NGT-21-002-080 & NGT-80001

SUBSELENEAN TUNNELER MELTING HEAD DESIGN

A Preliminary Study

NASA/USRA Project

Texas A&M University
Aerospace Engineering
College Station, Texas 77840

ISSUED: MAY 1988

Texas A&M University
Aerospace Engineering
College Station, Texas 77840

SUBSELENEAN TUNNELER MELTING HEAD DESIGN

A Preliminary Study

NASA/USRA Project

by

Bill Engblom *Eric Graham*

Jeevan Perera *Alan Strahan*

Ted Ro

Advisor

Stan Lowy

ABSTRACT

The placement of base facilities in subsurface tunnels created as a result of subsurface mining is described as an alternative to the establishment of a base on the lunar surface. Placement of the base facilities and operations in subselenean tunnels will allow personnel to live and work free from the problems of radiation and temperature variations. A conceptual design for a tunneling device applicable to such a lunar base application was performed to assess the feasibility of the concept. Designed was a tunneler which would melt through the lunar material leaving behind glass-lined tunnels for later development. The tunneler uses a nuclear generator which supplies the energy to thermally melt the regolith about its cone shaped head. Melted regolith is excavated through intakes in the head and transferred to a truck which hauls it to the surface. The tunnel walls are solidified to provide support lining by using an active cooling system about the mid section of the tunneler. Also addressed in this study is the rationale for a subselenean tunneler and the tunneler configuration and subsystems, as well as the reasoning behind the resulting design.

TABLE OF CONTENTS

APPENDICES

LIST OF ILLUSTRATIONS

INTRODUCTION

The rationale for the establishment of a lunar base is to further scientific investigation and to utilize lunar resources. Production of liquid oxygen from lunar material promises to reduce the cost of space development and manned exploration and ultimately provide the potential for an economically self-sufficient lunar base. However, since such objectives will require a permanent manned presence, the environment and protecting the personnel from it will be a primary concern. By locating the lunar base in subselenean tunnels, many of the problems of establishing a base can be resolved and the safety of the base personnel enhanced.

LUNAR SURFACE ISSUES

The traditional approach to lunar base establishment and development has been to place the facilities on the surface. Due to the radiation levels to which the lunar surface is exposed, the base facilities that will be accommodating personnel will require protection from radiation. Radiation protection can be accomplished by covering the facilities with lunar regolith. Proposed depth of coverage of these facilities for this purpose is about 2 meters in depth while depths of up to 7 meters may be necessary to protect personnel from radiation exposure during solar flares. Such shielding for the base facilities will require a significant effort in the establishment of a base. For crew activity outside of these shelters there are no means of protection from the radiation available.

Crew safety and productivity is also threatened by other conditions that will exist during surface operations outside of the base shelters. A safety risk to personnel exists due to the possibility of sudden depressurization of the EVA suit caused by an accident or micrometeorite puncture. Although the threat posed by meteorites to the safety of personnel in the short term is not high, this risk will grow with time. A greater threat is presented by high velocity particles produced by lander rockets or even the prospect of a lander crash. Finally, the near vacuum conditions will negatively impact on the efficiency of personnel surface activities due to the cumbersome nature of working in pressurized suits.

Strip mining has been the means advocated for obtaining the lunar regolith. The technique for strip mining is a straight forward one of

digging up the regolith and hauling it to the processing plant. The challenge is in minimizing the participation of the base personnel in these operations and in designing the equipment which will function efficiently and effectively in the lunar surface environment.

The difficulty in designing lunar surface equipment arises from the temperature gradient between day and night, the near vacuum conditions, and the properties of the lunar regolith. The temperature gradient resulting from the two week day night cycle is about 275 K (495°R), with temperatures reaching around 105 K (189°R) during the lunar night and about 380 K (684°R) during the day. These temperature conditions will require careful material selection and design to allow for the expansion and contraction which will occur in the equipment. The near vacuum conditions will require vehicles to be either pressurized, remotely controlled, or operated by crews in pressurized suits. Vacuum conditions will also require selection of special lubrications for exposed joints. The nature of the lunar regolith will also come into play. Lunar regolith is composed of very fine grains, which are abrasive and statically charged. Equipment operating in this regolith will accumulate a layer of regolith dust and must be designed so as not to incur dramatic wear or jamming of joints and moving components due to this accumulation. While none of these problems in themselves or their aggregate pose a prohibitive challenge, they will none the less likely raise, significantly, the cost of development and implementation of a lunar base.

Obtaining economic self sufficiency of the lunar base is essential for realization of long term development of the moon and space. Although paying off the initial establishment cost may take considerable

time, the key is to make the base pay for its day to day operations and to do so promptly. Achieving this will necessitate minimizing the weight and volume required for delivery to the moon both initially and during base expansion, and maximizing base productivity, all the while maintaining a high level of safety for base personnel.

SUBSELENEAN CONCEPT

The placement of base facilities in subsurface tunnels created as a result of subsurface mining is proposed as an alternative to the establishment of a base on the lunar surface. The rational for considering a subselenean base is primarily that it offers a radiation free environment for base habitation and operations. Other merits are that it offers a consistent temperature of 250 K (450°R), is free from the threat of meteoroids, and holds the potential of mining in a shirt sleeve environment.

In order to establish a subselenean base there must be available suitable underground space. Currently there exist lava tubes which could be utilized for this purpose. These lava tubes promise to provide abundant space for filling the needs of a lunar base. However, due to the questionable structural integrity of the lava tubes, as well as their lack of availability and accessibility, the reliance on the use of lava tubes for a subselenean base would not be appropriate. None-the-less, lava tubes could play a very beneficial role if the structural and accessibility issues can be resolved. However, instead of relying on lava tubes for suitable underground space, the use of man made tunnels to supply these needs should be considered.

By tunneling below the lunar surface, suitable underground space can be obtained. The structural integrity, location, depth, as well as the shape and amount of available volume of this underground space could then be controlled to suit the needs of a subselenean base. Once the tunnels are excavated, airlocks could then be installed and the tunnels pressurized. The necessary habitat interiors, such as flooring,

walls, utility lines, and equipment, could then be put in place. Since the tunnel walls themselves will provide the structural housing for the base only the interior of the base needs to be delivered, thus lowering the weight and volume required for delivery.

Excavation of large chambers by conventional methods could provide abundant space for agricultural use or processing plants. Excess tunnel space could be used for storage of liquid oxygen or other products and supplies. An abundant supply of lunar materials for processing would be available with little energy expenditure by simply extracting the regolith from above, using gravity to deposit it on the tunnel floor. This mining process however should be done remote from the main base as the process will eventually produce a large sink hole above with undetermined effects on other tunnels if they were in the immediate vicinity. The material gathered by this method could be placed on a conveyer belt system for delivery to the base processing plant. Should the abundant tunnel space be fully occupied, expansion would simply entail having the tunneler return and add more tunnel space adjacent to the base or at another depth. Tunnels could also provide a safe transportation environment between the various sites of a base and even between bases. Tunnels would be particularly well suited for providing structural support for a mass driver.

The subselenean base would provide a safer and friendlier environment than one located at the surface without restricting any of the objectives for establishing a lunar base. Such a base also appears to be more expedient and affordable than surface options. Before a subselenean base can be realized however, a viable means of tunneling must be available to do the job.

TUNNELING

The criteria established for the selection and development of a method for subselenean tunneling are; autonomy, reliability, maintainability, effectiveness in various ground formations, high advancement rate, and minimum weight and volume. Autonomy was set as a primary consideration due to the high cost of maintaining base personnel and the inherent safety risk involved. High reliability of a system is an essential criteria for obvious reasons. Unfortunately no system is free from failure, so features providing for maintainability and repair must be incorporated into the system. The system selected for tunneling should be capable of performing effectively in the various ground formations which can be expected to be encountered. Formations may range from loosely packed regolith to hard solid igneous rock or a heterogeneous mixture of the two extremes. A relatively high advancement rate is desirable to allow for expedient establishment and growth of the base. Finally, as with all projects requiring delivery of materials from the earths gravity well, the weight and volume of the system should be minimized.

There exist two basic approaches to tunnelling; blast dig and slurry, and tunnel boring machines. The blast dig and slurry methods are not considered to be viable for initial lunar base applications because of the high labor requirements involved with this approach. Tunnel boring machines are better suited for lunar applications because they are less labor intensive, potentially autonomous, and offer relatively higher advancement rates.

Tunnel boring machines can be categorized into two means of operation; mechanical and melter. Mechanical tunnelers operate by breaking down the medium through which it is boring with cutters on the leading surface and then passing the debris on for excavation. Mechanical tunnelers are a well-proven technology currently in use for many subterranean applications such as transportation tunnels. However, the difficulty with mechanical tunnelers is that they suffer from a high rate of down time, on the order of 1/4 of the time, for maintenance due to wear and system failures. Tunnels produced by mechanical tunnelers require, depending on the ground type, installation of lining to secure the tunnel walls. Lining is a significant factor both in the cost of tunneling and in limiting the rate of advancement.

Melter tunneling devices operate by melting the material before it with a heated leading surface as it advances and leaves behind a glass-like lining from the cooled molten material. Melting head tunnelers, however, still require development and need high levels of power. The potential merits of this type of tunneler are that it offers a relatively high advancement rate, good reliability, effective operation in all ground formation types, and, most importantly, it does not require liner installation.

There also exists a hybrid of the above two types of tunnelers, one which uses a mechanical cutter face and a heated band about the tunnelers circumference. This device operates like the mechanical tunneler except that it uses the heated band to melt the tunnel wall surface, which is then resolidified by cooling, thus producing a tunnel liner. However, the hybrid tunneler has not yet been developed and may have poor reliability comparable to that of the mechanical tunneler.

The melting head tunneler was selected as being the most suitable type of tunneler for lunar applications. This tunneler type was chosen since it was considered the most autonomous system. The expectation of the melting head tunneler being highly autonomous results from its being viewed as more reliable that the mechanical type and that it produces a tunnel with lining. The melter also provides a faster advancement rate than that of the mechanical tunnelers for rock type formations such as found in the mare regions and bedrock under the highlands. The principle concerns for the melting head tunneler are the high power requirements, materials and cooling requirements for the system and liner formation. An issue which must also be addressed, and one which is common to all the methods, is that of excavation and how it can best be accomplished.

To address the issues of a melting head tunneler to be used for subselenean applications, and thus provide an assessment of the feasibility of the concept, a conceptual design for such a device was performed.

MELTING HEAD TUNNELER

A conceptual design of a melting head tunneler was performed to develop and assess ways to resolve concerns for designing such a tunneler for lunar applications, to develop a tunneler system configuration, and to identify areas for technology development and further investigation. The principle areas of concern impacting on the design configuration were; power requirement, excavation, cooling systems, and autonomous operating capability (i.e. a distinct unit without continuous, direct physical link to the surface nor real time participation from personnel) which significantly challenged the resolution of the problems in providing sufficient power and cooling to the system, as well as a means of excavation. This section of the report will discuss the resulting configuration of a melting head tunneler and its components. Discussion of areas which need further technology development and investigation can be found in the Tunneler Research and Development section of this report.

Before discussing the tunnelers components and subsystems a synopsis of the configuration is given here. Refer to Figure 1 for a schematic of the tunneler. The tunneler uses a cone shaped head for its leading surface to melt the regolith before it. The head uses intakes for extracting all of the molten regolith as it advances. The molten regolith is then passed to a holding tank at the rear of the tunneler where it is maintained in its molten state, using excess heat from the generator, until it is transferred to the excavation truck. The required heat flux is delivered from a liquid metal nuclear reactor to the head via heat pipes. A turbine is also incorporated to convert the thermal power output of the nuclear

reactor to mechanical and electrical power. Electrical power is needed to operate the on-board general purpose computers and other electrical systems as well as charging batteries. The mechanical power is used by the propulsion system. The propulsion system has two sets of wheels, fore and aft, each set is composed of four pairs of tires with each pair placed opposing its counterpart. The

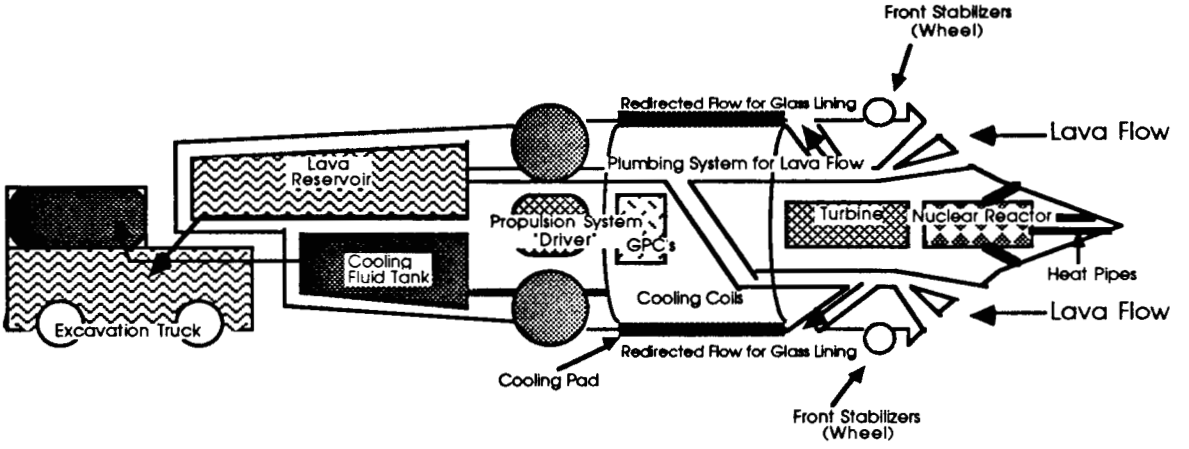

Figure 1.
Schematic of Tunneler

fore set of wheels are passive stabilizers while the aft wheels are axially driven, thus providing for forward movement. To provide for maneuverability, the aft wheels can be hydraulically offset from the center of the rear of the tunneler relative to the center of the tunnel, pivoting the tunneler about the stabilizer wheels. Note that the tunneler is slightly tapered towards the rear to allow for greater displacement and thus a higher turning angle than if it were not tapered. Just behind the fore set of wheels some of the extracted molten regolith is diverted from the pipes to the exterior of the tunneler. This molten regolith is then solidified using the cooling pads about the tunnelers mid-section. The cooling fluid is supplied from the coolant tank located at the rear of the

tunneler and is exchanged periodically, via the excavation truck, with recycled coolant from the surface where the heat was removed.

Utilizing the results of a tunneler systems analysis, pertinent overall parameters were assessed. This analysis produced an estimated total tunneler system mass of 300,000 kg (660,000 lb_f), a tunneler advancement rate of 25 m/day (81.25 ft/day), a total power requirement of 20 MWth, and an expected lifetime of between one and three years. On the pages that follow is a discussion of the tunneler systems analysis performed for this study.

HEAD DESIGN

Various head designs (both mechanical and thermal) were considered in the initial stages of this study. Each design was analyzed to meet the following criteria: (1) reliability, (2) maintainability, (3) autonomy, and (4) boring efficiency. All mechanical devices were later assumed to be unacceptable in terms of meeting a satisfactory reliability level. Furthermore, thermal heads were considered for their respective autonomy integrity; since all thermal heads were assumed to have relatively the same reliability and to a lesser extent, maintainability. Hence, based on this assumption and using the above criteria, a *conical* head utilizing a rock-melting technique was settled on.

Once the cone-shaped penetrator design was decided, specific features were implemented. First, the rock melting technique required that the surface temperature along the penetrator be higher than the melting point of the lunar regolith. In other words, a system was required which could deliver a sufficiently large heat flux to the melting face of the penetrator. The development of the heat pipe sufficiently filled this requirement. There has been a sufficient amount of improvement in heat pipe technology such that transportation of energy from a compact source to a melting device is possible. In addition, an inlet design for the excavation plumbing system required attention. Basically, a series of circumferential funnels with intakes located at the base of each funnel was conceived. The overall shape of the penetrator consists of two cones of different half angles molded into one unit. This dual-angle configuration will provide additional control of the lava flow. Finally, the base of the conical head was designed to be greater than the diameter of the tunneler body. This feature provides for a clearance

between the tunnel wall and the surface of the tunneler. The clearance will produce a net volume which will be utilized by the glass lining and the propulsion system. The overall structure of the head design is illustrated in Figure 2. A detailed description of the intake system will be provided in a later section.

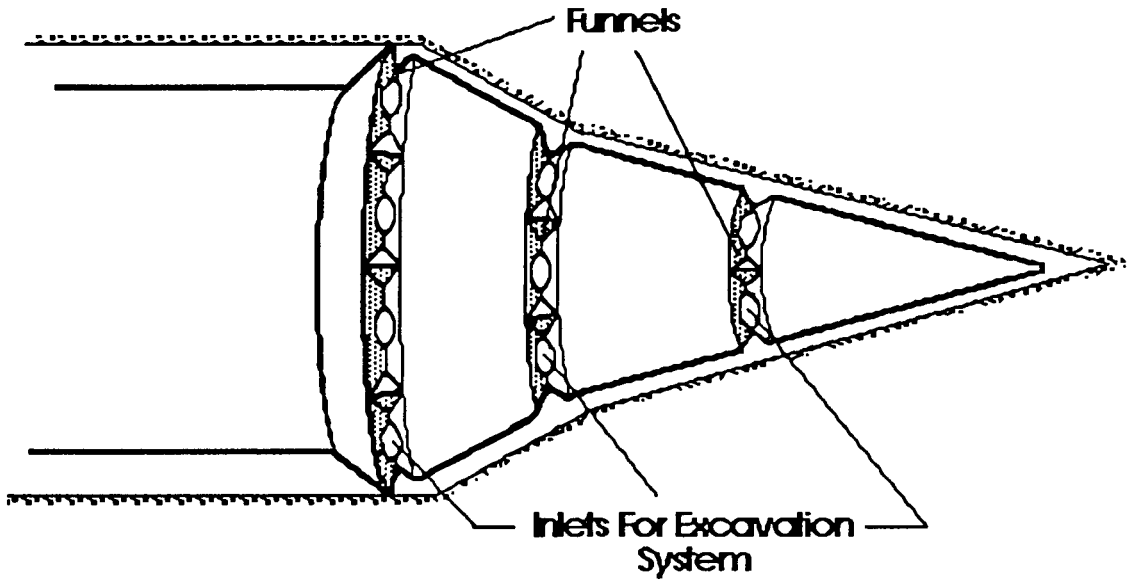

Figure 2.
Components of Head Design

The actual head dimensions were initially designed to account for fluid pressure along the surface. A model which the Los Alamos Scientific Laboratory developed for surface pressure due to viscous fluids in motion was incorporated into the design. This model did not account for excavation and hence, yielded extremely high pressures even for low-angled right circular cones (see Appendix D: Cone Pressure Distribution w/o Excavation). It was theorized that a steady state situation would result from continuous melting and simultaneous excavation. The pressure along the penetrator's surface would consist of shear stress resulting from viscous fluids in motion. Therefore, another model was

developed for this study which accounted for only shear stresses due to viscous forces (see Appendix E: Lava Flow Along the Head). As one would expect, this model yielded low viscous forces which could easily be compensated for by the propulsion system with minimal damage to the glass lining. Hence, the actual dimensions of the cone were not restricted by surface pressure.

In the actual determination of the head dimensions, a sufficient amount of freedom exists. The only overriding constraint is the base diameter, which must be slightly greater than the tunneler's body diameter of approximately 4 meters (13 feet). The rest of the head was designed to provide for a geometrically applicable means to direct the lava flow into the intakes. Furthermore, this design also should provide a sufficient net volume for the piping system, heat pipes, and reactor, of which all will be located inside the cone. The overall dimensions of the conical head may be examined in Figure 3. It should be noted, however, that the dimensions provided in this report may be easily changed without any serious effects on the rest of the tunneler design.

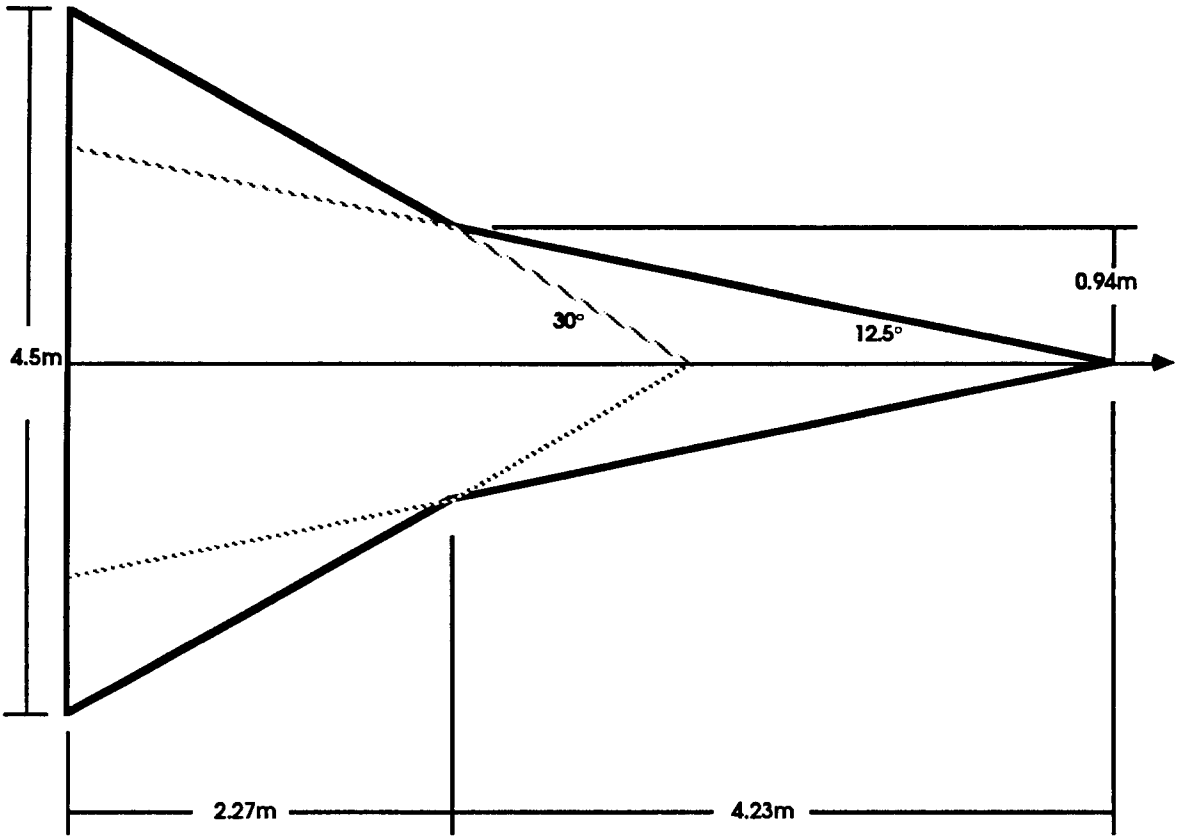

OVERALL DIMENSIONS FOR THE PENETRATING CONE

Figure 3.
Conical Head Dimensions

The obvious criterion in which the head material must be able to meet is the very high temperature originating within the penetrator and transmitted to the surrounding regolith environment. In addition, a variety of other areas of material criteria must be examined, such as head material-molten regolith (lava) interactions, internal power source (nuclear reactor)-head material interactions, surface erosion (particularly at the penetrator tip), and miscellaneous corrosion effects on the piping system. (Various scientific articles applicable to this study were examined and a complete summary of data collected from these

reports may be examined in Appendix F.) The high temperature involved with the total melt of surrounding regolith mandated the implementation of refractory alloys or materials for the proposed conical head. The major drawbacks with refractory alloys are its limited fabrication technology and corrosion resistance. Although fabrication and corrosion of refractory alloys are key concerns, recent improvement in these areas is encouraging. However, it is evident that continuing development is necessary in order to satisfy the specifications required for a melting head. Tentatively, a Mo 50%-V 50% alloy was selected because of its high temperature properties, respectable corrosion resistance, and improving fabrication technology.

INTAKE SYSTEM FOR LAVA FLOW

The main consideration in the design of the intake system was its impact on the power requirements imposed on the propulsion unit. Consequently, the piping for the lava intake system was designed to minimize pressure losses due to viscous forces internal to the pipes, and the pressure loss associated with transferring the weight of the lava to the top of the vehicle for deposit into the lava holding tank.

The molten regolith formed continuously just outside the surface of the cone is passed into the cone via circumferential ring-shaped openings. As shown in Figure 2 (see Head Design) three rings have been placed at strategic locations along the cone. One ring has been placed in the middle of the tip part of the cone to reduce the large pressures expected to develop on the front of the cone during the melting process. Another ring has been placed in the middle of the base part of the cone for the same purpose. The third ring is located at the base of the cone to ensure that lava which gets past the second ring is not pushed along with the vehicle, continually "stuck" between the base of the cone and the wall beside it. The thickness of the rings were chosen large 0.48 meters (1.6 feet), and in small number (3) to reduce the viscous losses in that phase of the intake system. The thickness was also chosen with respect to the pipe intake sizes, explained later, and the need to keep a relatively large amount of cone surface useful for heating purposes (above 60%). A heated filter may need to be added to reduce the particle sizes allowed to pass into the cone.

Obviously for structural reasons, the cone cannot be divided by circumferential rings that continue from the cone surface to the cone base. Consequently, the flow that passes into the circumferential rings

must be funnelled into pipes immediately. The number of pipes has been chosen small to increase the structural integrity of the cone and the amount of space available inside the cone for the incoming heat pipes. There are 4 pipes from the tip ring, 6 from the middle ring, and 8 from the final ring. The four pipes started at the tip are common to four of the pipes used by the other two rings. Similarly, the six pipes leading from the middle ring are common to six of the eight pipes used by the base ring. The cone piping commonalty is illustrated in Figure 4 on the following page. Note that the pipes must stay near the cone surface at all times since the inner-most part of the cone will be occupied by the nuclear reactor. All eight of the pipes leaving the cone will rendezvous aft of the nuclear reactor and before the turbine, forming one main pipe, to travel along the top of the vehicle so that the lava can eventually be poured into the holding tank without interfering with any of the other systems on-board the tunneler (refer to Figure 4).

In order to size the pipe diameters for the short (cone) pipes and the long (main) pipes, equations for pipe pressure loss as a function of length diameter ratio were developed and then used to find the optimum diameter for minimum pressure loss. A detailed development of these sizing calculations shown in Appendix G. Before correct equations could be produced an assessment of the Reynold's Number for the pipe flows had to be completed. It became apparent that, with any reasonable choice of pipe diameter, the Reynold's Number will be

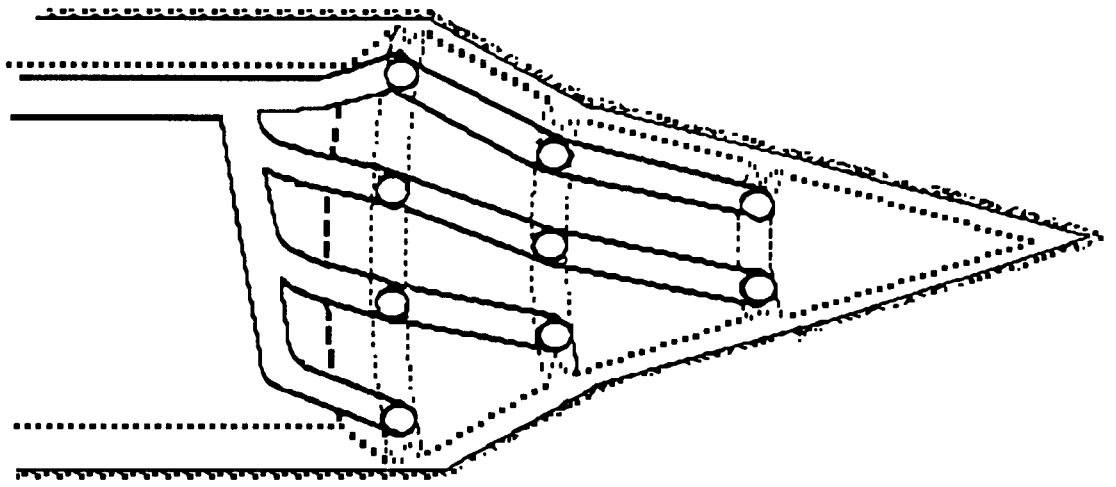

Figure 4.
Basic Piping Arrangement for Intake System

well below 2000, demonstrating that the flow will be laminar. Then, the laminar viscous forces as a function of pipe diameter were assessed. To account for the forces associated with bends in the piping system equivalent lengths for each bend were added to the actual lengths of the pipes when calculating the viscous forces. Additionally, the forces required to raise the level of the flow in the pipes were approximated as hydrostatic pressure losses (i.e., the specific weight multiplied by the height change). The viscous losses at the circumferential ring were assumed small. Also, the static pressure losses due to the increase in flow rate from the cone surface to the short pipes have been calculated to be negligible.

Finally, equations for the total losses imposed by the intake system on the propulsion unit as a function of diameter were produced and then minimized with choices of a diameter of 0.48 meters (1.6 feet) for the short pipes and 0.36 meters (1.2 feet) for the long pipe. The resulting losses amounted to about 6,000 and 2,400 Newtons (1346 and 538 lb_f) lost in the short and long pipes, respectively, for a total of 8,400 N (1884 lb_f). This is the force the propulsion system will have to produce to move the

vehicle forward at a constant speed. The intake piping system has been optimized with respect to the assumption that the tunneler will most often be travelling at a zero degree inclination.

However, the tunneler must travel at various inclinations; and so, the forces imposed on the propulsion system as a function of inclination must be understood to assess the full impact of the intake system on the propulsion unit. Appendix H contains a detailed development of an equation for the forward forces imposed on the propulsion system as a function of inclination. To accomplish this evaluation, the component of weight of the vehicle and all of the lava it contains that acts against the forward movement of the vehicle must be accounted for. Using the dimensions of the piping system and the holding tank and assuming a mass for the vehicle, the total additional forces to be overcome may then be approximated as simply the maximum weight of the vehicle and its contents multiplied by the sine of the inclination angle. The worst case scenario would involve a 90° fully-upward inclination at maximum weight. In this case the propulsion unit would be required to produce 400 kN (90 klb_f) with a safety factor of 1.5. Note that a full decline involves similar values, and hence, only inclinations of 0 to 90 degrees were evaluated.

PROPULSION SYSTEM

The propulsion unit is a wheel-driven system that utilizes two sets of wheels, called assemblies, to guide and move the tunneler. One of the assemblies is located at the aft portion of the vehicle and is called the "driver", illustrated on the next page as Figure 5. It is responsible for producing the frictional forces needed to propel the vehicle forward. To accomplish this, the driver gets shaft power from the turbine which is converted via a gearing system, along a torsional shaft, into a wheel torque which produces the necessary frictional loads.

Hydraulic actuators have been placed on each wheel of the driver to produce the normal loads needed to promote these frictional forces and are responsible for the alignment of the rear portion of the vehicle in the tunnel. The hydraulic system is used to manipulate and stabilize the position of the vehicle. The on-board computer regulates all of the actuator fluid levels and pressures, independently, to compensate for unexpected loads on the vehicle and to initiate maneuvers (i.e., turns). The power to drive the electric motors used to operate the actuators comes from a battery that is continually recharged by the turbine. Note that when the fluid level in a hydraulic actuator changes the arm length changes (e.g., wheel pushes outward). Consequently, to allow the torsional bar to deliver the shaft power to the wheel, despite these arm length changes, another bar that is fixed to the wheel that can be moved up and down the torsional bar will be needed to collect the torque.

The other assembly is called the "stabilizer", located in the forward part of the tunneler, and is only responsible for maintaining a relatively fixed alignment of the frontal portion of the vehicle (see Figure 6). A hard

spring system will be connected to each wheel of the stabilizer to minimize the alignment changes seen in the front of the tunneler, even under maximum load conditions. It is assumed that the surface of the

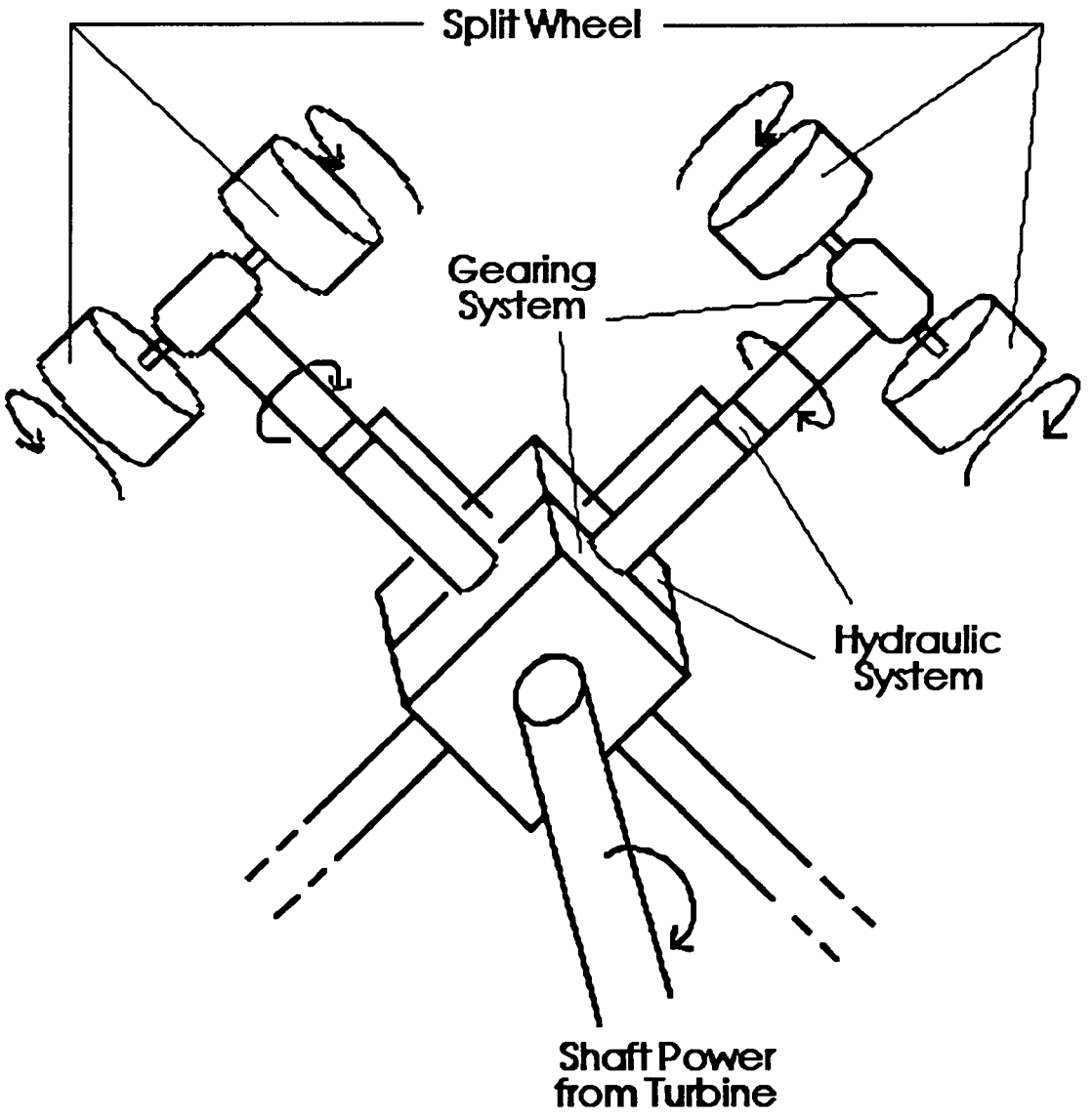

Figure 5.
Propulsion System--"Driver"

tunnel at this location is hard enough for wheels to roll upon. However, if the temperature of the surface is too high the rock will be too soft for wheels to grip and some kind of pads (skids) may be more effective

stabilizers. Note that the "driver" was placed in the aft portion of the tunneler to protect the hydraulics from the excessive heat and to avoid overcrowding the forward portion of the vehicle.

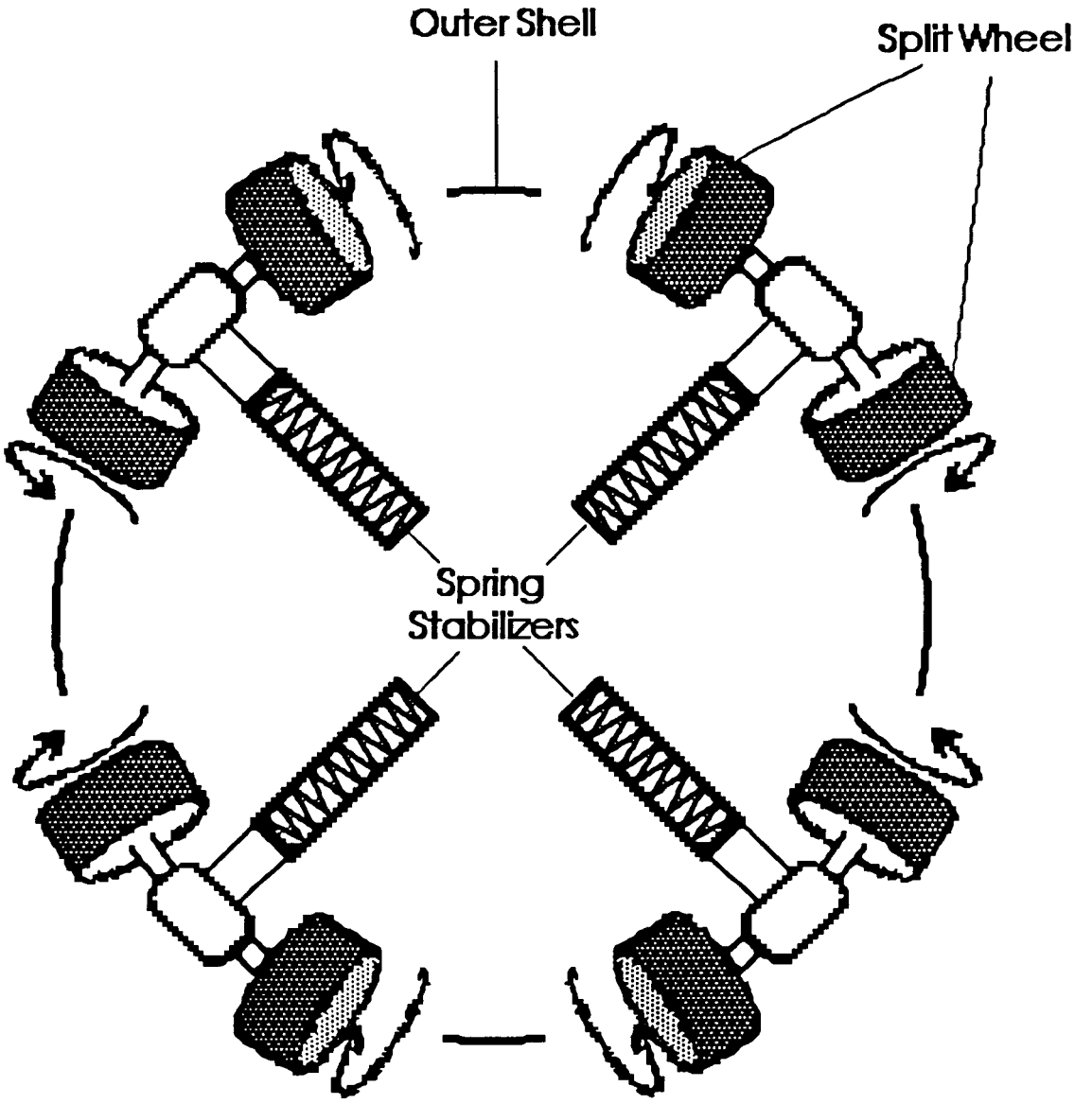

Figure 6.
Propulsion System--"Stabilizers"

Each of the assemblies have four wheels -- the minimum needed to perform turns in any direction (maneuvers will be explained later). The

wheels have been positioned on the assemblies for the best weight distribution. Each wheel of the "driver" has a slightly compressible tread and has been designed in a split-wheel configuration to maximize the amount of surface area in contact with the glass liner this minimizing the normal and radial stresses in the glass liner.

This propulsion system is unlike the ones typically used and proposed for conventional tunnel-boring machines which are often pad systems that operate in a caterpillar-type of motion. Mechanical tunnelers used for subterranean applications have great strength and stability capability because considerable forward power is needed from these propulsion units. However, this tunneler melts through the rock and is moon-based, thus lowering power requirements dramatically. According to calculations herein, a wheel-driven propulsion unit can produce the necessary forward thrust and perform all needed alignment functions for the tunneler without harming the glass liner. Moreover, wheel driven units operate in a more continuous manner and are much less complex than pad systems. Consequently, it seems that a wheel-driven system is more appropriate for a melting tunneler on the Moon than a pad system.

The "driver" must be able to produce the required frictional force to propel the tunneler forward and help support the weight of the vehicle in the tunnel at various inclinations. From the analysis performed in the Lava Intake System section, the frictional loads the propulsion unit must overcome varies with inclination and would be a maximum at 272 kN (61,000 lb_f), in a 90° climb, without a safety factor. These frictional forces will be produced via a torque applied to each wheel to promote a frictional force equal to the torque times the radius of the wheel

provided the normal force is sufficient to avoid wheel slipping (this problem has been modelled in Appendix I). For a constant speed the torque required corresponds to the frictional requirements. For example, the maximum frictional force requires a torque of 200 kN-m (146,000 lb_f-ft). This corresponds to a power requirement of only 0.5 kilowatts for all four wheels combined, due to the low angular velocity corresponding to the relatively slow advance rate of ~ 25 meters/day (82 ft/day). Moreover, the tunneler may be accelerated or decelerated by changing the shaft torque being delivered to the propulsion unit.

The gearing system would need a main transmission box, controlled by the on-board computer, to transfer the power along two separate torsional bars. At both ends of both bars the power will be converted to the wheel axles using four gear boxes. The weight of the gearing system: the main transmission box, the four gear boxes, and the two torsional bars, should not exceed 2.24 kN (500 lb_f).

The hydraulic system for the driver must be able to produce the required normal loads to help propel the tunneler forward and support the weight of the vehicle in the tunnel at various inclinations. The calculations of the normal forces required as a function of inclination are detailed in Appendix J. The required normal forces depend on the frictional forces required to prevent slippage of the wheels since the frictional forces required must be less than the normal forces, at the point of contact between the wheel and the glass liner, times the static friction coefficient. In Appendix J the friction coefficient has been assumed to be low (0.2: rough glass on elastomer polymer tread), making for a maximum required normal force, for each of the four actuators, at a 90°

inclination, of 340 kN (76,000 lb_f) including no safety factor. At low inclinations the required normal loads for frictional purposes are relatively small.

However, normal forces are also needed for normal support of the weight of the tunneler, to maintain the alignment of the vehicle. In supporting the vehicles weight two of the hydraulic actuators and two of the hard springs of the stabilizer on the bottom-side of the vehicle will always be responsible. In contrast to the needs of the frictional loads, the hydraulic normal support needed for the vehicle weight will be a maximum at zero inclination, a value of 94 kN (21,000 lb_f), and will gradually decrease to zero at an inclination of 90°. At approximately a 15° inclination the normal force requirements imposed by the frictional requirements and the support requirements are equal at 91 kN (20,000 lb_f). It follows that above this inclination the normal force requirement imposed on the hydraulic actuators by the frictional forces dominate, whereas, below this angle the normal support requirements dictate the necessary hydraulic forces.

To be able to bore at any inclination, the hydraulic actuators must be able to produce 340 kN (76,000 lb_f) or 510 kN (114,000 lb_f) for a safety factor of 1.5. A maximum pressure of 7 MPa (1 ksi) was chosen for these actuators since it is a typical maximum pressure and would be less likely to produce leakages than an actuator with a higher maximum pressure. The diameter of the actuated cylinder would only need to be about 0.30 meters (1 ft)--this cylinder size would not pose any problems. Note that during level boring the actuators need only operate at 30% maximum pressure with a safety factor of 1.5.

The fluid levels within the hydraulic actuators play an important role in the maneuvering of the tunneler. Maneuvers, or turns, will be initiated within the hydraulic system, as described below. The fluid levels in the four cylinders will increase or decrease to correspond to the desired alignment of the rear portion of the tunneler. The maximum angle of the vehicle, with respect to the tunnel, is limited by the clearance between the fuselage and the wall (1.4 degrees). The vehicle has been tapered to allow for an extra degree to be added to this angle making for a maximum turning angle of 2.4 degrees, but a conservative value of 2 degrees will be used as the maximum turning angle. This angle is the change in inclination the tunneler can achieve for every vehicle length it travels (2° change every 20 meters or 66 feet). The fluid levels in the actuators must be able to change 0.38 meters or 1.2 feet (provided the distance between the two assemblies is about 10.7 meters or 35 feet), meaning each cylinder will need the capacity to hold about a 1 meter (3.28 ft) height of fluid. The extra weight associated with this capacity is only around 300 N (67 klb_f) for all four cylinders. The actuator size of 0.3 meters (1 ft) wide and 1 meter (3.28 ft) high will easily fit within the tunneler radius of 1.9 meters (6.2 ft). The hydraulic system will require the wheels to function properly despite the variance in actuator levels of 0.76 meter (2.5 ft).

Once the fluid levels have been altered, setting the new alignment, the "driver" wheels will need to be rotated to orientate the wheels parallel with the present tunnel direction. Then, by creating a forward force ahead a torque in the direction of the turn will also be created, forcing the vehicle to maintain the turn. Also, due to the misalignment of the cone with the lava flow, the new pressure distribution

will cause the head to be pushed in the direction of the turn. To complete the turn the fluid levels must be returned such that the vehicle is again completely aligned with the tunnel. It should be noted that these fluids will be subjected to temperature of from 873 to 1073 degrees Kelvin (1571 - 1932 degrees Rankine) , and so, a fire-resistant fluid (e.g., water-oil) will be needed to maintain a high enough viscosity to avoid leakages.

According to vendor data the weight of four such hydraulic actuators, as described, with the associated motors, reservoirs, accumulators, etc., would not exceed 2.23 kN (0.5 klb_f). Also, from vendor data, the power required to operate the cylinders under normal conditions would be negligible, but could be around 80 kilowatts if all cylinders were being fully actuated simultaneously. For this reason a battery will be included in the hydraulic system to be used during periods of large power requirement. The size of this battery has not been determined but has been assumed not to be a major weight factor.

As mentioned previously, the "stabilizer" will be expected to maintain the front alignment of the vehicle in the tunnel using a hard spring system attached to each of its four wheels. The maximum normal force these springs will encounter will be the same as those encountered by the hydraulic actuators on the driver with respect to normal support--94 kN (21 klb_f). However, if a turn is initiated at any inclination an additional force will be encountered due to the misalignment of the cone-shaped head. This force will equal the normal component of the frictional force, up to a maximum of 9500 N (2000 lb_f), making for a required hard spring normal force of 104 kN (23 klb_f). Picking a maximum allowable displacement of 0.1 meters or 0.33 feet (0.34 degree inclination change), an approximate stiffness equivalent of 1 MN-m (735 klb_f-ft) is

needed for each hard spring system. Note, 1.8 kN (0.4 klb_f) has been allotted for these spring systems.

The wheels for the "driver" were designed to minimize the stress on the glass liner. To maximize the surface area of the wheels, a split-wheel configuration was chosen. Each half-wheel is 1 meter (3.28 ft) wide. Nearly half of the circumference of the tunnel wall will be in contact with the wheels. To keep the wheels in contact with the wall despite the maximum hydraulic fluid displacement of 0.38 meters (0.09 feet), the nominal clearance between the fuselage and the wall must be at least the same amount. A wheel radius of 0.5 meters (1.6 ft) would ensure safe wheel contact. Note that to keep the wheel axle below the fuselage at all times would be desirable in order to better protect the driver, however, this would require a large radius of 0.76 meters (2.5 ft). Never the less, with a wheel radius of 0.5 meters (1.6 ft), assuming a tread compressibility that would allow at least 30° of the circumference to be in contact with the wall, the resulting area of contact for each of the four wheel locations would be 0.52 square meters (5.6 ft^2). It follows that with a maximum normal force of 510 kN (114 klb_f) and a maximum radial force of 400 kN or 90 klb_f (with a safety factor of 1.5), the maximum normal and radial stresses seen by the glass liner will be 974 kPa (0.14 ksi), and 191 kPa (0.03 ksi), respectively. These values are well within the structural limit of the assumed SiO_2 glass structure of approximately 50 MPa (7 ksi). Note, the stabilizer will never come in contact with the glass liner since the liner is formed aft of the assembly. The contact area of the wheels (or pads) for this assembly should not need to be much larger than the driver wheels since the normal forces to be dispersed are nearly equivalent.

The weight of the four split-wheels and the four similar wheels (or pads) should not exceed 7.1 kN (1.6 klb_f), allocating 900 N (200 lb_f) to each split-wheel of 1 meter (3.28 ft) diameter and 2 meters (6.6 ft) in total length. The total propulsion unit is then estimated to weigh about 14 kN (3 klb_f). The total nominal power requirements for the propulsion system from the turbine is 0.5 kW for the needed torque plus an almost negligible power to recharge the battery that runs the actuators. In the most extreme case, with a dead battery and a need to slightly accelerate, the power requirements would be about 21 kW. The space required by the propulsion unit is slightly more than a 1 meter (3.28 ft) section of the tunneler.

POWER

Thermodynamic Cycles

Power generation, distribution and heat rejection are important aspects for any type of regolith melting system. To generate and manage the energy used by the lunar tunneler three separate though interactive thermodynamic power cycles are proposed. The loops are defined as follows;

(a) The primary power cycle, conducting heat from a nuclear reactor to the regolith.

(b) The secondary power cycle, using heat exchanged from the reactor to drive a work producing turbine.

(c) The thermal rejection cycle, dumping the waste heat into space with a surface radiator.

These cycles and their major components are shown in the schematic in Figure 7 and are described either in the following sections or elsewhere in the report. It should be noted here that liquid metals were chosen as the working fluids for all three loops. One advantage of liquid metals, such as lithium or sodium, is that they are excellent heat storage and transferring agents. Also liquid metals can be pumped by electromagnetic pumps that do not require moving parts. This is beneficial for a system that must operate unmanned and as maintenance-free as possible. Preliminary calculations associated with the state changes in the thermodynamic cycles are included in Appendix A.

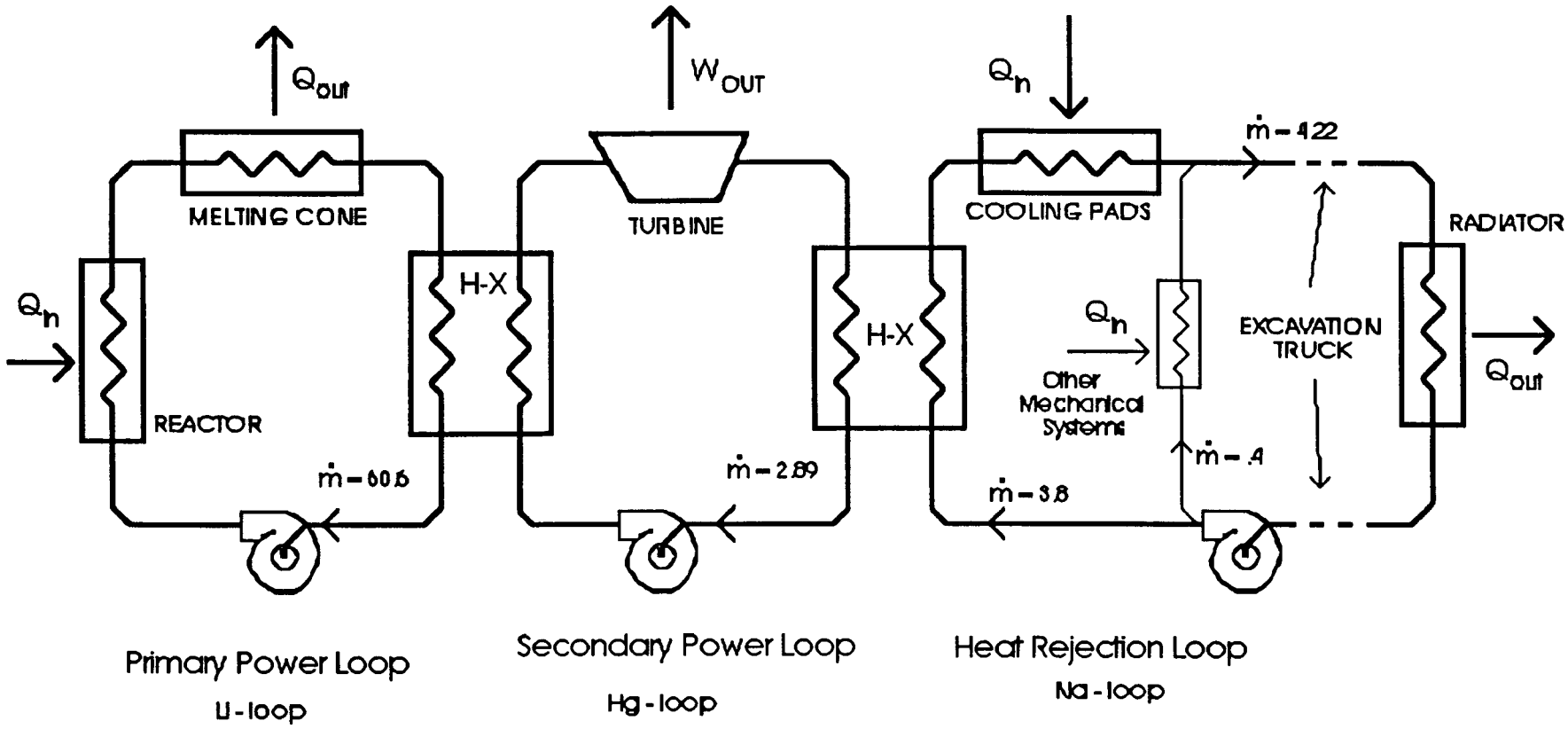

NOTE: All mass flow rates in Kg/sec

Figure 7.
Schematic of Tunneler Power Systems

Primary Power Cycle

The melting of selenean regolith requires an immense amount of power in the form of continuous heat energy. In this design, such power is provided by a lithium cooled, liquid metal, nuclear reactor. Lithium was chosen as the cooling medium because it can operate at higher temperatures than most other liquid metals (e.g. sodium, potassium or mercury). After inefficiency losses, 95 % of the power generated by the reactor is transferred into the regolith. The heat is transferred by flow of lithium coolant through heat pipes in the tunneler cone. The other 5 % of the net reactor thermal output is transferred to the secondary power cycle by a heat exchanger. This provides energy for the secondary loop to convert into power for tunneler systems use. The heat transfer process is supposed to be isobaric but some pressure loss is expected, hence a pump is included in the primary loop to maintain lithium pressure and velocity at the entrance to the reactor.

The primary power cycle is only concerned with heat transfer and would ideally expend or receive no mechanical work but only absorb and radiate heat. The actual cycle is plotted in Figure 8 on a temperature-entropy (T-S) diagram. Heat is added to the fluid in a nearly constant pressure process from states 1 to 2 by the reactor, and absorbed in a nearly constant pressure process from states 2 to 3 by the regolith. Heat is transferred to the secondary power cycle between states 3 and 4. In actuality, the temperature at state 4 must be slightly below the reactor entrance temperature to allow for heat gain while pumping the fluid. This temperature rise is essentially negligible however. In Figure 8, pressure loses through the system are also seen as increases

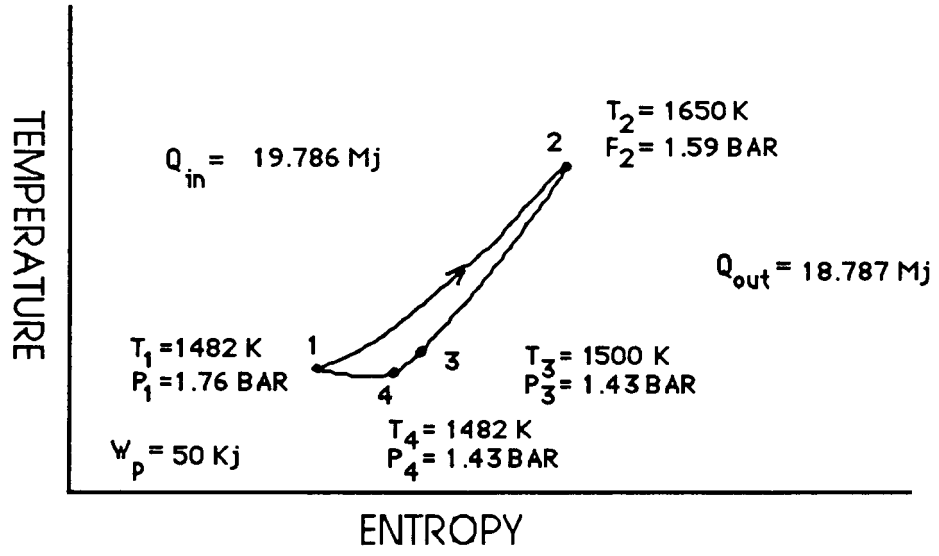

Figure 8.
T-S Diagram for Primary Power Cycle

in entropy. It should also be noted that the temperature at the reactor exit is above the boiling point for lithium at one earth atmosphere so the lithium is pressurized up to almost two earth atmospheres (Faires, 1978).

Secondary Power Cycle

The second thermodynamic loop is one in which mercury is used to absorb thermal energy from the primary power cycle and convert the energy to turbine work. This work is used to drive the propulsion system and generate electricity for the tunneler systems. The power the turbine needs to provide, calculated in Appendix B, has been set at 300 kW.

The secondary power cycle is a two phased Rankine cycle which is commonly used in power generating systems throughout the world. The thermodynamic changes of the secondary loop are illustrated in the T-S diagram in Figure 9. Mercury was chosen for this cycle because it transcends from liquid to vapor at reasonable pressures (atmospheric) over the temperature range involved in this cycle. Liquid mercury

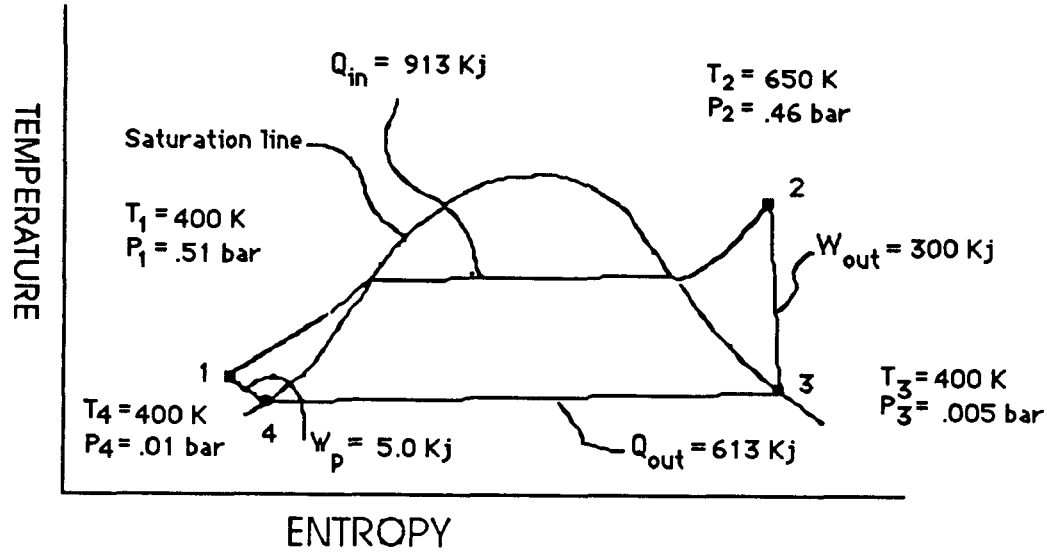

Figure 9.
T-S Diagram for Secondary Power Cycle

receives heat from the primary loop from states 1 to 2 through a heat exchanger. The mercury is seen to enter the liquid-vapor mixture region and ultimately receive heat until it is a vapor at state 2. The vapor metal then expands through an axial turbine in what would ideally be an isentropic process from states 2 to 3, though as evident in the figure, a slight increase in entropy due to losses in the turbine occurs. The expansion results in the mercury returning to a liquid-vapor mixture that is condensed at constant pressure from states 3 to 4. This is accomplished in a heat exchanger that rejects heat from the condensing mercury to the heat rejection cycle. The mercury is then pumped to restore its state 1 pressure at which it will again absorb thermal energy.

Thermal Rejection Cycle

The thermal rejection loop is similar to the primary power cycle in that it is strictly a heat exchanging loop. Hence, the T-S diagram for this cycle is not included as it would have the same shape as that in Figure 8. The state properties for the heat rejection loop are included in Appendix

A with the calculations for all three cycles. One difference from the primary loop, evident in Figure 7, is that the sodium coolant actually follows two paths, the majority cooling the secondary loop from about 400 to 600 Kelvin (720 to 1080 R) and the regolith to form the glass lining from 600 to 800 Kelvin (1020 to 1440 R), while the remainder cools tunneler mechanical systems and components. Sodium was chosen for this cycle because of good thermal conduction and rejection properties over the temperature range involved and like the other coolants, it was a liquid metal. The amount of sodium used in this cycle was originally sized just for glass wall and tunneler system cooling, but as it became evident that heat would have to be rejected from the power cycle, the low end temperature of the heat rejection cycle was reduced to allow for further heat rejection without increasing the amount of sodium used. This is important as the sodium ultimately rejects heat in a surface radiator and must be stored in a limited volume in the tunneler for a period of time before the rejection process can occur. The procedure involves storing 'hot' thermally saturated sodium in a holding tank until it can be exchanged with 'cool' sodium which is brought in by truck from the surface. The 'hot' sodium is then carried in the truck to the surface where it cools in the surface radiator. After being returned to the tunneler, the sodium is pumped up to the initial pressure at which the cycle began (Faires, 1978).

An important feature of the power generation and heat rejection systems of the tunneler is the ability for some of the fluid mediums to be redirected around the loops. In the primary cycle, lithium can be directed just through the melting cone, (or a portion of it) or just the heat exchanger depending on the situation. Two paths are available for the

liquid sodium to follow while in the tunneler, going either to cool the secondary power system and the cooling pads or to cool the other tunneler mechanical systems. Additional sodium, lithium and mercury are also stored in the tunneler surface support system/ lander and these mediums can be brought to the tunneler when needed. It should be emphasized that specific heating or cooling pipes can be shut off and the tunneler still operate, provided the other pipes can compensate the heating or cooling. All of the fluids are directed and controlled by valves which are in turn controlled by the tunneler general purpose computers. The heat pipes and coolant pipes are described in more detail in the heat transfer section of this report.

It should also be noted that the electrical systems, such as the general purpose computers, can not be cooled at the 400 - 800 K (720 - 1440 R) used for glass formation and mechanical cooling. A small amount of another coolant, working in a lower temperature range and managed in the same way as the sodium, will need to be provided for electrical and possibly some mechanical cooling. The issue of additional coolant was not addressed here due to the small amount involved and secondary nature of the issue.

Alternatives for Power and Thermal Rejection Systems

Several ideas were considered for the heat source and arrangement of the turbine driving cycle. One possibility considered was to drive the turbine with heat recovered from the glass forming process, hence recycling energy output from the reactor. This idea was questioned, however, as it appeared that the cycle efficiency at the high operating but narrow temperature range would be extremely low (Carnot efficiency of 25 % or less) and not enough energy would be

recoverable. The prospect of reducing the lower temperature of the sodium loop was considered to improve efficiency, (and the temperature was eventually reduced, though to cool other systems). Ultimately it was decided that cycle temperatures were too low or the metals too dense to allow for the use of a metal in a two-phase Rankine cycle, at least while maintaining the metal at a manageable pressure and volume (Gary, 1963). Placing the turbine directly in the lithium power cycle was also considered but this environment would be very hot and corrosive. The use of non-metals, such as ideal gases, was considered as well in the secondary power loop or even a combined secondary and heat rejection loop but they did not offer the advantage of being electro-magnetically pumped. Electro-magnetic pumping was desirable for minimizing moving mechanical systems that could fail.

Power and Heat Rejection System Components

Detailed design of any of the following components is beyond the scope of this report, however, other space based nuclear reactor designs (former USRA projects) were reviewed and some basic ideas borrowed or suggested as possibilities here. To get approximate masses and powers for the entire tunneler system, masses and dimensions of the following components were approximated. In most cases these were either taken directly from components used in the space based reactor designs mentioned, or extrapolated or interpolated from them. Most of the actual numbers are included in the "Tunneler Specifications" at the end of the main body of this report. Some basic observations and component requirements as they apply to the lunar tunneler are included below.

Nuclear Reactor

The power source for the entire tunneler system is a liquid lithium cooled nuclear reactor. The nuclear reactor requires the capability to produce 20 Megawatts of thermal energy. The regolith composition assumed in this study requires 18 Megawatts of thermal energy and the tunneler power systems, essentially 1.0 Megawatt of thermal energy. The tunneler progression rate will be monitored, as well as some type of sensing of the density and makeup of the rock being melted, such that if small variations in total melting heat are required the reactor can compensate. Although there is a time delay in the reactor to allow for the lithium to absorb heat, the lithium flow through the reactor is relatively fast at 60.6 Kg/sec (133.6 lbm/sec) requiring some efficient and rapid heat transfer in the core. The reactor must have a reliable control system with the capability of varying the neutron excitations versus absorptions to control the intensity of the reaction, hence controlling the amount of heat produced. The regolith being melted will not be homogeneous and the need will arise for varying the heat into the rock by varying the heat from the reactor so that other tunneler systems, such as excavation, can keep up. An alternative design noted in the heat transfer section of this report calls for the possibility of vaporizing some or all of the coolant in the reactor core. This would be less efficient for heat transfer in the core but more efficient for heat transfer, via heat of fusion, in the heat pipes. Therefore, a trade study is necessary to determine if a net gain results from vaporizing the coolant in the core.

Reactor Shielding

A sizeable reactor of the 20 Megawatt range, such as the one employed for the lunar tunneler, produces a considerable amount of radiation, primarily in the form of neutrons and gamma rays. Both of these are harmful to man and the amount of shielding required to make the tunneler man rated would most likely be prohibitive both from a mass and volume perspective. The problem is aggravated by the fact that the reactor activates (irradiates) the surrounding tunneler body, the regolith, and the primary coolant and these all would require more shielding of the reactor to make the system man rated (Schmidt,1988).

The modest amount of shielding used here (varying between .4 and 1 meters thick (1.3 and 3.3 ft), and with a mass of 15000 Kg (33075 lbm)) was only for protection of the tunneler electrical components and the regolith. The value is 50% of that similar to that used on other space reactor designs that were man rated at a distance of 300 meters (985 ft) beyond the shield. It is hoped that this will be sufficient for the purposes here of protecting electronics at 5 meters (16.5 ft). Less shielding is provided around the perimeter of the reactor due to volume constraints. It is hoped that the regolith will not remain activated for a long period of time but no study has been made of the issue at this point and will have to be conducted some time in the future. The shielding suggested is that of two layers, with the closer layer made of tungsten to absorb high energy gamma rays and the thicker outer layer being lithium-hydride for a light but efficient neutron shield (University of Washington, 1986).

Pumps

There are a total of four pumps used in the power and thermal rejection systems. Because the mediums in each loop are liquid metals helical rotor electromagnetic pumps are used to move the fluids and increase their pressures. Such pumps require no moving parts and are therefore more reliable than conventional mechanical pumps. The efficiency of electromagnetic pumps is low, however, presently being around .25 to .30. The largest pump used is that in the primary power loop increasing the pressure of and accelerating liquid lithium just prior to its entrance into the nuclear reactor. A large pump of similar size is mounted in the underside of the truck to rapidly pump the sodium coolant into the elevated truck tank. Two additional smaller pumps are used in the secondary and heat rejection cycles to also pressurize and accelerate the respective mediums (Blumberg, 1984).

Heat Exchanger

Two heat exchangers are incorporated into the tunneler system. They are between the primary and secondary loops, and the secondary and heat rejection loops respectively. Both exist to support the secondary cycle, one by adding heat and the other by absorbing heat. Approximately 1.0 Megawatts of thermal energy is continuously transferred across each heat exchanger when it is in use. The design selected for tunneler application was a relatively simple counter flow concentric pipe design. This design was selected for both exchangers because of its use in a similar application for an exchange between lithium and potassium in a space based reactor design (Blumberg, 1984).

Turbine and Generator

One turbine is included in the secondary loop for power generation and is one of the few mechanical systems used with the selenean tunneler. The turbine generates shaft work that is mechanically transferred to the gear box of the propulsion system by an axle. The turbine also mechanically drives a generator producing electricity. The type of turbine required is an axial turbine with its medium being a liquid-vapor mixture of mercury. The amount of electricity required by the tunneler and its auxiliary systems was calculated to be 200 kW (see Appendix B). The amount of power actually supplied by the turbine was 300 kW, with the extra amount for contingency. A suggested blade material would be a titanium or other high operating temperature alloy possibly coated with another corrosion resistant alloy. Sizes and weights for the turbine and generator were both estimated from similar components in other space nuclear power systems (Blumberg, 1984).

An alternative to a mechanical turbine that should be considered in the future is that of a Stirling engine which converts thermal energy to mechanical work in a manner suggestive of a piston, only the Stirling engine is completely contained with no fluids crossing its boundaries. The Stirling engine requires only a hot and cold source, which could readily be provided, and a linear actuator which would produce electricity. These systems are presently in an experimental stage and none have been produced that provide more then a few kilowatts according to sources (Schmidt, 1988).

Radiator

The sodium in the secondary loop enters the radiator at a temperature around 800 degrees Kelvin (1440 R) cools through the heat exchanger/radiator to a temperature of 400 degrees Kelvin (720 R). The radiator is an above ground system, separate from the tunneler, but still a very critical part of the heat rejection cycle described previously. Sodium coolant is exported to the surface by the excavation truck where it is circulated through a radiator emitting thermal energy to space. The radiator is sized to emit about 2.4 Mw in standard continual operation. Several radiator proposals considered by other space nuclear design groups were reviewed for this application with a relatively simplistic option ultimately chosen. The design chosen was similar to that used in a USRA study (Blumberg, 1984) for a space based nuclear reactor, being that of a double fin-tube radiator. The fin-tube radiator has pipes set between two planes or 'fins' of radiative material. Heat is conducted from the pipes into the fins and ultimately into space. This design, though less sophisticated than others, did not require an prohibitive amount of mass or size, at least not in this first order study. The validity of the design could be attributed in part to the use of a liquid metal that has good heat transfer properties and in part to the high operating temperature in which the sodium is passed through the radiator (University of Washington, 1986).

A more advanced option that was rejected but that would warrant further study was the Liquid Drop Radiator proposed by the University of Washington (University of Washington, 1986). The idea involves actually exposing the heat rejection fluid to the vacuum of space by emitting and collecting small droplets of the fluid which fall a distance through the

vacuum. This increases surface area and eliminates secondary less efficient radiator encasement. One limitation of the liquid droplet radiator is that the heat rejection medium must be at a temperature such that its vaporization pressure is less than that of the lunar vacuum. Any type of two phase (liquid-vapor) heat rejection medium would be eliminated by such a criteria. Many other liquid metals would also be eliminated due to the near vacuum at the moon. Also while the mass of such a radiator was very light, the size necessary to allow for the droplets to fall a sufficient distance for heat radiation was comparatively large and such a radiator would not easily lend itself to portability once established (University of Washington, 1986). It should be noted that if such a liquid drop radiator is persued for the selenean tunneler, one working fluid that might withstand the lunar vacuum without boiling off would be molten tin with an extremely low vapor pressure at high temperatures (Gary, 1963).

SUPPORT SYSTEMS

Regolith and Heat Excavation Truck

The task of heat and regolith excavation is a formidable one, but essential to the operation of a regolith boring system. One of the significant limitations on a tunneling device is that advancement rate is limited by the rate at which bored material can be relocated behind the tunneler. This task was initially accomplished by the melting head itself. Once the regolith is molten, it can flow through the tunneler. The excavation problem is not solved at this point however, as the molten regolith must be transported out of the tunnel before solidifying otherwise the tunnel will be refilled and defeat the initial purpose. When melting, an

enormous amount of heat is generated that must be released. Fortunately most of the heat generated in melting stays in the regolith and is excavated with the regolith. It should be mentioned here that ultimately, it would be beneficial to recapture most of the heat in the regolith excavated to the surface.

The Excavation Truck

The actual excavation of the molten regolith and the tunneler liquid sodium coolant is accomplished by a separate vehicle, appropriately named the excavation truck. The basic function of this truck is to transport molten regolith to the surface where it would be dumped, and to transfer 'cool' replacement liquid sodium back to the tunneler. All other truck systems would be to support these ends. The first task in excavation truck design was to size the tanks necessary to carry the regolith and the liquid sodium coolant. From such sizes, a general configuration could be defined. To this end an excavation scenario was assumed, and after an initial study (elaborated on in Appendix M) some critical parameters were defined.

The basic excavation scenario called for the truck to support the tunneler at a penetration of 3 kilometers (9843 ft) without restricting the tunneler's advancement rate due to the turn around-time of the truck. The scenario defined a dumping cycle which began with the excavation truck attached to the tunneler with an empty regolith holding tank and a full tank of 'cool' sodium coolant. Molten regolith would then pour into the truck while simultaneously 'cool' for 'hot' sodium would be exchanged and other necessary functions, such as acquiring power for its excursion, would be performed. The truck would then detach, proceed to the surface, dump the hot regolith, exchange the 'hot'

coolant with 'cool' coolant from the radiator, and return to the tunneler to resume the cycle. A lag-time of about 21 minutes for coupling, dumping and fluid exchange, both on the surface and in the tunnel, was allowed. With the respectable amount of non-travelling time, the exchange rate of the coolant (originally .25 m^3/sec (8.8 ft^3/sec)) was reduced to ease the pumping requirements. Some critical parameters for the truck excavation scenario were defined as follows:

V truck = 4.5 m/sec (14.76 ft/sec)

Regolith dump rate = 0.25 m^3/sec (8.8 ft^3/sec)

Coolant exchange rate = 0.048 m^3/sec (1.69 ft^3/sec)

Dump cycle time = 2591 sec

Volume regolith tank = 11.89 m^3 (419.6 ft^3)

Volume coolant tank = 14.44 m^3 (509.5 ft^3)

It should be noted that the coolant tank was sized to take out the total heat required to be absorbed by the cooling pads and an additional 1.0 % of the amount of heat being generated by the nuclear reactor. The additional heat was estimated to account for heat being radiated from mechanical systems and carried by the sodium coolant not passing through the cooling pads. A volume was found for the amount of coolant required to perform this cooling task for the period of the dump cycle (2591 sec). With these parameters in mind, and using two semicircular tanks for the regolith and the coolant, the truck configuration, shown in a schematic in Figure 10, was developed.

The truck defined in Figure 10, has a coolant tank in the upper portion of the vehicle and the regolith tank shifted forward, and in the lower section of the vehicle. This allows for ease of regolith

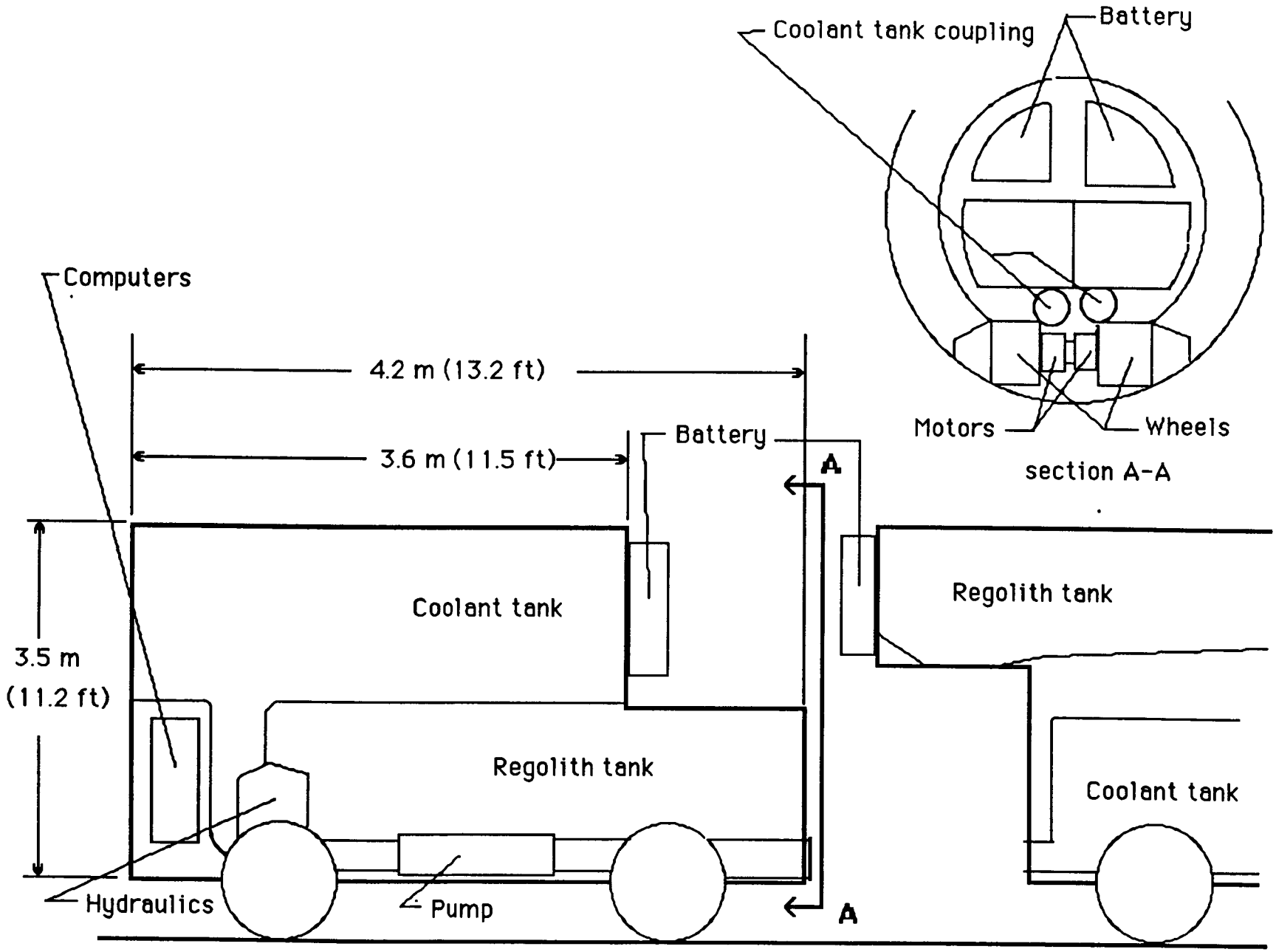

Figure 10.
Excavation Truck

dumping from the tunneler into the excavation truck when the vehicles are mated. The regolith tank is also lined with heating elements to keep the regolith molten in the truck. At the front end of the coolant tank is a battery and battery holder. One battery is always attached to the truck, supplying power while the other battery is attached to the tunneler being recharged. Coolant pipes run along the bottom of the truck, both connecting to the rear portion of the coolant tank. A vertical membrane of a highly insulative material runs the length of the coolant tank. It is not shown in the schematic as it would appear only as a cross section of the tank, but this membrane separates the 'hot' and 'cool' liquids and can move across the tank as the volumes of the two liquids change during exchange. A pump is placed on one line to load coolant while gravity and a pressure differential (it is anticipated though not thoroughly studied) will force coolant out. Four independent motors drive four independent wheels to propel the truck. From the end view in Figure 10, the wheels can be seen to be cylindrical on the inside but tapered on the outside. The flat contact point of the cylinder section allows for surface locomotion while the tapered end allows for travel in the tunnel. Hydraulic actuators are located over the surface facing two wheels to elevate the rear portion of the truck to allow for regolith dumping. Computers and communications equipment for guidance and control of the vehicle are also located on the same end. A mass break down of the truck is included in Appendix C.

The power requirement for the truck is listed in Appendix B but is approximately 10 kW of continuous power. The possible battery for this application would be a lead acid traction battery, a design in use today to power various electric vehicles. Contemporary batteries of this

design can survive 6000 cycles of recharging if the drain is only 20 % of the battery's capacity. To allow for such a long life, the battery sized for the truck is 5 times the size needed to provide the power required for truck operations (Kordesch, 1977).

Excavation Truck Interface

Referring again to Figure 10, the interface between the tunneler and the truck can be understood, as the end of the tunneler is also included in the figure. When the excavation truck attaches to the tunneler, the tunneler regolith buffer tank extends over the excavation truck holding tank. Once secured, the molten regolith pours into the excavation truck due to a slight incline in the tunneler tank floor. The drain of the regolith buffer tank, situated over the excavation truck tank, is crossed by a few heating elements to insure that the regolith is generally in a molten state. The fluids exchange through the pipes at the base of the systems, which are connected upon mating of the vehicles. As alluded to previously, the batteries, attached to the top of both the tunneler and the truck are exchanged during docking to always keep the truck powered.

Tunneler Communication and Guidance

Communication with the tunneler is vital as the vehicle will not be man tended, due to the radioactivity and heat of its operating systems. Communication with the tunneler will be established by very low frequency electro-magnetic (radio) waves. The telemetry will be transmitted though the lunar regolith at a distance of up to at least 3 kilometers between the tunneler and its landing/support station on the surface. This type of communication through dolomite has been

successful at a distance of 120 meters at Los Alamos Laboratory but much work in this technology is still required (Smith, 1971). The landing/support station will maintain radio contact with the tunneler's control point, be it the earth, space station, or elsewhere on the moon.

The control will be little more than observation except in critical situations, as the tunneler will have a degree of artificial intelligence on board. For guidance, a desired path will be programmed into the tunneler and it will follow that path until told otherwise. Changes in any directions will be measured for control by a gyroscopic system internal to the tunneler. Progress will be measured by distance from the lander/support base telemetry source and confirmed with measured wheel rotation provided slip is not very likely or can be detected.

Maintainability

As the tunneler and glass lining will be relatively 'hot' with radiation, maintenance by man is not possible. All repair work to the tunneler and its systems will have to be performed by some type of teleoperated system. To this end some type of access corridor through the tunneler must be provided for access to various tunneler systems. One possibility is to have a teleoperated system already built into the tunneler that could traverse along some type of rail network in the access corridor and that would have one or two 'arms' for minor or even major servicing tasks if so designed. Such a system is consistent with other capabilities sought for lunar activities so its technological development is consistent with other significant lunar activities (Sliwa, et al. , 1988).

Some spare parts, such as pipes, valves, and spare logic boards could be stored on the lander and the excavation truck could have the

capability to bring back whatever part when needed for the teleoperated robot to install. Spare lithium, sodium, mercury and hydraulic fluid will be stored on the lander or in the tunneler because they will leak from the pipes and valves in which they are operating.

Surface Systems

The list of all the surface equipment has not been thoroughly studied but individual systems, some noted previously, have been identified. These include.

(a) A lander/support facility, possibly containing some spare parts.

(b) A radiator for dumping waste heat.

(c) A radio transmitter/receiver for communication, possibly mounted on the lander.

(d) A surface transportation system such as a tow truck, unless the excavation truck could perform such a task if given enough power.

Landing, Set-up, and Modularity

A complete breakdown of all the tunneler system power and masses is included in Appendices B, and C, respectively. The total set-down mass, with a safety factor of 25 %, was found to be about 300000 Kg (661500 lbm). One aggressive lunar scenario development being studied at the Advanced Programs Office at the NASA Johnson Space Center has defined as part of its study a lunar lander with a 25000 Kg (55125 lbm) payload (Alred, 1988). The problem with such a vehicle is that it would require 12 trips to carry the tunneler to the moon. Many of the tunneler systems could be separated or modularized, along with 4 - 5 meter (13.1 - 16.4 ft) section of the tunneler body but the challenge to

reassemble, especially by teleoperated robotics would be a formidable factor of this design. Another option would be that of landing the tunneler on one transfer vehicle that would be uniquely designed for the tunneler mission. This option is demanding also, but perhaps a scaled up version of the 25000 Kg (55125 lbm) lander could be built. The systems and lander would not have to be shipped by one enormous booster all the way from the earth to the moon but could be shipped, in pieces, to the space station. Once there, the systems could be assembled, and then transferred in one flight, already assembled, to the moon. While this is a demanding option, it was assumed for the following possible start up scenario.

(1) Tunneler, lander/support systems touch down on moon.

(2) Thermal double-fin radiator is deployed and set up adjacent to lander.

(3) Lander platform with tunneler extends down at an angle to the lunar surface for the tunneler to start boring.

(4) Lead-acid batteries that will power the truck, power the heat elements around the various lithium, sodium and mercury systems to start the fluid mediums melting.

(5) The tunneler begins boring into ground, initiating excavation when necessary.

(6) As the tunneler approaches the desired depth, it gradually levels off to form a horizontal tunnel, though a gradual lateral curve left or right may be executed over a period of days.

(7) The tunneler digs until shut down.

HEAT TRANSFER

The projected scope and depth of the subselenean melter development program suggests that a sound theoretical basis must be established for the heated cone motion through the melting rock. The development of this theoretical foundation will consist of a heat transfer and fluid flow analysis of melting cones in addition to the development of appropriate numerical analysis methods, including the generation of required computer programs. The ultimate goal will be to apply the results of these theoretical analyses to the performance optimization of a rock-melting tunneler. Under certain initial conditions (e.g. extremely high surface temperatures) or depending upon the properties of the fluid rock melt, contributions from free convection and thermal radiation should be considered. However, as a result of the very high viscosity and opacity of molten rocks free convection and thermal radiation may be ignored. This seems an acceptable methodology to adopt for preliminary study calculations. In a later study, when the dynamics of the problem are being analyzed completely, contributions from these effects could be accurately assessed.

The power source requirements for the subselenean melting head design can be estimated knowing the regolith characteristics. The following initial conditions and properties are used in the calculations. Some of these variables (e.g. specific heat) are functions of temperature, however, only constants could be located. It must also be noted that these characteristics vary from one lunar sample to another. Additionally, values are difficult to obtain since test regolith samples are limited. Hence, the complete validity of these numbers for future in depth analyses should not be assumed.

Latent heat:	$L_f = 483027.08 J/kg$	*Density:*	$\rho = 2600 kg/m^3$
Specific heat:	$c_p = 755.52 J/kg°K$	*Melting Temperature:*	$T_m = 1500°K$
Thermal Diffusivity:	$\alpha = 1.12 \times 10^{-7} m^2/s$	*Initial Temperature:*	$T_i = 250°K$
Thermal Conductivity:	$k = 1.7 W/m°K$	*Maximum Tunnel Length:*	$L = 3000m$

The maximum tunnel length is needed for several reasons, notably for sizing the excavation truck. The maximum tunnel length was set at 3000 m (9843 ft) to account for the possibility of transportation tunnels linking various remote lunar base sites.

The use of an average regolith melting point temperature appreciably higher than its constituent melting points is to account for the additional sensible energy transfer required to super-heat the rock melt adjacent to the cone head surface. Thus, a high thermal gradient is maintained which provides a lower viscosity shear boundary layer. This additional energy consumption is needed to attain the comparatively high advancement rate desired.

The results of the computational analyses are graphed in the Appendix N. Most of the variables in the iterations were coupled, but by holding all but two constant, a two-dimensional relationship could be determined. These relational charts were used to determine the design points. Thus, an insight was gained into the effects of changing any variable.

Heat Pipe Issues

This section will address the theoretical assumptions and calculations that are necessary for an acceptable modeling of the heat flow behavior at the melter head location. As previously stated, since convection and radiation are assumed negligible, conduction is the only process that is considered.

The tunneler speed must be determined before any further calculations are performed. The effect of ground or rock type on advance rate is illustrated in Figure 11. This figure is based on data from existing earth tunnelers. The common igneous rocks, which are especially difficult to penetrate mechanically, become, in general, fluid at temperatures between ~1370°K and ~1470°K (2470°R and 2650°R).

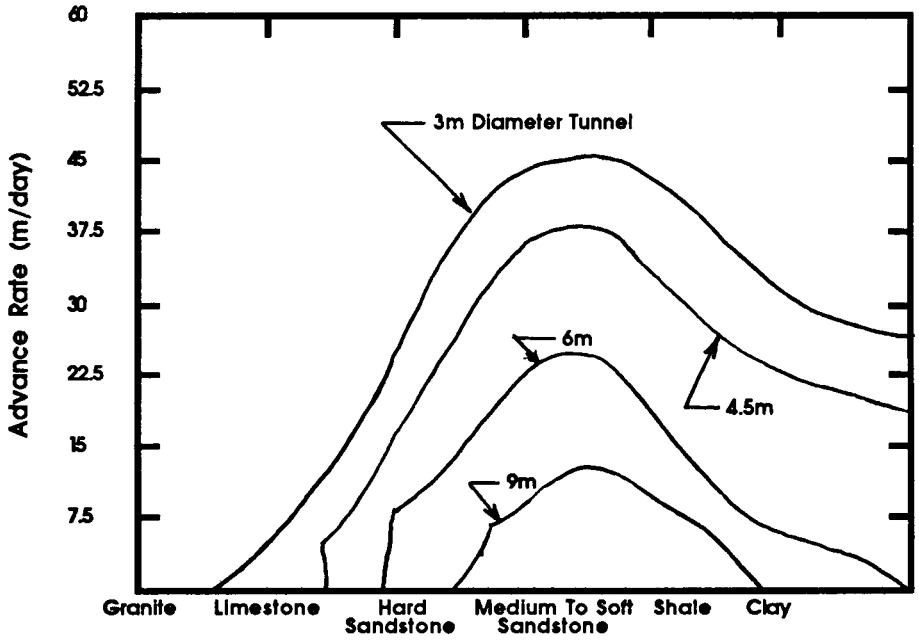

Figure 11.
Effect of Ground Rock Type on Tunneler Advance Rate

From the previous figure, it can be seen that for hard to medium sandstone (close to the consistency of regolith) an advancement rate of 25 m/day (82 ft/day) for a tunneler radius of 4.5 m (14.76 ft) is achievable. Tunneler speed is of preliminary importance when determining the other characteristics of the heat pipe (e.g. mass flow rate). Once the tunneler speed is known, a mass balance can be performed to yield the capacity of the rear regolith reservoir. Through calculations this was determined to be 13.1 m^3 (463 ft^3).

Energy transfer from the reactor to a melting cone head at the rates and densities required appears feasible by means of liquid heat pipes. Refractory metals, with their high melting points, are available for the development of the required rock melting structures. When designing this structure, a good insulator material must be chosen so that heat transfer between different segments of the structure are suppressed. The proposed excavation method, which is relatively insensitive to variations in rock formation, produces a liquid melt whose behavior can be predicted by the laws of fluid dynamics. The basic rock heat transfer and melting processes are relatively well-defined and close to theoretical analyses and predictions.

The selection of the penetration mode is automatic depending on the characteristics of the constituents (controlled by sensing devices, computer routines and an integrated valve system). Taking the extreme case (first excavation mode) where melting and near complete consolidation takes place, the density of the chilled glassy liner is much greater than the in-situ rock. In this condition the mass of the excavated regolith is almost the same as that of the glassy tunnel lining. Thus, the volume of the regolith taken out approaches zero. But usually the

densities of both are relatively the same, so in this second mode almost all the excavated regolith must be taken out. The liquid regolith (lava) is transferred from the inlet nose cone openings by direct heated pipes to a rear holding tank. The design is such that it maintains the lava in a liquid state for transport and utilization purposes, so any heat energy dissipated through the removal process is restored by the heated pipes.

As a result of the high surface temperature of a melting penetrator cone and the low thermal conductivity of the regolith, the rock structure preceding the cone will be disintegrated by thermal stress fracturing. The individual segments forming the melter head could be provided with separate thermal control so that differential melting for guidance and alignment purposes can be achieved.

Heat pipe technology is now sufficiently advanced that it appears evident that the pipe can indeed transport energy from a compact source to an extended melting penetrator while progressing at a relatively high rate. Development work on systems that would optimize the energy transfer from a nuclear power source to a melting penetrator cone has led to the utilization of specialized heat pipes. One heat pipe under consideration is a cylindrical gas-tight tube that contains liquid lithium and its vapor (this system was developed by a Los Alamos Scientific Laboratory team). The liquid-metal heat pipe and its basic components are illustrated in Figure 12. For subselenean applications, the evaporator end of the heat pipe is embedded within the liquid lithium from the nuclear heat source, and the condenser section would be adjacent to the rock-melting surface. An inert gas reservoir should be placed between the condenser section and the actual cone head surface so as to maximize heat transfer. The cylindrical cavity is lined with

a wick, i.e. a capillary structure normally consisting of multiple layers of woven-wire screen. The liquid within this wire matrix is heated and evaporated by the evaporator section of the heat pipe. The continuously forming vapor fills the interior of the heat pipe and flows toward the slightly cooler condenser end. At the condenser, it rejects its latent heat of vaporization and returns to the evaporator section as a liquid by capillary action through the wick matrix. The unique advantage of the heat pipe is its ability to maintain extremely high heat fluxes with only small temperature differences between the evaporator and the condenser sections (because as previously stated, the thermal

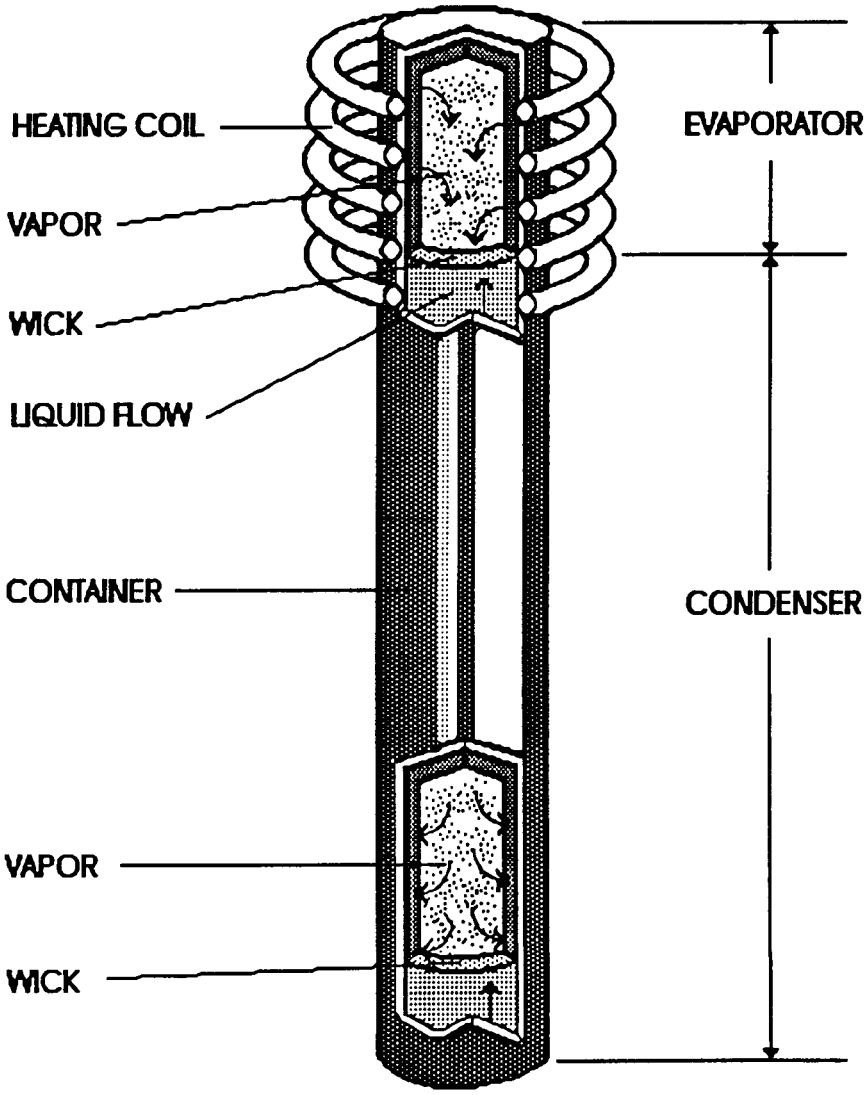

Figure 12.
Components of a Liquid Metal Heat Pipe

exchange involves the latent heat of vaporization rather than a sensible temperature difference). A heat pipe of this design should be able to transmit in excess of 10 MW/m^2 ($3.17x10^6$ $Btu/hr\ ft^2$) which far exceeds this study's requirements.

The second option for the heat pipes is considerably more simplistic. The basic requirement of the pipe structure is to allow the heat to be transmitted from the lithium to the regolith. This is accomplished without using a phase change, only a temperature differential. The lithium exiting the reactor at 1650°K (2970°R) will be reduced to 1500°K (2700°R) so that the required heat energy can be released. This may be less efficient than option one, but has the advantage that in the reactor no vaporization occurs. For design considerations and calculations, this second option was modeled. Since subselenean applications require extremely high temperatures 1650°K-1500°K (2970°R-2700°R), the heat pipe shells should be constructed of refractory metals.

From theoretical foundations, a concise but accurate procedure must be developed so that the thermal energy requirements of the heat pipes for total melt can be calculated. If the system is modeled as a semi-infinite solid, an analytical solution may be obtained. Since such a solid extends to infinity in all but one direction, it is characterized by a single identifiable surface (see Figure 13). If a sudden change of conditions is imposed at this surface, transient, one-dimensional conduction will occur within the solid. The heat equation for transient conduction in a semi-infinite solid is given by equation 1,

$$\partial^2 T/\partial x^2 = 1/\alpha(\partial T/\partial t) \qquad (1)$$

where α is the thermal diffusivity, and t is time. The initial condition is prescribed by equation 2,

$$T(x,0) = T_i \qquad (2)$$

and the interior boundary condition is of the form,

$$T(\infty,t) = T_i \qquad (3)$$

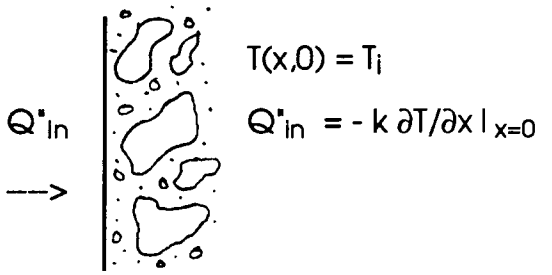

Figure 13.
Constant Surface Heat Flux

where k is the thermal conductivity. Figure 13 depicts the surface conditions present along with the governing equation and boundary conditions. Closed form solutions have been obtained for the above case, instantaneously applied at t=0. The solution to the equation is,

$$T(x,t)-T_i = 2Q''_{in}(\alpha t/\pi)^{1/2}/k \exp(-x^2/4\alpha t) \qquad (4)$$

Equation 4 is used to solve for t with x=0 and $T(x,t)=T_m$. This t , renamed t_{init}, will be the initial set-up time (the time from when the melter head is placed on the regolith to the time when melt conditions are occurring at the boundary). Solving for t_{init},

$$t_{init} = \pi(k(T_m-T_i)/(2\alpha Q''_{in}))^2 \qquad (5)$$

From the analyses an acceptable t_{init} was determined to be 23 seconds. Now, suppose that the solid is heated by a constant flux Q''_{in} at its surface, with any melted material being continuously removed. Note that the plane at which melting takes place is constantly referenced as x=0, and the solid in the region x>0 is being regarded as moving towards it with speed U (tunneler speed). Then, if T_m is the melting temperature and T_i is the initial regolith temperature, the temperature T(x) in x>0 is the solution to the conduction equation (note, T tends to T_m as x->0, and to T_i as x->∞). That is,

$$T(x) = T_i+(T_m-T_i)e^{-Ux/k} \qquad (6)$$

Using this value of T(x), it follows that the rate of heat from outside must be equal to its rate of heat removal with the melt, or,

$$Q''_{in} = (L_f + c_p(T_m-T_i))\rho U \qquad (7)$$

(note ρ is density, c_p is specific heat and L_f is latent heat of fusion).
From the analyses the required Q''_{in} was determined to be 1.18 MW/m^2 ($3.74x10^5$ Btu/hr ft^2).

A certain mass flow rate is required to transmit this heat energy from the heat pipes to the regolith (see the Appendix K).

$$\dot{m} = 9.4436x10^{-5}Q''_{in}D^2/(\int c_p dT) \qquad (8)$$

where D is tunnel diameter, and T is temperature. In order for the above equation to be applied, specific heat needs to be obtained as a function of T. Lithium was selected as the reactor/heat pipe solution since it provides the necessary characteristics. Experimental data points for the temperature of lithium versus its specific heat were curve fitted using a fifth order polynomial. This function can now be integrated to determine a value for mass flow. The lithium exiting the reactor is at the initial temperature 1650°K (2970°R), and the lithium in the heat pipe at the melter head end (after thermal energy has been dissipated) is at 1500°K (2700°R). These two temperatures are therefore the limits of integration. The lithium cannot be reduced any further because the correct sign on the heat flux needs to be maintained. This also creates a substantial benefit since it enables the preceding turbine to have a large temperature drop to obtain necessary mechanical work. After the lithium leaves the turbine it once again reenters the reactor creating a closed loop system. The mass flow rate for the heat pipes through iteration was determined to be 61 kg/s (134.2lb/s).

Coolant Pipe Issues

The rock melt can be chilled to a glass and formed into a dense, strong, firmly attached tunneler lining. Thus, the melting penetrator can produce permanently self-supporting tunnels even in unconsolidated sediments. A glass forming section conditions this molten rock into a smooth, continuous glass lining. Separate thermal control and access for servicing will again be provided. The process for the cooling will utilize the opposite of the heat pipe design (seen in the previous section).

The time-temperature-transformation (TTT) curve describes the locus of times required to reach the given fraction crystallized on isothermal treatment at various temperatures. The transformation temperature effects the fineness of the structure, the time required for transformation, and even the arrangement of the two phases (crystalline and non-crystalline). This occurs because the cooling rate determines the amount and distances of diffusion that can take place. Consequently, this diagram permits the prediction of the structure, properties and cooling treatment required for optimal SiO_2 ceramics. It is beneficial to achieve as much non-crystalline structure as possible (i.e it is desirable to force this part of the structure to be the matrix material). Now, if some small non-continuous hard brittle crystalline particles (i.e. precipitate) can be dispersed in this matrix, dispersion strengthening is achieved. When cracks are initiated, they first form in the discontinuous brittle precipitate and are soon arrested by the precipitate-matrix interface. This procedure will optimize the ultimate strength of the glass lining. As previously stated, the method of achieving this is obtained by choosing the correct cooling rate from the TTT curve. The optimum cooling rate from previously tabulated TTT curves indicates that a

judicious 1°K/s should be adopted for the average lunar sample tested. Deviations from this can be accommodated by adjusting the mass flow rate in the cooling pipes. This can be accomplished by an automated closed loop/feed back sensing device that is integrated with a valve system network.

The thickness of the wall lining should be about 2% of the tunnel diameter for acceptable tolerances and safety. Therefore, a value of 0.09 m (0.30 ft) was chosen. From the analysis, the coolant pad length that will facilitate this desired cooling rate is 0.2 m (0.66 ft). This analysis was conducted assuming a continuous mass flow rate in the coolant pipes. The direct dependence between cooling pad length and coolant mass flow rate can be eliminated if this mass rate is staggered (i.e. sending impulse waves). On a side note, a good ceramic insulator between the cooling pad and the melter head is recommended so that heat conduction through the tunneler structure does not interfere with the process.

The amount of heat flux that must be removed is dependent on the latent heat of fusion, the mass of the glass lining required per unit time and the final temperature of the glass lining. In Appendix L, the heat flux equation derived is,

$$Q''_{out} = (2r\Delta y+\Delta y^2)\rho U(c_p\Delta T+L_f)/(2r\Delta x) \qquad (9)$$

(note ρ is density, c_p is specific heat, Δy is lining thickness, Δx is cooling pad length and L_f is latent heat of fusion). Through iteration the optimal value of 384 kW/m^2 (1.22x10^5 Btu/hr ft^2) was chosen for Q''_{out}.

A certain mass flow rate is required to extract the heat energy from the melted regolith to the coolant pipes so that the desired solidification will occur (see the Appendix L). This mass rate obeys the following equation:

$$\dot{m} = Q''_{out}\pi D\Delta x/(4183.8515\int c_p dT) \quad (10)$$

where D is tunnel diameter, and T is temperature. Next, specific heat must be obtained as a function of T for the selected coolant. Through investigation it was determined that sodium provides the best characteristics for the design's cooling system. Experimental data points for sodium that relate temperature and specific heat were curve-fitted using a fifth order polynomial (see the curve fitted function in Appendix N). This function can now be integrated to determine a value for mass flow. The limits of integration are from 600°K (1080°R) (initial temperature) to 800°K (1440°R) (final temperature). This range of temperatures is the best operating range for sodium. The only disadvantage is that the wall lining can be cooled to only 800°K. No effective coolants are known to have all the desired prerequisite properties and yet operate near 250°K (the temperature at which the wall lining would equal the surrounding regolith , with time the wall will naturally cool back to 250°K). The coolant will be in a closed loop system; after it leaves the coolant pad pipes it reenters the coolant holding tank with the "other" coolant. This coolant is then taken to the surface by the excavation truck, cooled to 600°K (1080°R) and brought back for subsequent use. There will be multiple units of cooling fluid supply so as to provide for continuous operation.

Through assessments, the mass flow rate of the wall coolant yielded an optimal value of 3.8 kg/s (8.4 lb/s).

"Other" coolant is necessary for cooling of the reactor as well as other systems like the turbines. A judicious estimate was needed for the amount of cooling required here. A conservative value of 1% of the melting heat energy was assumed for this portion. Additionally a surface area was needed such that a mass flow rate through which these "other" coolant pipes act could be approximated. Again, after some analysis an acceptable area of 30 m^2 (323 ft^2) was used. The value for this mass flow rate was determined to be 0.4 kg/s (0.9 lb/s). Once both these mass flow rates are known, a mass balance can be performed to yield the capacity of the rear coolant reservoir. This was calculated to be 14.4m^3 (508.6 ft^3).

SUBSELENEAN BASE SCENARIO

To show how a subselenean base might be established with a melting head tunneler, a brief scenario is given here.

Establishment of a lunar base could be performed with a precursor landing of the tunneler. The tunneler would bore itself into the lunar subsurface to a depth of 20 meters (65 feet) and then level out. Once it has leveled out, the tunneler would then follow a preprogramed path creating tunnel space for the lunar base which would be safe for later occupation. Along with the tunneler is an excavation truck working to remove the regolith. Once the path pattern was completed the tunneler would resurface at another location and be relocated to another site to begin the process over. Once a site had been tunneled the initial base hardware and personnel could arrive to begin set up. With the bases hardware moved into the tunnels and the airlocks installed the tunnels could then be pressurized and the base interiors installed in a shirt sleeve environment. With the establishment phase complete the base can now go into its regular operations phase.

Regular operations imply scientific investigation and mining. By excavating large chambers, using well established techniques, abundant space can be obtained for a processing plant and for agricultural purposes. Should such large spaces be needed for immediate use then location of the base could be situated adjacent to a lava tube, accessing it with the tunneler. Once mining and agricultural facilities are in place the base should become economically self-sufficient.

TUNNELER RESEARCH AND DEVELOPMENT

In the conceptual design of the melting head tunneler for lunar application certain areas were identified where further research and development are needed. Two key areas are power generation and materials. The design of the tunneler relies on a liquid metal nuclear reactor to produce 20 MWth, uses a high coolant flow rate, and operates at a temperature of 1500° K (2700° R). Such a reactor is not currently available, although it appears one could be developed. Thus, further research and development in this area is needed. The biggest difficulty for the system, including the development of the nuclear reactor, is that special materials, namely refractory metals, are needed for the system due to the high operating temperatures. This problem, and better definition of the operating parameters for the materials, needs further investigation. Initial investigation appears to indicate that there are materials available for such application and that materials limitation does not pose a prohibitive problem to development of the tunneler. However, this possibility has not been excluded as such.

Areas where development would help facilitate the implementation of a subselenean tunneler system are robotics, artificial intelligence, and communication transmission through regolith. Robots, or tele-operated devices, would be of benefit for maintenance purposes, due to the radiation from the nuclear generator, while artificial intelligence would greatly improve on the autonomy of the system. In order to monitor, communicate, and control the tunneler system a means of transmitting information to and from the tunneler while operating below the lunar surface is needed.

For further development of this concept, two areas where more complete information is needed is (1.) on the subselenean composition and its properties, and (2.) how it may become radiated from the radiation output of the nuclear generator. Information on the subselenean environment will allow design of the tunneler for optimal performance for the densities it will encounter, melting temperatures and other appropriate factors yet to be recognized. Radiation of regolith needs to be understood so that necessary measures can be implemented to prevent radiating the tunnels.

Further design work for the melting head tunneler would enable better weight and size estimates. Effort in the areas of material selection, structural design and configuration refinement would be of particularly value. Refinement of the power generator parameters followed by a design effort for a generator to meet these needs should also be performed.

If the above areas for further research and development are pursued then a tunneling device for subselenean application should be available within the time frame currently being forecast for when a lunar base program may be pursued.

CONCLUSION

The placement of base facilities in subsurface tunnels created as a result of subsurface mining was proposed as an alternative to the establishment of a base on the lunar surface. Placement of the base facilities and operations in subselenean tunnels will allow personnel to live and work free from the problems of radiation and temperature variations. A conceptual design for a tunneling device applicable to such a lunar base application was performed to assess the feasibility of the concept. Designed was a tunneler which would melt through the lunar material, at an advancement rate of 25 m/day (81 ft/day), leaving behind glass-lined tunnels for later development. The tunneler uses a 20 MWth nuclear generator to supply the heat flux necessary to melt the regolith about its cone shaped head. Melted regolith is excavated through intakes in the head and transferred to a truck which hauls it to the surface. The tunnel walls are solidified to provide support lining by using an active cooling system about the mid section of the tunneler. Results of the conceptual design analysis indicate that the concept is viable given further research and development in a few key areas, namely nuclear power production and high temperature tolerant materials. The benefits resulting from locating a lunar base in subselenean tunnels merit the concept and tunneling technology receiving further investigation in the future.

REFERENCES

Alred, John, conversation with John Alred, NASA Johnson Space Center, March 1988.

Askeland, D.R., The Science and Engineering of Materials, PWS Engineering, Boston, Massachusetts, 1984.

Blumberg, Marc et. al., USSR-1, A Liquid-Metal Cooled Fast Space Reactor, report for nuclear engineering design project, Texas A & M University, April 1984.

Carslaw, H.S., et. al., Conduction of Heat in Solids, Oxford at the Clarendon Press, Second Edition.

Dehart, Mark et. al., SNAFU - Space Nuclear Advanced Fuel Unit, report for nuclear engineering design project, Texas A & M University, 1984.

Faires, Virgil Moring and Simmang, Clifford Max, Thermodynamics, 6th edition, MacMillan Publishing Co.,Inc. New York, 1978.

Gary, Robert ed., and Nesmeyanov, A. N., Vapor Pressure of the Chemical Elements, Elsevier Publishing Company, New York, 1 1963.

Hanold, R.J., Large Subterrene Rock-Melting Tunnel Excavation Systems, Los Alamos Scientific Laboratory of the University of California, Los Alamos, New Mexico, February 1973.

Incropera, F.P., et. al., Fundamentals of Heat and Mass Transfer, John Wiley & Sons, New York.

Kordesch, Karl V. ed., Batteries, vol 2, Lead-Acid Batteries and Electric Vehicles, Marcel Dekker, Inc., New York, 1977.

Moses Jr, W.M., Conversations with Dr. Moses, Mechanical Engineering Department, Texas A&M University, February 1988.

Multimegawatt Nuclear Power System for Lunar Base Application, Spacecraft Systems Design, NASA - University Pilot Program, Department of Aeronautics and Astronautics, University of Washington, Seattle Washington, June, 1986.

Perera, J.S., Curve-fitting Basic Routine, Eagle Engineering, Inc., Houston, Texas, 1986

Schmidt, Paul, conversations with Paul Schmidt, graduate Nuclear Engineering student at Texas A & M University, April 1988.

Simonds, C., Conversations with Chuck Simonds, Eagle Engineering, Inc., Houston, Texas, February 1988

Sliwa, Nancy et. al., Automation and Robotics Considerations for a Lunar Base, Lunar Bases and Space Activities in the 21st Century Conference, April 1988. LBS-88-184

Smith, M.C. ed., A Preliminary Study of the Nuclear Subterrene, LosAlamos Scientific Laboratory of the University of California, Los Alamos, New Mexico, April 1971.

Uhlmann, D.R. et. al., "Simplified model evaluation of cooling rates for glass-containing lunar compositions." Proceedings of the Twelfth Lunar And Planetary Science Conference. LPI, Houston, Texas, March 1981.

SUBSELENEAN TUNNELER SPECIFICATIONS

(FOR EXCAVATION UTILIZING THE ROCK MELTING TECHNIQUE)

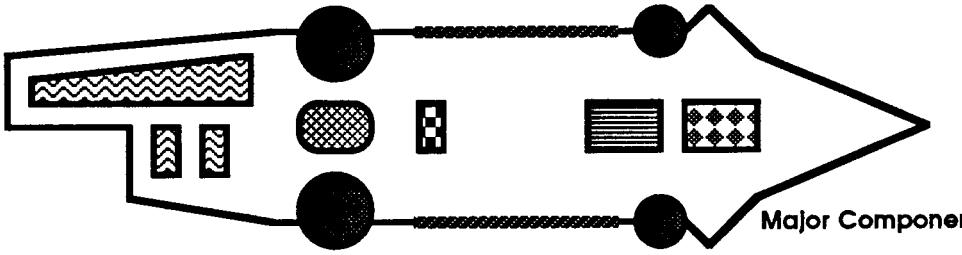

Major Components of Tunneler

Nuclear Reactor

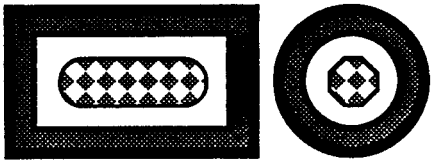

Sources: Snafu, 1986
USSR - 1, 1984

Power Output - 20 MWth
Working Fluid - lithium
Operating Temperature - 1650K
Mass Flow Rate - 60.6 kg/s
Mass - 8800 kg
Geometry - Cylindrical
Radius - 1m
Length - 2m
Shielding Material - W and LiH
Mass of Shielding Material - 15100 kg
*Control Druims for neutron absorption

Head

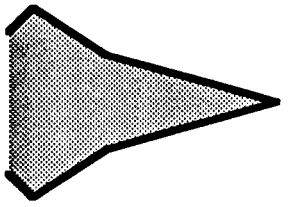

Geometry - Bi-Conic
Length - 6.5 m
Base Radius - 2.25 m
Half angle1 - 12.5°
Half angle2 - 30°
Thickness - 0.08 m ~ 3 in.
Material Composition - Mo50%-V50%
Shell Volume - 1.9 m^3
Total Volume - 23 m^3
Mass - 15500 kg
Weight on Earth - 1.5 (10^5) N ~ 34000 lbf

Propulsion System

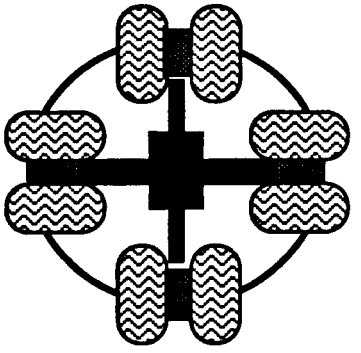

Power Requirement (Hydraulics) - 80 kW
Power Requirement (Gearing Subsystem) - 1kW
Spring Coefficient (Hard Spring Subsystem) - 1MN·m
Total Weight on Earth - 13350 N
Number of Wheels (Driver) - 8
Number of Wheels (Stabilizer) - 8
Wheel Radius (Driver) 0.5 m
Wheel Thickness - 1 m
Max. Pressure of Hydraulic Actuator - 7 MPa
Fluid Level in Hydraulic Actuator - 1 m
Fluid Level Variation - 0.38 m

Turbine

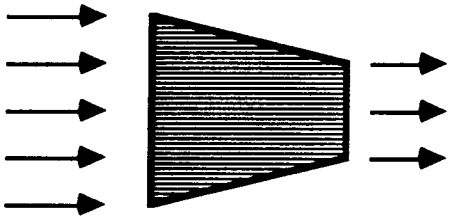

Type - Axial
Working Fluid - mercury
Inlet Temperature - 650K
Inlet Pressure - 0.46 bar
Exit Temperature - 400K
Exit Pressure - 0.005 bar
Work Output - 300 kJ
Mass - 600 kg
Average Diameter - 1m
Length - 2 m

Source: USSR - 1, 1984

Pumps

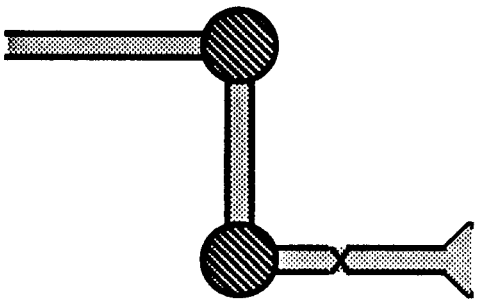

Source: USSR - 1, 1984

Lithium Pump (Large)

Number of Pumps - 1
Type - electro-magnetic coil
Mass - 2500 kg
Dimensions - 3.2 x 1.2 x 0.5 m

Sodium Pump (Large)

Number of Pumps - 1
Type - electro-magnetic coil
Mass - 2500 kg
Dimensions - 3.2 x 1.2 x 0.5 m

Sodium Pump (Small)

Number of Pumps - 3
Type - electro-magnetic coils
Mass - 200 kg (each)
Dimensions - 0.7 x 0.4 x 0.25 m

Tunneler Body (Shell)

Length - 15.7 m
Forward Diameter - 3.74 m
Aft Diameter - 3.2 m
Taper Angle - 1°
Volume - 150 m^3
Assumed Mass -100,000 kg
(Including internal structures)

Lining System

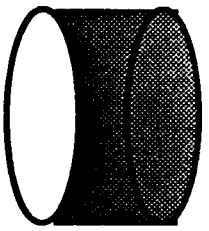

Cooling Pad

Length - 0.2 m
Width - 4.5 m
Volume - 0.15 m^3
Mass - 800 kg

Insulator Pad

Length - 0.5 m (x2)
Width - 4.5 m (x2)
Volume - 0.7 m^3 (x2)
Mass - 1000 kg

Radiator

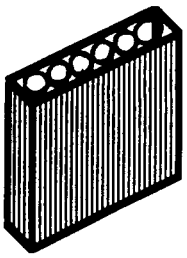

Configuration - double-fin pipes
Mass - 4000 kg
Dimensions - 4 x 15 m (deployed)
Working Fluid - sodium
Mass Flow Rate - 4.22 kg/s

Top View

Source: USSR - 1, 1984

Heat Exchanger

Configuration - series of pipes
Mass - 100 kg
Dimensions - 0.5 x 0.16 x 0.16 m

Source: USSR - 1, 1984

Generator

Mass - 2000 kg
Dimensions - 0.81dia x 1.24 m

Source: USSR - 1, 1984

APPENDICES

APPENDIX A: CALCULATIONS FOR T-S DIAGRAMS (Faires, 1978)

T - S Calculation for Primary Power Cycle (Figure 8)

m_{rate}=60600g/sec c_p=2.0667j/g-K

State - 1 , T_1= 1482 K Given Conditions set for cold side of operations
P_1= 1.76 bar Given almost 2 earth atm to prevent vapor lithium

State - 2 , T_2= 1650 K target maximum temperature of cycle
P_2= 1.59 bar 90 % of P_1 to account for system losses

State - 3 , T_3= 1500 K melting point of regolith assumed in this study
P_3= 1.43 bar 90 % of P_3 to account for system losses

State - 4 , T_4= 1482 K low point (actualy slightly less than 1482 K)
P_4= 1.43 bar about the same as state 3

$Q_{in} = mc_p (T_1 - T_2) = (60600g)(2.0667J/g\text{-}K)(1482\ k - 1650\ K) = 19.788$ Mj

$Q_{out\ reg} = mc_p(T_2 - T_3) = (60600g)(2.0667j/g\text{-}K)(1650\ k - 1500\ K) = 18.787$ Mj

$Q_{out\ 2nd} = mc_p(T_3 - T_4) = (60600g)(2.0667j/g\text{-}K)(1500\ K - 1492\ K) = 1.002$ Mj

W_p= scaled from other electro-magneto pumps = 50.0 Kj

T - S Calcuclations for Secondary Power Cycle (Figure 9)

m_{rate}= 2857g/sec c_p=.1256 j/g -K

For Carnot efficiency $e_c = 1 - T_{low}/T_{high} = .38$, It was decided to expand mercury across a turbine dropping from 650 K to 400 K. Enthalpies were optained for these values (and an initial pressure of 1/2 earth atm) from a mercury 'steam' table. The energy sought from the turbine was 300 Kj so a mass flow rate could be determined as follows.

H_1 = 24.5 Kj/Kg H_2 = 344 Kj/Kg

$W_T = H_2 - H_1 = 344 - 24.5 = 105$ Kj/Kg per unit mass

m_{rate} = Power $_{req}/W_T$ = (300 Kj/Kg-s)/(105 Kj/Kg) = 2857 g/sec

State -1, $T_1 = 400$ K $H_1 = 24.5$ Kj/Kg
$P_1 = .51$ bar

State - 2, $T_2 = 650$ K $H_2 = 344.0$ Kj/Kg
$P_2 = .46$ bar

State - 3, $T_3 = 400$ K $H_3 = 239$ Kj/Kg
$P_3 = .005$ bar

State - 4, $T_4 = 400$ K $H_4 = 20.8$ Kj/Kg
$P_4 = .01$ bar

$$Q_{in} = (H_1 - H_2)m = (24.5 - 344.0)(2857\ g) = 912.8\ Kj$$

$$W_T = (H_2 - H_3)m = (344 - 239)(2857g) = 300\ Kj$$

$$Q_{out} = (H_3 - H_4)m = (239 - 24.3)(2857g) = 613.4\ Kj$$

$$W_p = 5.0\ Kj$$

T-S Calculations for the Heat Rejection Cycle

As this cycle is very similar to the Primary Power Cycle, the actual heat and work calculations will be omitted, and just the results listed. It should be remembered that the sodium is flowing through two different systems in this cycle.

$m_{rate\ total} = 4.22$ Kg/sec $C_p = 1.42$ j/g-K

For the mechanical systems cooling;

$m_{rate} = 0.4$ Kg/sec

State -1 $T_1 = 400$ K
$P_1 = 1.01$ bar

State - 2 $T_2 = 800$ K
$P_2 = .91$ bar

State -3 $T_3 = 400$ K
$P_4 = .82$ bar

$Q_{in} = 187.8$ Kj $Q_{out} = 187.8$ Kj

pump work is mentioned below.

For cooling the secondary cycle and the regolith

m_{rate} = 3.82 Kg/sec

State -1 T_1 = 400 K
P_1 = 1.01 bar

State - 2 T_2 = 600 K
P_2 = .96 bar
(state - 2 is at the entrance to the cooling pads)

State -3 T_3 = 800 K
P_3 = .91 bar

State - 4 T_4 = 400 K
P_4 = .82 bar
(state - 4 is at the entrance to the pump)

Q_{in} = 1.7 Mj Q_{out} = 1.7 Mj W_p = 5.0 Kj

APPENDIX B: POWER BREAKDOWN

COMPONENTS		POWER, or ENERGY
Truck		
regolith heating in tank		15.0 kW
propulsion		1.5 kW
hydraulics	(20 kW pk)	0.15 kW
pump	(60 kW pk)	10.0 kW ave
computers, and other systems		1.0 kW
		27.65 kW
Body		
lithium pump		50.0 kW
mercury pump		5.0 kW
sodium pump		5.0 kW
proppulsion system		20.0 kW
regolith heating tank		15.0 kW
heating regolith pipng networks		60.0 kW
electronics/computers		5.0 kW
radio system and gyroscope		5.0 kW
		165.0 kW
truck	+	27.65 kW
		192.65 kW
approximately	=	200.0 kW
plus safety factor (allow for losses)	+	100.0 kW
		300.0 kW - target output

APPENDIX C: CALCULATION OF VEHICLE MASS

Mass Breakdown

COMPONENTS	MASS - KG	(lbm)
Truck		
battery	5000.0	(11025)
wheels (4)	400.0	(880)
motors (2)	400.0	(880)
pump large	2500.0	(5510)
body	25000.0	(55125)
computers	1000.0	(2200)
	34300.0	(75630)
Body		
melting cone	15400.0	(33960)
heating & cooling pipes	3500.0	(7720)
propulsion system	1000.0	(2200)
nuclear reactor	8800.0	(19400)
shielding	15100.0	(33300)
liquid lithium	7300.0	(16100)
liquid sodium	38300.0	(84450)
liquid mercury	300.0	(660)
pump large	2500.0	(5510)
pumps small (2)	400.0	(880)
turbine	600.0	(1320)
generator	2000.0	(4410)
radiator	4000.0	(8820)
heat exchanger	200.0	(440)
battery	5000.0	(11025)
body & support structure	100000.0	(220500)
computers	3000.0	(6620)
	207400.0	(457320)
+ truck mass +	34300.0	(75630)
	241700.0	(532950)
+ safety factor 25 % +	60400.0	(133240)
TOTAL MASS =	302100.0	(666190)

APPENDIX D: AN ANALYSIS OF PRESSURE DISTRIBUTION ALONG THE HEAD (w/o Excavation)

The following analysis was developed by members of the Los Alamos scientific laboratory located at Los Alamos, New Mexico and was extracted from *A Preliminary Study of the Nuclear Subterrene*, 1971.

It is convenient to consider that the penetrator stands still and the rock moves toward it, so that the problem becomes one of hydrodynamic flow around a hot barrier. Velocity of the rock far from the penetrator is v^*. Rock temperature decreases exponentially with distance, z, from the drill face, as exp $(-c\rho v^* z/\lambda)$. For a typical basalt, λ = 0.01 cal/cm•sec•°C, c = 0.3 cal/g•°C, ρ = 2.8 g/cm^3, v^* = 0.05 cm/sec, and the characteristic decay distance of temperature , $\gamma/c\rho v^*$, is ~ 0.3cm. Rock viscosity varies with temperature as exp (E/RT) so that, for E = 140 kcal/mole and T_1 = 1700°K, the characteristic decay distance for viscosity, E/RT, is about 1/40 of that for temperature, or about 0.01 cm. Within 0.3 cm of the penetrator face, then, rock viscosity increases by many orders of magnitude. Flow of the molten rock therefore occurs within a very thin, film-like channel along the face of the penetrator.

The hydrodynamic problem is well represented by regarding the viscosity to vary as

$$\eta = \eta_o e^{\beta z}$$

where η_o is viscosity at the penetrator face (z = 0) and

$$\beta = \frac{E}{RT_1} \quad \frac{(T_1 - T_o)}{T_1} \quad \frac{c\rho v^*}{\lambda}$$

The Navier-Stokes equation for incompressible materials is represented in cylindrical coordinates by

$$\frac{2}{r}\frac{\partial}{\partial r}\left(r\eta\frac{\partial u}{\partial r}\right) - 2\lambda\frac{u}{r^2} + \frac{\partial}{\partial z}\lambda\left(\frac{\partial u}{\partial z} + \frac{\partial v}{\partial r}\right) = \frac{\partial p}{\partial r}$$

$$\frac{1}{\partial r}\frac{\partial}{\partial r}\left(r\eta\left(\frac{\partial u}{\partial z} + \frac{\partial v}{\partial r}\right)\right) + 2\frac{\partial}{\partial z}\eta\frac{\partial v}{\partial z} = \frac{\partial p}{\partial z}$$

Together with the equation of continuity, this system was solved exactly (in Armstrong *et al.*, 1965) with the assumption that v = v(z), yielding the solution

$$v = -v^*\left(1 - e^{-\beta z}(\beta z + 1)\right)$$

$$u = \beta^2 v^* z\, e^{-\beta z}(r^2 - a^2/2r)$$

$$p = -\eta_o v^* \beta^3 (z^2/2 + z/\beta + r^2/4 - a^2/2 \ln r) + \text{const.}$$

A result of this development is an expression for the total applied force, in which the force is proportional to $\eta_o v^* \beta^3$. Furthermore, since β is itself proportional to v^*, the force increases as the fourth power of the velocity, unless the penetrator temperature is raised to decrease η_o. Hence, the final conclusion of the early theory was that, as higher penetration rates were sought, the device should be constructed to apply very large pressures to the rock, thus requiring strong, rugged construction.

Much of the above development can be adapted to a cone-shaped penetrator doing only melting of the rock (with no cracking), toward which the regolith moves with velocity v^*. In such a case, the temperature distribution projected onto a horizontal plane is the same

as that for a cylindrical penetrator, but the heat flux from the surface is reduced by sin α, and the channel width, $1/\beta$, is increased, i.e., $\beta = \beta_o \sin \alpha$. The flow lines in rock far ahead of the penetrator are almost parallel to its path, and near the penetrator they represent fanning radial flow nearly parallel to its conical surface. The pressure gradient in lava flowing along the surface of the penetrator is reduced by the factor $\sin^3 \alpha$. These factors become very significant for a sharp cone in which, for example, $\sin \alpha \sim 10^{-1}$.

For the pressure distribution along the surface of a conical penetrator, the above development gives an expression of the form

$$P = p(a) + 1/4 \left(\eta_o \beta_o^3 v^* \sin^2 \alpha \, (a^2 - r^2) \right) .$$

This is the equation of a parabola whose apex coincides with that of the cone (r = 0). For a small drill with typical values; base radius = 10 cm, η_o = 100 g/cm-sec, v^* = 0.1 cm/sec, $\beta_o = 2000 v^* = 200$ cm^{-1}, sin α = 0.1, the pressure drop along the surface of the penetrator is only about 20 bar (204 kPa). If however, the same values are applied to a large Subterrene with a radius of 1 m (3.28 ft), the pressure at the apex of the penetrator is 2 kbar (20 MPa) above that at its shoulder. In this case the solid rock adjacent to the apex would certainly fracture, the flow of liquid melt would no longer be along the surface from point to shoulder, and the above analysis breaks down.

This concludes the section extracted from Los Alamos' *A Preliminary Study of the Nuclear Subterrene.*

The equation for pressure was taken and analyzed for a lunar boring device with a dual angled conical penetrator. Utilizing the values collected in the investigation of lunar regolith properties and dimensions from one of the conical head designs for this study, a calculation of

pressure along the surface was performed and a pressure distribution graph (Figure D.1) was constructed. (It should be stressed that the following graph represents no excavation of the melted regolith.)

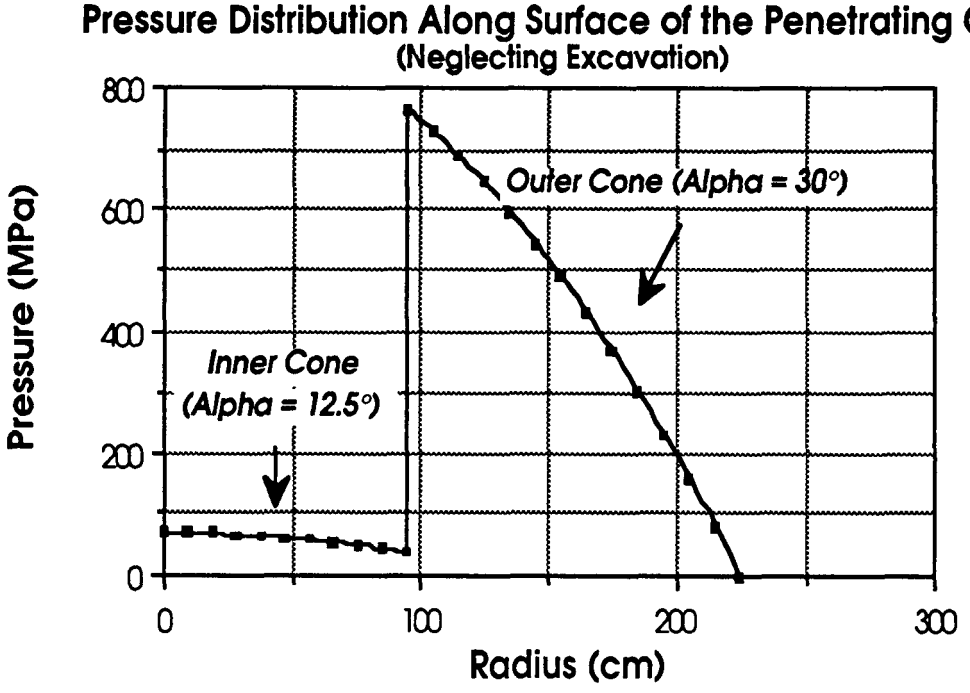

values:

base radius = 2.25 m
v^* = 30 m/day = 0.035 cm/sec
$\beta_o = 2000v^*$

Figure D.1
Pressure Distribution Along Conical Head

First, notice that the pressures along the penetrator are extremely high. This phenomenon was predicted by Los Alamos' study. An obvious result of this model would be fracturing of the rock ahead of the tunneler. However, another result which is not obvious at first inspection would be that an extremely high horizontal force (thrusting force) is required to drive the tunneler forward. The force required to drive the penetrator

would be excessive, limiting the tunneler's usefulness to weak, highly porous rock or unconsolidated material. Furthermore, the proposed glass lining would be subjected to an extremely high shearing force and higher normal forces. Consequently, these forces would put the lining in jeopardy of irreparable damage.

In conclusion, the probability of damage to the glass lining due to the extreme pressures at the conical penetrator, as well as other factors, contributed to the introduction of excavation inlets located at various points in the head. Hence, the pressure due to fluid build-up would be relieved by the availability of these intakes.

APPENDIX E: AN ANALYSIS OF VISCOUS FORCES ALONG THE HEAD

The following analysis was developed for this study and involves a determination of viscous forces along a conical head with an assumption that a steady state situation, resulting from continuous melting and simultaneous excavation, is present. With this assumption in mind, a model was developed which only accounted for shear stresses due to frictional forces and is provided below.

First, consider the lava flow along the surface of the cone as fluid flow in a channel. Next, consider the steady flow of an incompressible liquid in this channel. If the mean velocity is v_m, the shear stress at the surface of the cone τ_o is defined by

$$\tau_o = 0.5 \bullet c_f \bullet \rho \bullet v_m^2$$

where c_f is the skin friction coefficient . Furthermore, neglecting losses due to inlets and bends, the pressure drop, Δp, is given by

$$(\Delta p) \bullet \text{area} = \tau_o \bullet \text{surface area}$$

Incorporating this equation into the model for a bi-angled right circular cone (see Figure E.1) yielded,

$$(1) \quad p_2 \bullet \pi\,(2r_2 \bullet \text{length} + \text{length}^2) - p_1 \bullet \pi \bullet \text{length}^2 = 0.5 \bullet \rho \bullet v_m^2\,(c_{f\,\text{upper}} \bullet SA_{\text{upper}} + c_{f\,\text{lower}} \bullet SA_{\text{lower}}) \sin \alpha$$

p = pressure
SA = surface area

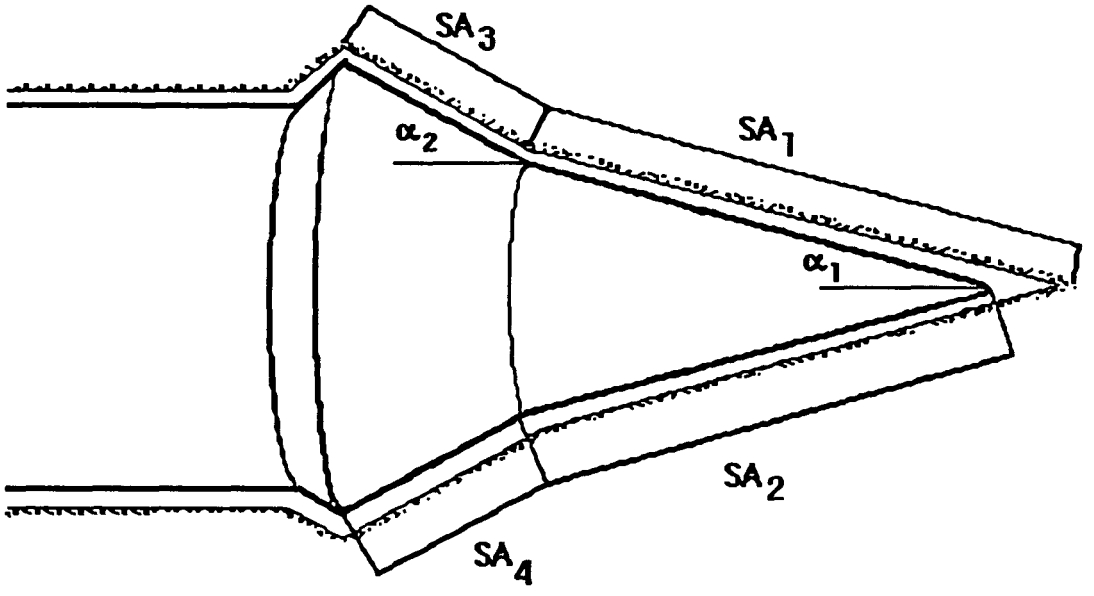

Figure E.1.
Conical Head

However, the ultimate goal of this analysis is to determine the viscous forces along the surface of the conical head. Therefore, it is only necessary to consider the right side of the equation 1.

For a biangle conical head with the values; $v_m = v_{max}/2 = 1.8(10)^4$ m/s $(5.9(10)^4$ ft/s), $\rho = 2800$ kg/m^3 (0.1 psi), $SA_1 = 13$ m^2 (140 ft^2), $SA_2 = 20$ m^2 (215 ft^2), $SA_3 = 26$ m^2 (280 ft^2), $SA_4 = 31$ m^2 (333 ft^2), $c_{f1} = c_{f2} = c_{f3} = c_{f4} = 16/Re = 416$, $\alpha_1 = 12.5°$, $\alpha_2 = 30°$, the total horizontal viscous force was less than 1 N (0.224 lb_f). (The skin friction coefficient was high due to the extremely low Reynold's number of the lava). Further analysis for viscous forces within the plumbing system for excavation of the lava yielded similar results.

In conclusion, the shape and dimensions of the conical head does not appear to constrain the propulsion system in its struggle to overcome any resistance encountered in the tunneling process.

APPENDIX F: MATERIALS SELECTION

A major effort into materials science and technology applicable to rock melting excavation has been accomplished by the Los Alamos Subterrene Program, at the Los Alamos Scientific Laboratory. Much of Los Alamos' study was directed towards the feasibility of a rapid excavation tunneler for *earth*-bound applications. However, a large majority of their research can be utilized in this feasibility study of a tunneler for *lunar*-bound applications. The high operating temperatures proposed for a melting head mandated the use of refractory alloys. The following pages contain a brief overview and comprehensive investigation of refractory alloys suitable for this study. The investigation incorporates much of Los Alamos' research and to a lesser extent, individual research.

Refractory Alloys

The refractory alloys are alloys based on relatively common metals which have extremely high melting temperatures. Specifically, molybdenum, tungsten, and columbium make up the basis for most refractory alloys.

The nuclear, aerospace, chemical processing, etc., industries have many applications which require metallic-type properties at temperatures over 1475°K (2656°R). Obviously, the melting head tunneler concept falls in this category. It should be noted that none of the more well-known systems, including the superalloys, can be used. A glance at the melting points of the refractory metals compared to iron, nickel and cobalt (Table F.1) clearly shows the increased temperature capability and justifies the previous statement.

Metal	*Melting Temperature* °K
Chromium (Cr)	2145
Columbium (Cb)	2738
Molybdenum (Mo)	2880
Tantalum (Ta)	3266
Tungsten (W)	3680
Vanadium (V)	2189
Iron (Fe)	1805
Cobalt (Co)	1763
Nickel (Ni)	1722

Table F.1
Melting Points of Refractory Metals
*Data taken from *Rare Metals Handbook*, Clifford A. Hampel, Editor, 2nd Ed., Reinhold Publ. Corp., 1961.

However, there are fundamental problems, one of which is low-temperature brittleness of tungsten, molybdenum and chromium due to low transition temperatures. Furthermore, refractory metals and alloys display poor oxidation resistance or corrosion due to reaction with an oxygen-rich atmosphere. The latter problem is not a concern for lunar-bound *applications* but is a concern for *production* of refractory alloys. The existence of a ductile-to-brittle transition temperature would necessitate careful "handling" of the proposed melting head below this temperature (e.g., pre-operation stages). The actual transition temperatures for refractory alloys vary depending on the metal, the alloy composition, the working history, and the heat treatments used. Generally, columbium and tantalum alloys are ductile well below *room* temperature while molybdenum, chromium and tungsten alloys have transition temperatures occasionally above room temperature.

Production of refractory alloys is understandably more difficult than of the lower melting metals. The high melting temperatures, high working

temperatures, poor oxidation resistance and low temperature brittleness (in some cases) of the refractory alloys all contribute to difficulty. Two general methods are in use for production: consolidation of powder and vacuum melting (arc or electron beam). In vacuum melting, close control of impurities must be maintained. After melting, the ingot formed is usually protected by an oxidation-resistant metal container and either extruded, forged or rolled into shape. The powder metal method involves compacting and sintering at high temperature in a protective atmosphere, followed by oxidation-protection and forging or rolling.

Fabrication of refractory alloys parts can be accomplished by standard processes, with some precautions. Those alloys having transition temperatures at room temperature or higher should be handled carefully because of their low ductility. Furthermore, bending or forming must be done above the transition temperature. Similarly, refractory alloys can be welded or brazed by standard methods which provide oxidation protection (e.g., inert arc welding, electron beam welding, inert atmosphere or vacuum brazing, etc.). Finally, for molybdenum and tungsten, the large temperature differences between melting and room conditions plus the high modulus of elasticity can set up large thermal stresses which can cause cracking. Preheating the material, localizing the heat input, etc., aids in reducing the stresses.

C-2

Refractory Alloy-Lava Interactions

A major area of concern for the conical penetrator is the interaction of the refractory alloy and the molten regolith. Since, the regolith may be compared to a typical basalt, research material involving refractory alloys in basalt as the rock media may be directly analyzed. The interaction between the conical head and the molten lava justifies an investigation of possible failures due to corrosion or corrosive effects. At Los Alamos, the corrosion effects within a series of basalts (basalts are commonly compared to lunar regolith) for molybdenum and tungsten alloys were determined. Significant test results obtained from the Los Alamos laboratory study (*Rapid Excavation by Rock Melting,* 1976) as well as comments pertaining to the lunar environment are listed below:

- Since corrosion occurs due to at least three general mechanisms: direct solution, electrochemical, and gas bubble oxidation, the details of these corrosion mechanisms have never been determined completely. "Gross variations in chemical composition, viscosity, density, and flow rate differences with their effects upon diffusion rates, solution thermodynamics, and variable rock oxygen potentials makes such determinations formidable tasks."[1] However, it can be assumed that the large majority of corrosion which might take place will be due to chemical corrosion, or direct solution. To a lesser extent, an electrochemical cell might be produced, depending on the actual material composition, and electrochemical corrosion would result. Gas

1. Hanold, R.J., "Rapid Excavation by Rock Melting", Sept. 1973 - June 1976, p. 28.

bubble oxidation will be a negligible since the head will not come into contact with an atmosphere. It should be further noted, with the proposed installation of the nuclear reactor within the conical head, large amounts radiation could alter the head material structure.

- In all rock types tested by Los Alamos, molybdenum tested superior to tungsten in terms of corrosion resistivity. Furthermore, it was determined that molybdenum is less soluble than tungsten with factors ranging from 4 to 20.
- "A significant correlation was obtained at constant temperature, time, and similar viscosity between metal solubility and the ferric-ferrous ratio, Fe^{+3}/Fe^{+2}, of the various basaltic compositions."[1] Higher degrees of this ferric-ferrous ratio increases the amount of corrosion which takes place on refractory materials. Lunar regolith exhibits a low ferric-ferrous ratio, with high amounts of Fe^{+2} and little to no traces of Fe^{+3}. Hence, based on this statement, low amounts of corrosion will take place due to the ferric-ferrous ratio in the lunar regolith.
- Overall, rock melts (lava) with a higher degree of silicon in its composition results in lower degrees of corrosion on the refractory surface. Silicon is abundant in the regolith and a logical conclusion would be that lower degrees of corrosion may be expected.

1. Hanold, R.J., "Rapid Excavation by Rock Melting", Sept. 1973 - June 1976, p. 28.

• "Based on geometric considerations and the static test data, a model for the surface recession rate of the outer surface of a cylindrical penetrator was derived. Combined with engineering design data, it was thus possible to make estimates of penetrator lifetime based on chemical action alone. Mechanical erosion effects were not considered although these add to the surface wear, particularly at the penetrator tip. The surface recession rate, $\Delta r'$, is given as

$$\Delta r'(mm/s) = 0.5\,(10)^{-3}\,D_p\,V\,\{\,1 - (\,1 - 4f\,(1+f)\,K')^{1/2}\,\}$$

where:

D_p = penetrator diameter, mm

V = penetration velocity, mm/s

$f = \partial / D_p$

∂ = thickness of dissolved metal boundary layer in the glass lining, mm

$K' = 1/H_p \bullet (d_g/d_p)\,\alpha_p$

H_p = penetrator length, mm

d = density of glass (d_g) or penetrator (d_p)

α_p = solubility by weight of metal in glass

Assigning certain engineering parameters and average 1900°K (3421°R) solubility values, the curves shown in Figure F.1 were constructed."[1]

1. Hanold, R.J., "Rapid Excavation by Rock Melting", Sept. 1973 - June 1976, p. 29.

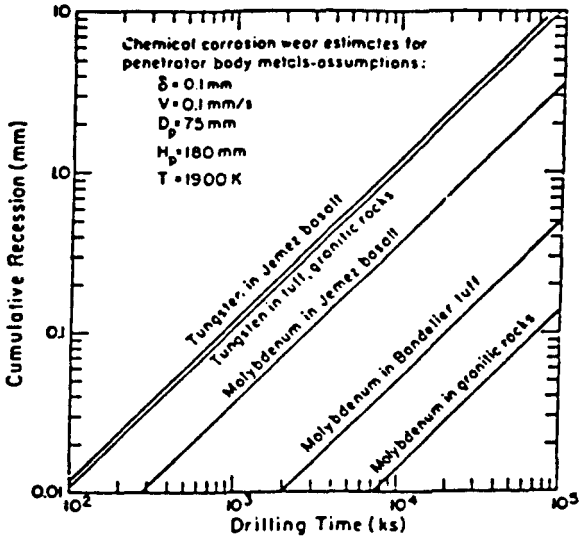

Figure F.1
Estimated Lifetimes of Mo and W Penetrators in Basalt and Granitic Rocks
* graph supplied by Los Alamos Scientific Laboratory

This model has been generated from data obtained from dry basalt and hence, may be directly analyzed for this study. Notice the lifetime estimates from this graph indicates that the chemical corrosion rate for molybdenum is less than tungsten as was previously mentioned. Analyzing the molybdenum corrosion rate line a liquid Jemez basalt media shows that drilling lifetime increases with recession rates. Larger penetrators would permit much larger surface recessions and hence a long operating lifetime may be expected for the proposed head (~ 300 - 900 days). A specific lifetime expectancy would require further testing and evaluation of scale models in a simulated lunar environment.

- A study conducted by Professor A. Muan of Pennsylvania State University determined that severe corrosion of molybdenum or tungsten-based heads should not occur due to interactions with FeO within basalt-based lava. In other words, a severe oxidation

reduction reaction which might occur due to reactions between the refractory metals and indigenous FeO may be neglected.

- Due to the geometry of the proposed conical head, a variety of surface velocities (hot lava against the refractory shell) could result. This scenario of forced convection of a fluid is known to increase corrosion rates on refractory materials.

In conclusion, it is obvious that more research must be completed if serious consideration is given to a boring device utilizing the rock melting technique. As previously stated, corrosion is a phenomenon which is difficult to predict and requires extensive physical experimentation.

Refractory Material Fabrication

Because of the high temperatures, (internal and external to the head), involved with the process of melting the lunar regolith into a lava state, the utilization of refractory materials is essential. Hence, an extensive study involving the collection of refractory metal fabrication techniques to accommodate large stock sizes would also be deemed essential. It should also be noted that requirements would exist for corrosion resistance at various design joints, and hence a high temperature braze program would be needed.

In 1976, the Los Alamos Subterrene Program, in its effort to asses the feasibility of earth-bound tunneling devices, conducted a nationwide survey to locate facilities and organizations that handle molybdenum and tungsten. Although this survey desperately needs updating it has still

been deemed a good source of reference. Following is a completed list reproduced from *Rapid Excavation by Rock Melting*, 1976, p. 34.

(1) Vacuum-arc-cast, extruded molybdenum bar: Climax Molybdenum (Amax Specialty Metals) Cleveland, OH.

(2) Powder-metallurgy, extruded molybdenum bar: Climax Molybdenum, General Electric, Cleveland,OH.; Sylvania, Towanda, PA.

(3) Powder-metallurgy tungsten blanks: General Electric, Cleveland, OH; Sylvania, Towanda, PA.

(4) Extruded tungsten bar: Canton Drop Forging and Mfg, Bo., Canton, OH. Nuclear Metals, W. Concord, MA.

(5) Upset forging--molybdenum and tungsten: Oak Ridge National Laboratory, Oak Ridge, TN.; Ladish Co., Cudahy, WI.; Northwest Industries, Albany, OR.

(6) Molybdenum sheet spinning: Laeger Metal Spinning, East Linden, NJ.

(7) Chemical vapor deposition: Ultramet, Pacoima, CA.

(8) Ring rolling; Ladish Co., Cudahy, WI.; Airco Viking, Verdi, NV.

(9) Silicide coating: Vac-Hyd Processing, Torrance, CA.

(10) Machining: Los Alamos Scientific Laboratory, Los Alamos, NM.; Northwest Industries, Albany, OR.; Thermo Electron, Woburn, MA.

(11) Medium-temperature brazing: Los Alamos Scientific Laboratory, Los Alamos, NM.; Air Vac, Carrollton, TX.; Thermo Electron, Woburn, MA.

(12) High-temperature brazing: Oak Ridge National Laboratory, Oak Ridge,TN.; Thermo Electron, Woburn, MA.; Advanced Technology, Pasadena, CA.

(13) Electron-beam welding: Los Alamos Scientific Laboratory, Los Alamos, NM.; Electrofusion, Menlo Park, CA.; Electron Beam Welding, Inc., Los Angelos, CA.; Thermo Electron, Woburn, MA.

(14) Alloy development (in conjunction with LASL): Climax Molybdenum, Cleveland, OH.; Wah Chang, Albany, OR.

Table F.2
Fabricators for Tungsten and Molybdenum Parts
* Table supplied by Los Alamos Scientific Laboratory,
Rock Excavation By Rock Melting, p. 34

Utilizing current technology, the fabrication of a large molybdenum-based conical head, with all its intricacies of intakes and

joints, would be quite possible. However, serious consideration of the proposed melting head tunneler would require an extensive development program.

APPENDIX G: LAVA INTAKE PIPE DIAMETER SIZING

A. Reynold's Number determination for flow through cylindrical pipes:

$$R = (4\ \rho\ Q)/(\pi\ \mu\ D) \qquad (1);\ \textit{if } R < 2000 \textit{ then flow is always laminar}$$

ρ = density = 2900 kg/m^3 (maximum)
Q = volumetric flow rate = AR (advance rate)•A_t (tunnel area)
AR = 0.000289 m/s (25 m/day)
A_t = 15.9 m^2 (4.5 diameter) = 0.0046 m^3/sec (note only a fraction of this flow travels through one short pipe)
μ = dynamic viscosity = 31.6 N-sec/m^2 (assumed worst case at 1200°C, barely melted)
D = pipe diameter

R = 0.538/D (for D > 0.0003 m, laminar flow exists)

Therefore, laminar flow is always present.

B. Loss of pressure due to laminar flow in cylindrical pipes:

$$\Delta P = (128\ \mu\ L\ Q\ )/\ (\pi\ D^4) \qquad (2)$$

L = pipe length = 4.5 m (short pipe), 18 m (long pipe)

it follows,

$$\Delta F = (4.65\ L)/D^2$$

Adding equivalent length of 30D for each 90° turn (18 turns for all short pipes, 2 turns for long pipe), the total viscous losses become,

$$\Delta F_S = 4.65\ (4.5 + 18 \bullet 30D_S)/D_S^2$$

$$\Delta F_L = 4.65\ (18 + 2 \bullet 30D_L)/D_L^2$$

Including the losses due to the pressure drop in raising the fluid level (approximated as $\rho g \Delta h$), and ignoring the cone surface inlet losses, the total forces imposed on the propulsion unit by the lava intake piping during level tunneling is:

$$\Delta F_S = 4.65\ (4.5 + 18 \bullet 30D_S)/D_S^2 + (3/8)\ 7448 \bullet D_S^2$$

$$\Delta F_L = 4.65\ (18 + 2 \bullet 30D_L)/D_L^2 + 7448 \bullet D_L^2$$

Now, minimizing these losses with respect to the pipe diameters, we get,

$$D_S = 0.48 \text{ m}, \Delta F_S = 6\text{kN}$$

$$D_L = 0.36 \text{ m}, \Delta F_L = 2.4\text{kN}$$

Note: equation (1) and (2) were taken from page 177 and 187, respectively, of *System Dynamics* by Katsuhiko Ogata.
Note: viscosity and density data was taken from the Apollo 16 samples.

APPENDIX H: FORWARD FORCE REQUIREMENTS ON PROPULSION SYSTEM

Varying the inclination of the tunneler will effect the forces needed from the propulsion unit to move forward due to the opposing component of the vehicles weight and all the lava contained in it, as follows:

$$\Delta F = g\,(M_{vehicle} + M_{lava})\sin\theta + \Delta F_{\theta=0^\circ}$$

θ = inclination of tunneler
$M_{vehicle}$ = 100,000 kg (assumed value)
$M_{lava\ contained} = M_{piping} + M_{holding\ tank} =$
$\rho\,(V_{pipe\ system} + V_{holding\ tank})$

Incorporating the lengths and diameters of the piping system and the reservoir volume into the above equation yields,

$$\Delta F = g\,(100{,}000 + 62{,}200)\sin\theta + 6.4\text{kN}$$

$$\Delta F = (265\text{kN})\sin\theta + 6.4\text{kN}$$

$$\Delta F_{max} = 272\text{kN}\ (\theta = 90^\circ, \text{straight up})$$

Therefore,

ΔF_{max} ~ 400kN or 90 klb_f (with a safety factor of 1.5 (maximum force imposed on propulsion unit)

APPENDIX I: TORQUE AND POWER REQUIREMENTS FOR THE GEARING SYSTEM

The torque required by each wheel to produce enough friction to sustain a constant tunneling speed has been modelled as shown below:

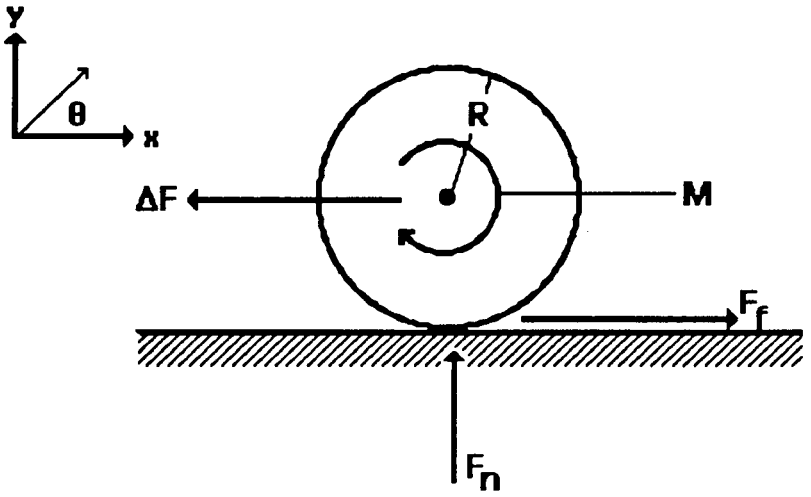

ΔF = force to overcome (see Appendix H)
R = radius of wheel
M = torque (shaft)
F_n = normal force (can be adjusted by hydraulic actuator)
F_f = frictional force generated

Figure I.1
Wheel (Propulsion System) Model

Using Newton's law:

$$m\ddot{x} = F_f - \Delta F$$

$$J\ddot{\theta} = M - R \bullet F_f$$

(note: this assumes $F_f \leq \mu_s \bullet F_n$, no slipping, only rolling)

For constant speed: $\ddot{\theta} = 0, \ddot{x} = 0$

and,

$$F = \Delta F$$

$$M = R \bullet F$$

Thus,

$$\mathbf{M = R\Delta F,}$$
where $\Delta F \leq \mu_s \bullet F_n$

Torque must be equal to the wheel radius times the forces imposed on the propulsion unit by the lava intake system. The tunneler can be accelerated or decelerated by changing the shaft torque.

For a maximum ΔF of 400kN (90 klb_f) (see Appendix H) and wheel radius of 0.5 m (1.6 ft):

M_{max} = 200 kN-m (147 klb_f-ft) = the maximum torque required

The power delivered can be calculated as follows:

$P = M \bullet \omega$

ω = angular velocity = $(AR)/R$ = 0.000578 rad/sec

therefore, P_{max} = 0.115 kW/per wheel

P_{max} ~ 0.5 kW (0.7 HP)

APPENDIX J: ACTUATOR LOAD REQUIREMENTS

The normal forces delivered by the actuators must be enough to keep the wheels from slipping and support the weight of the vehicle.

To avoid slipping:

$$F_f \leq \mu_s \bullet F_n \quad \text{(from Appendix I)}$$

assuming $\mu_s \sim 0.2$ (tread on glass lining), and using $F_f = \Delta F$ (shown in Appendix I), and using 4 wheels to generate F_f, we get:

$$\Delta F = 4\,(0.2)F_n = 0.8\,F_n$$

where $F_n = P_n \bullet A_h$

P_n - hydraulic normal pressure
A_h - hydraulic actuator area

Therefore,

$$P_n = \Delta F/(0.8 \bullet A_h)$$

For $\Delta F = 265\text{kN} \bullet \sin\theta + 6.4\text{kN}$ (see Appendix H),

$$\mathbf{P_n = (332\ kN \bullet \sin\theta + 8\ kN)/A_h}$$

$$\mathbf{P_n = 340\ kN/A_h\ (76\ klb_f/A_h)}$$

to avoid slipping of the wheels.

To support the weight of the vehicle (normal support) the bottom two wheels for the driver and the bottom two wheels for the stabilizer will be used. Note that all 4 points are angled 45° to the weight vector at all times. Consequently,

$$4(F_n)\cos 45° = g(M_{vehicle} + M_{lava\ contained})\cos\theta$$

F_n = normal force needed by the hydraulic actuators
$M_{vehicle}$ = 100,000 kg (assumed value)
$M_{lava\ contained}$ = 62,200kg (from Appendix H)
θ = inclination of tunneler

thus,

$$F_n = (94kN)\cos\theta$$

$$F_{n\,max} = 94kN$$

or,

$$\mathbf{P_n = (94\ kN/A_h)\cos\theta}$$

$$\mathbf{P_{n\,max} = 94\ kN/A_h\ (21\ klb_f/A_h)}$$

It may then be shown that the normal force requirements imposed on the hydraulic actuators are 94 kN (21 klb_f) at $\theta = 0°$, 340 kN (76 klb_f) at $\theta = 90°$, and a minimum of 91 kN (20 klb_f) at $\theta \sim 15°$.

Picking P_n = 1 ksi, for a maximum normal load of 510kN (including a safety factor of 1.5), D_h must be 0.3 meters (1 ft).

APPENDIX K: HEAT PIPE ISSUES

This section of the appendix will address the derivations required to obtain the necessary equations. From the explanations provided in the heat transfer section, equations (4), (6), & (7) are restated,

$$T(x,t)-T_i = 2Q''_{in}(\alpha t/\pi)^{1/2}/k \exp(-x^2/4\alpha t) \quad (4)$$

$$T(x) = T_i+(T_m-T_i)e^{-Ux/k} \quad (6)$$

$$Q''_{in} = (L_f+c_p(T_m-T_i))\rho U \quad (7)$$

Evaluating equation (4) at x=0,

$$T(0,t)-T_i = 2Q''_{in}(\alpha t/\pi)^{1/2}/k$$

Solving for t (t_{init}),

$$t_{init} = \pi(k(T_m-T_i)/(2\alpha Q''_{in}))^2 \quad (5)$$

To determine the mass flow rate in the heat pipes, the acting surface area must be calculated.

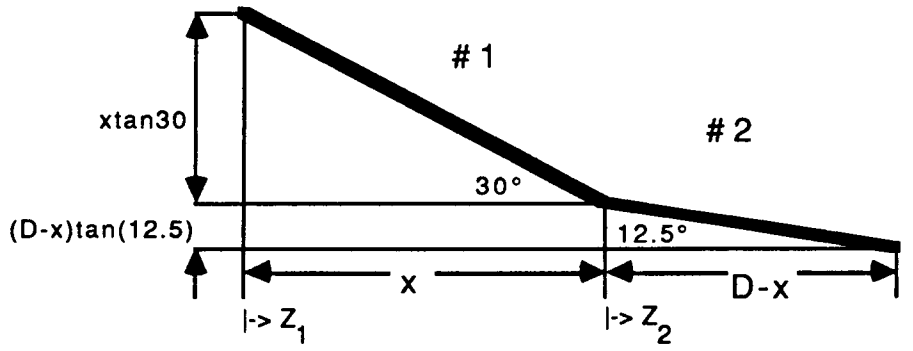

Figure K.1.
Geometry of Head

The head length is known to be one diameter, D, as shown above in Figure K.1, so

$$x\tan(30)+(D - x)\tan(12.5) = D/2$$

$$x(\tan30 - \tan12.5) = D(1/2 - \tan(12.5))$$

$x = D(1/2 - \tan(12.5))/(\tan(30) - \tan(12.5))$

$x = 0.7825136D$

Now calculating the surface area of section #1 above (SA_1),

$SA = \int 2\pi R dZ$

$R_1 = D/2 - Z_1\tan(30)$

$R_1 = D/2 - 0.57735Z_1$

$SA_1 = \int 2\pi R_1 dZ_1$ $\qquad SA_1 = \int_{0.04821D}^{0.7825136D} 2\pi(D/2-0.57735Z_1)dZ_1$

$SA_1 = 2\pi(DZ_1/2 - 0.57735Z_1^2/2)\Big|_{0.04821D}$

$SA_1 = 2\pi(0.7825136D^2/2 - 0.57735(.7825136D)^2/2) - \pi(0.048216D^2/2 - 0.57735(0.04821D)^2/2)$

$SA_1 = 0.382118D_2$

Now for surface area #2

$R_2 = 0.2174864D\tan(12.5) - Z_2\tan(12.5)$

$R_2 = 0.048216D - 0.221695Z_1$

$SA_2 = \int 2\pi R_2 dZ_2$ $\qquad SA_2 = \int_{0.0}^{0.048216D} 2\pi(0.048216D - 0.221695Z_2)dZ_2$

$SA_2 = 2\pi(0.048216DZ_2 - 0.221695Z_1^2/2)\Big|_{0.0}$

$SA_2 = 2\pi((0.048216D)^2 - 0.221695(.048216D)^2/2)$

$SA_2 = 0.0129879D^2$

$SA_{tot} = 0.3951059D^2$

By definition,

$Q_{in} = Q''_{in}SA_{tot} = \dot{m}\int c_p dT$

Solving for $\dot{m}$,

$\dot{m} = (Q''_{in}SA_{tot})/(4183.8515\int c_p dT)$ $\qquad$ 4183.8515 - conversion factor cal/g to J/kg

$\dot{m} = (9.4436\text{x}10^{-5}Q''_{in}D^2)/(\int c_p dT)$

APPENDIX L: COOLANT PIPE ISSUES

This section of the appendix will address the derivations required to obtain the necessary equations. The amount of heat energy to solidify the lining is the latent heat of fusion plus the specific heat times the temperature differential,

$q''_{out} = \dot{m}c_p\Delta T/A + \dot{m}L_f/A$ $\quad q_{out} = q''_{out}A$ $\quad Q''_{out} = q''_{out}/t$

$t = \Delta x/U \rightarrow$ $\quad Q''_{out} = q''_{out}U/\Delta x$

$\dot{m} = \Delta x\pi((r+\Delta y)^2 - r^2)\rho$ note Δx - cooling pad length, Δy - lining thickness

$\dot{m} = \Delta x\pi(2r\Delta y+\Delta y^2)\rho$

$A = 2\pi r\Delta x$

Combining the above equations,

$Q''_{out} = (2r\Delta y+\Delta y^2)\rho\Delta x\pi U(c_p\Delta T+L_f)/(2\pi r\Delta x\Delta x)$

$Q''_{out} = (2r\Delta y+\Delta y^2)\rho\pi U(c_p\Delta T+L_f)/(2\pi r\Delta x)$

$Q''_{out} = Q_{out}/A$ $\quad A = \pi D\Delta x$

For a heat exchanger (in the coolant pipes)

$Q_{out} = \dot{m}_{wc}\int c_p dT$ note $\dot{m}_{wc}$ - mass rate in wall coolant

$Q''_{out}\pi D\Delta x = 4183.8515\dot{m}_{wc}\int c_p dT$

$\dot{m}_{wc} = Q''_{out}\pi D\Delta x/(4183.8515\int c_p dT)$

therefore, by summing the volume up, the volume of coolant tank, υ_{ct}, is

$\upsilon_{ct} = (\dot{m}_{wc}+\dot{m}_{oth})t_{tot}/(\rho 1000)$ note $\dot{m}_{oth}$ - mass rate of other coolant, t_{tot} - total return time for truck

$t_{tot} = 2L_{tunn}/V_{tru} + t_{lag} + \upsilon_{ct}/\varepsilon_c$ note L_{tunn} - maximum length of tunnel, V_{tru} - truck speed, t_{lag} - lag time for truck incidental, ε_c - dump rate for coolant

similarly,

$\dot{m}_{oth} = Q''_{out}0.2A_{oth}/(4183.8515\int c_p dT)$ 0.2 - factor for other coolants, 4183.8515 - conversion factor, A_{oth} - acting area of other coolants

$$\rho \upsilon_{ct} 1000/(\dot{m}_{wc}+\dot{m}_{oth}) = 2L_{tunn}/V_{tru} + t_{lag} + \upsilon_{ct}/\varepsilon_c$$

$$(\rho 1000/(\dot{m}_{wc}+\dot{m}_{oth}) - 1/\varepsilon_c)\upsilon_{ct} = (2L_{tunn}+t_{lag}V_{tru})/V_{tru}$$

$$\upsilon_{ct} = ((2L_{tunn} + t_{lag}V_{tru})/V_{tru})((\dot{m}_{wc}+\dot{m}_{oth})\varepsilon_c/(1000\rho\varepsilon_c-\dot{m}_{wc}-\dot{m}_{oth}))$$

$$t_{tot} = 2L_{tunn}/V_{tru} + t_{lag} + \upsilon_{ct}/\varepsilon_c$$

$$L_{ct} = 6\upsilon_{ct}/(\pi(D-0.5)^2)$$

L_{ct} - length of coolant tank
1.5 - safety factor
0.5 - less diameter used for support systems

APPENDIX M: EXCAVATION ISSUES

This section of the appendix will address the derivations required to obtain the necessary equations. The regolith tanks are sized depending an several variables (e.g. tunnel length and tunneler speed)

Total time for return is,

$$t_{tot} = 2L_{tunn}/V_{tru} + \upsilon_{rt}/\varepsilon_r$$

$$\upsilon_{rt} = 1.1V_{tunn}t_{tot}\pi D^2/4$$

$$\upsilon_{rt} = 1.1\pi D^2V_{tunn}(2L_{tunn}/V_{tru} + t_{lag} + \upsilon_{rt}/\varepsilon_r)/4$$

$$\upsilon_{rt} = (1 - (1.1\pi D^2V_{tunn})/4\varepsilon_r) = V_{tunn}1.1\pi D^2(2L_{tunn}/V_{tru}+t_{lag})/4$$

$$\upsilon_{rt} = (1.1V_{tunn}\pi D^2\varepsilon_r/V_{tru})(2L_{tunn}/V_{tru}+t_{lag})(4\varepsilon_r/(4\varepsilon_r - 1.1\pi D^2V_{tunn}))$$

$$\upsilon_{rt} = 1.1V_{tunn}\pi D^2\varepsilon_r/V_{tru}((2L_{tunn}+t_{lag}V_{tru})/(4\varepsilon_r - 1.1\pi D^2V_{tunn}))$$

ε_r - dump rate for regolith

υ_{rt} - volume of regolith tank

1.1 - factor of safety

V_{tunn} - tunneler speed

t_{lag} - lag time for truck incidental

υ_{rt} is also,

$$\upsilon_{rt} = 0.5\pi/4(D - 0.5)^2L_{rt}$$

$$L_{rt} = 8\upsilon_{rt}(1.5)/(\pi(D - 0.5)^2$$

$$L_{rt} = 12\upsilon_{rt}/(\pi(D - 0.5)^2$$

L_{rt} - length of regolith tank
first 0.5 - only using half diameter for tank sizing
second 0.5 - less diameter used for support systems

1.5 - factor of safety

Appendix N Design Charts

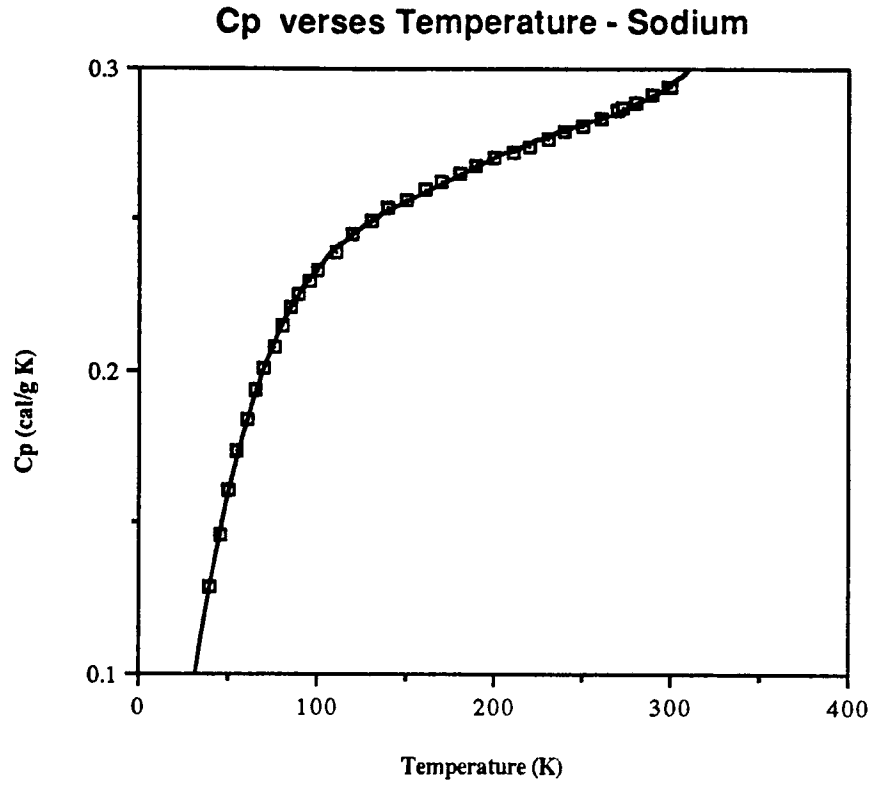

Cp = - 0.0826 + 0.0078T - 7.703e-5T^2 + 3.909e-7T^3 - 9.848e-10T^4 + 9.787e-13T^5

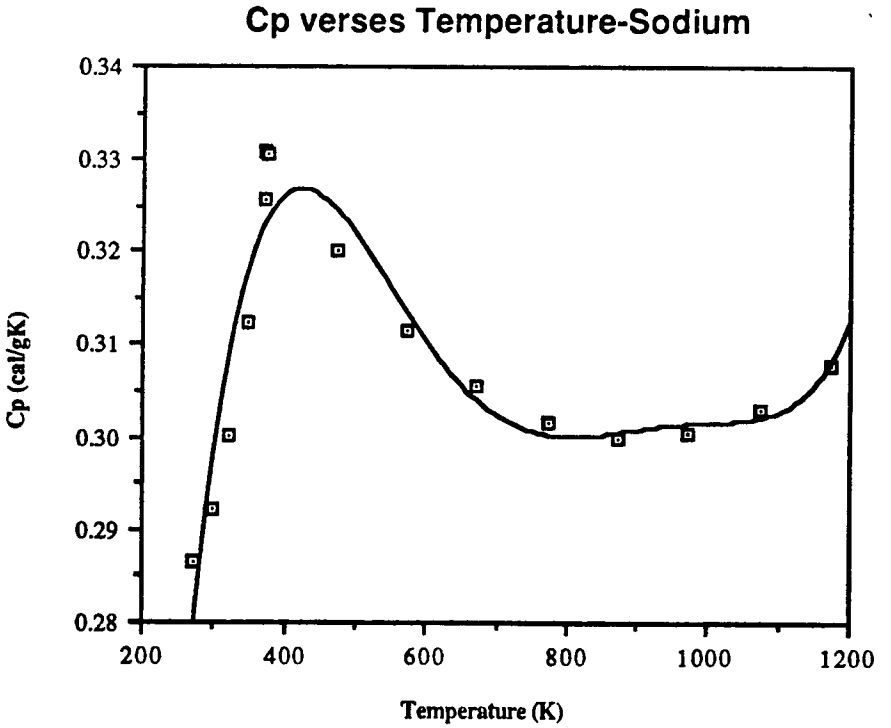

Cp = - 0.5034 + 0.0061T - 1.703e-5T^2 + 2.240e-8T^3 - 1.416e-11T^4 + 3.480e-15T^5

Cooling Pad Length Ve Heat Flux Out

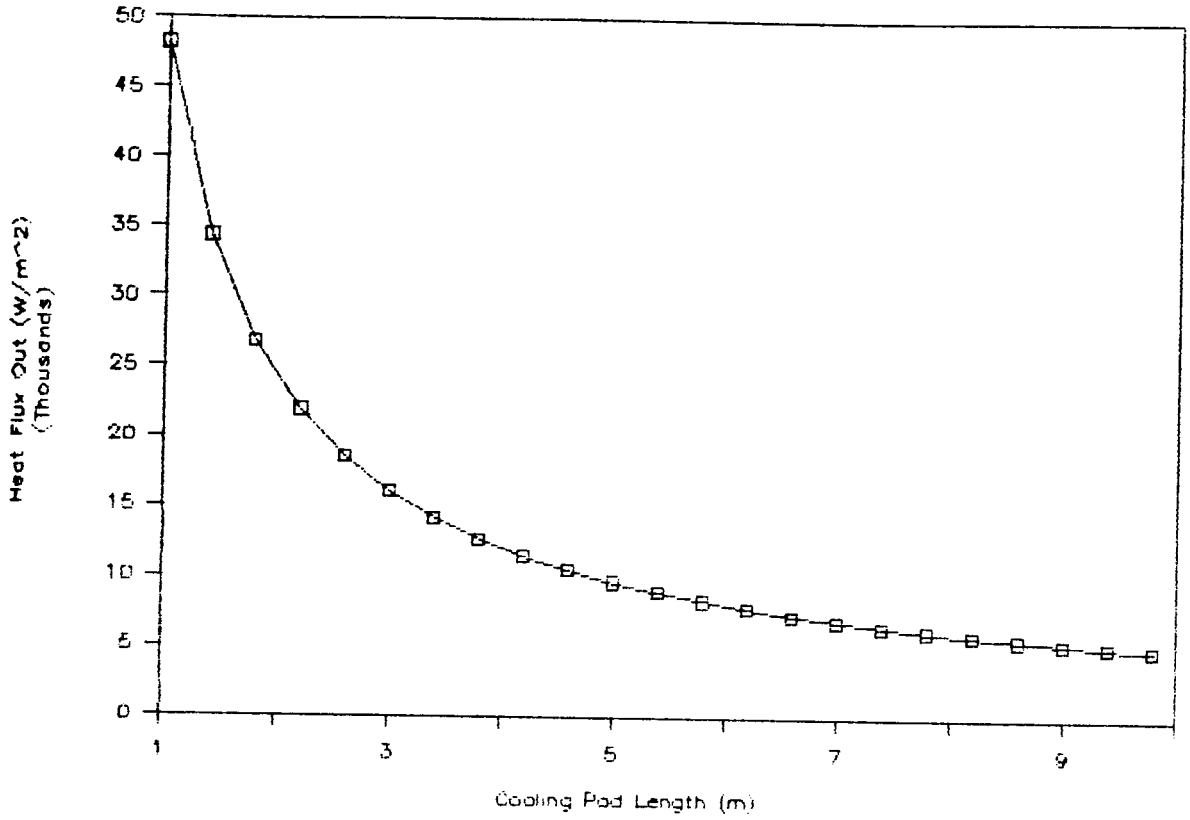

Tunnel Radius Vs Mass Rate in

Heat Pipes

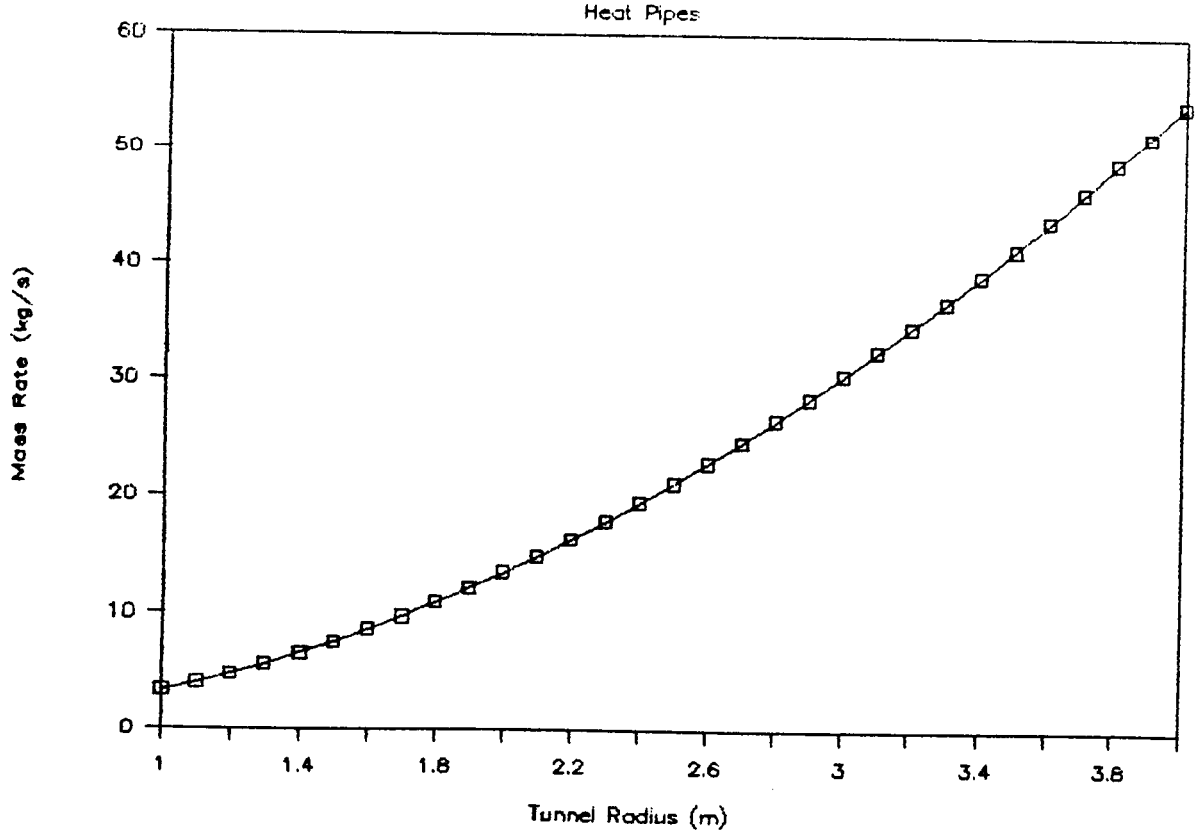

Tunnel Radius Vs Mass Rate of

"Other" Coolant

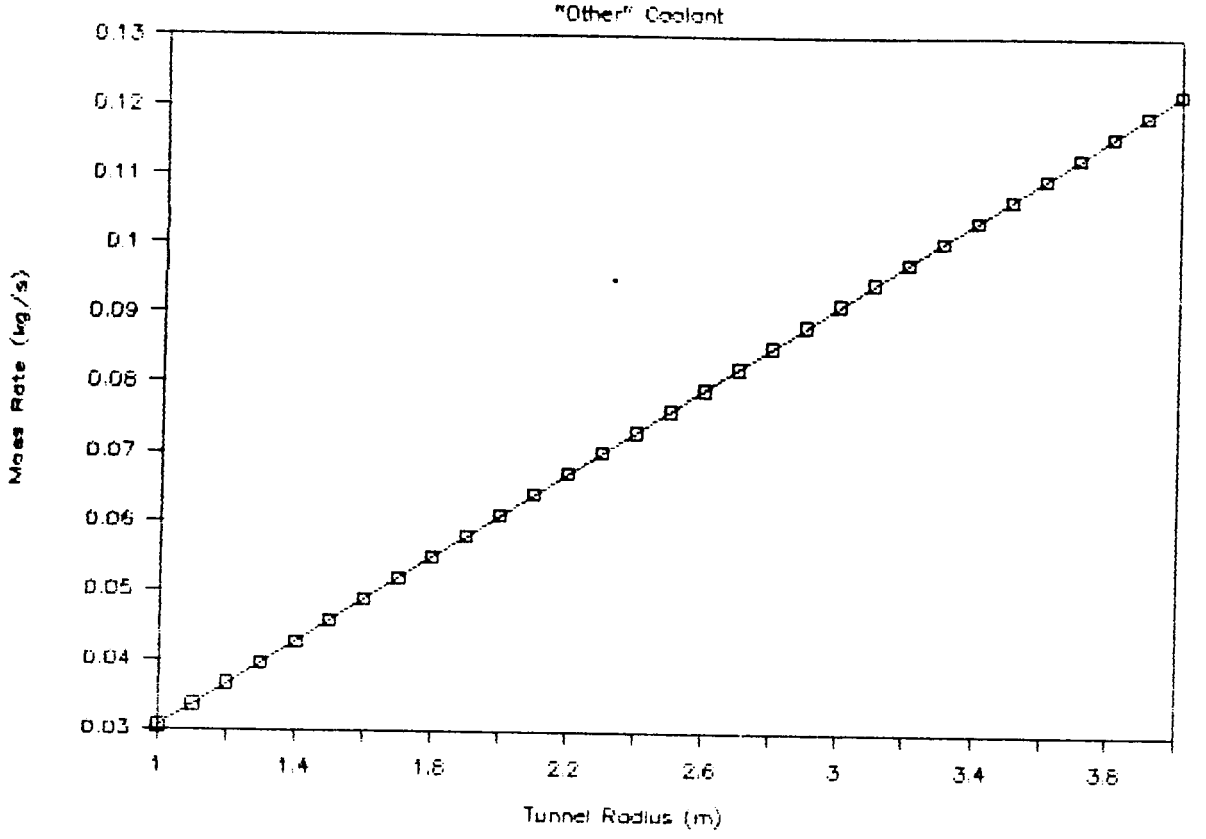

Tunnel Radius Vs Mass Rate of

Wall Coolant

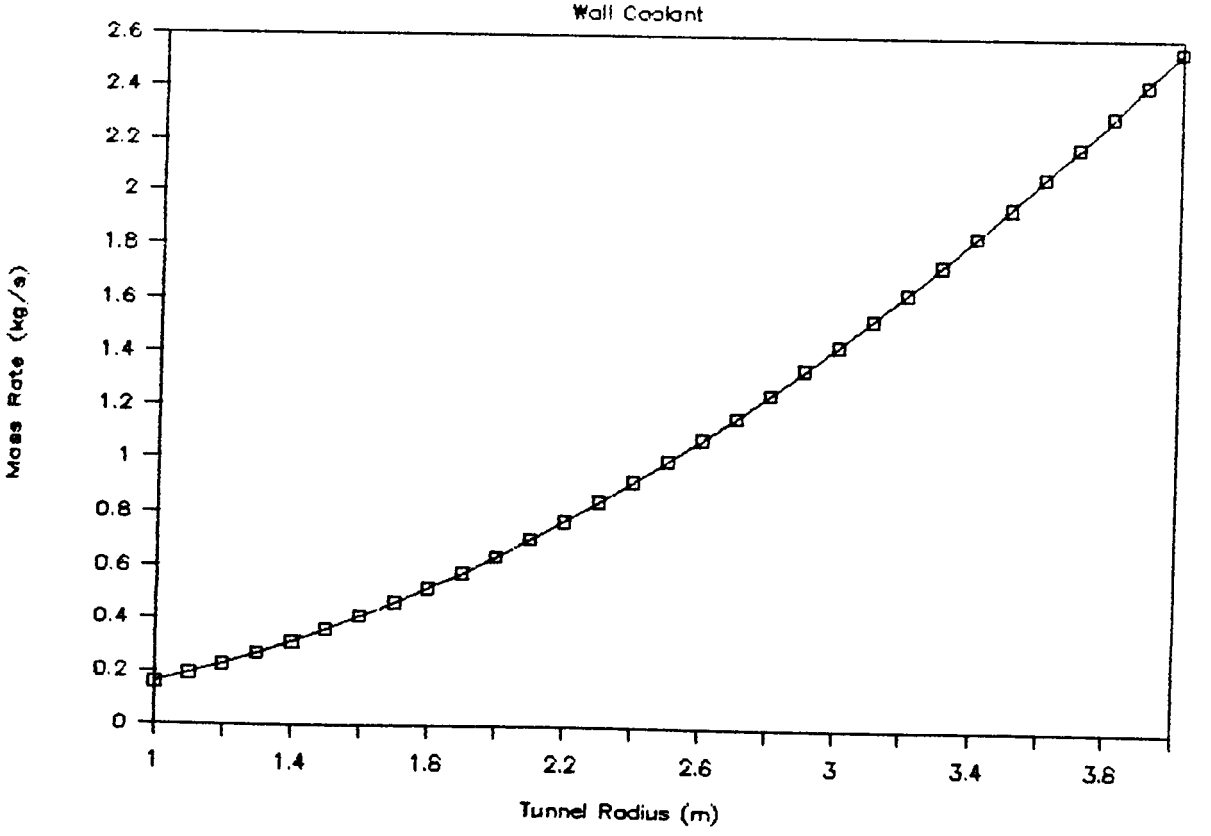

Tunneler Speed Vs Mass Rate of

Heat Pipes

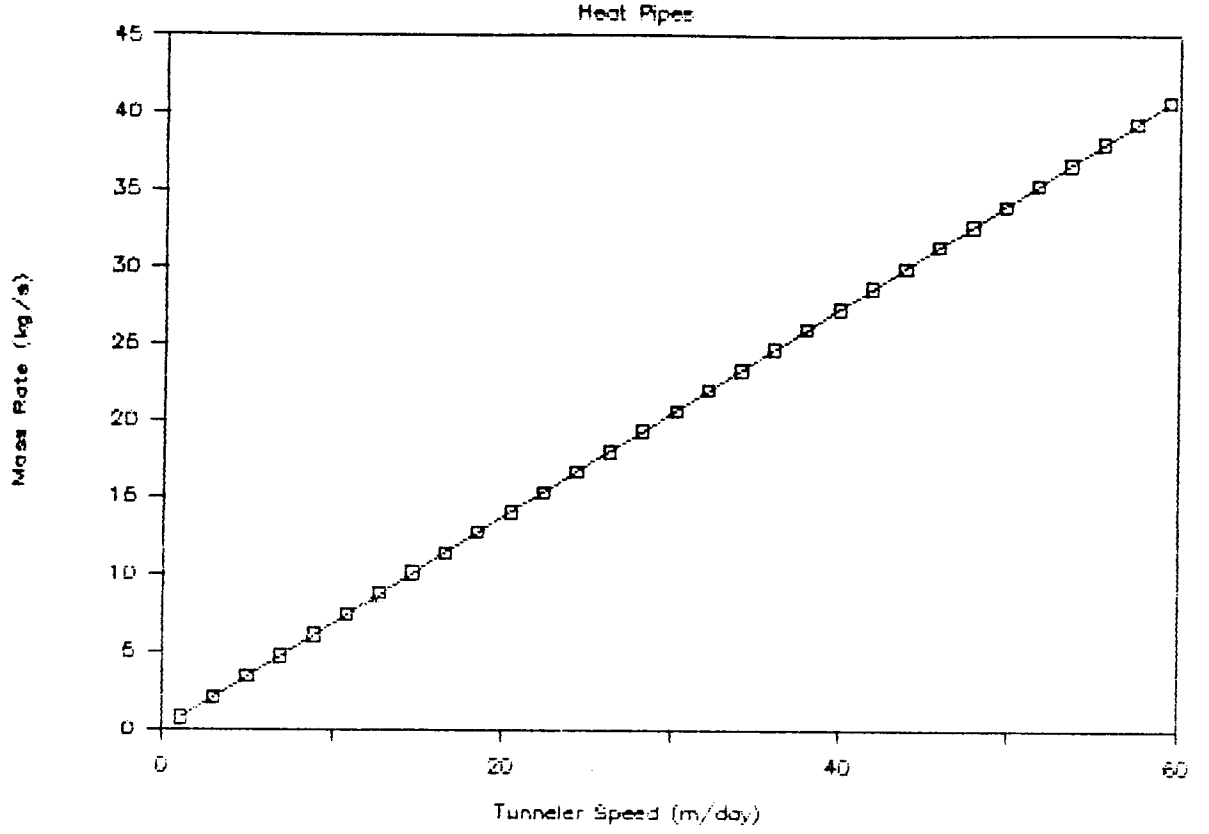

Tunneler Speed Vs Mass Rate of

"Other" Coolant

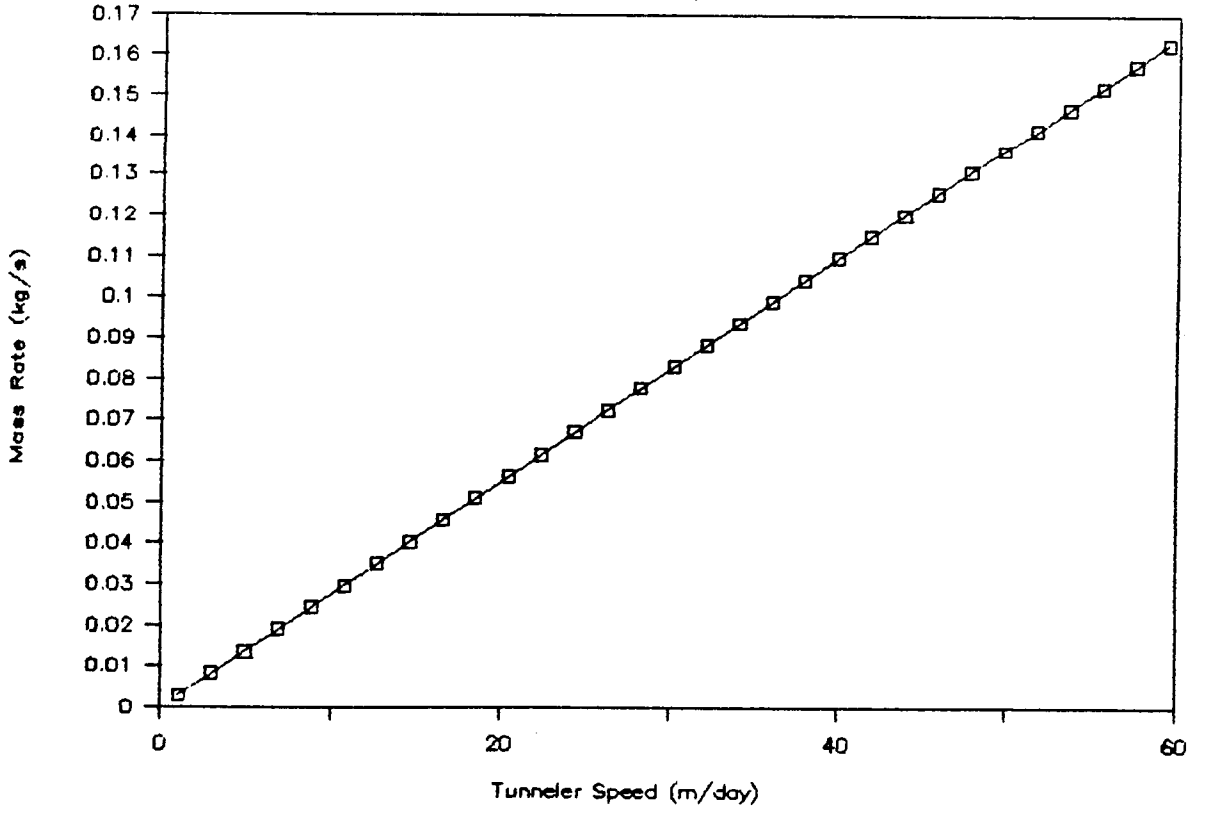

Tunnel Radius Vs Heat Flux Out

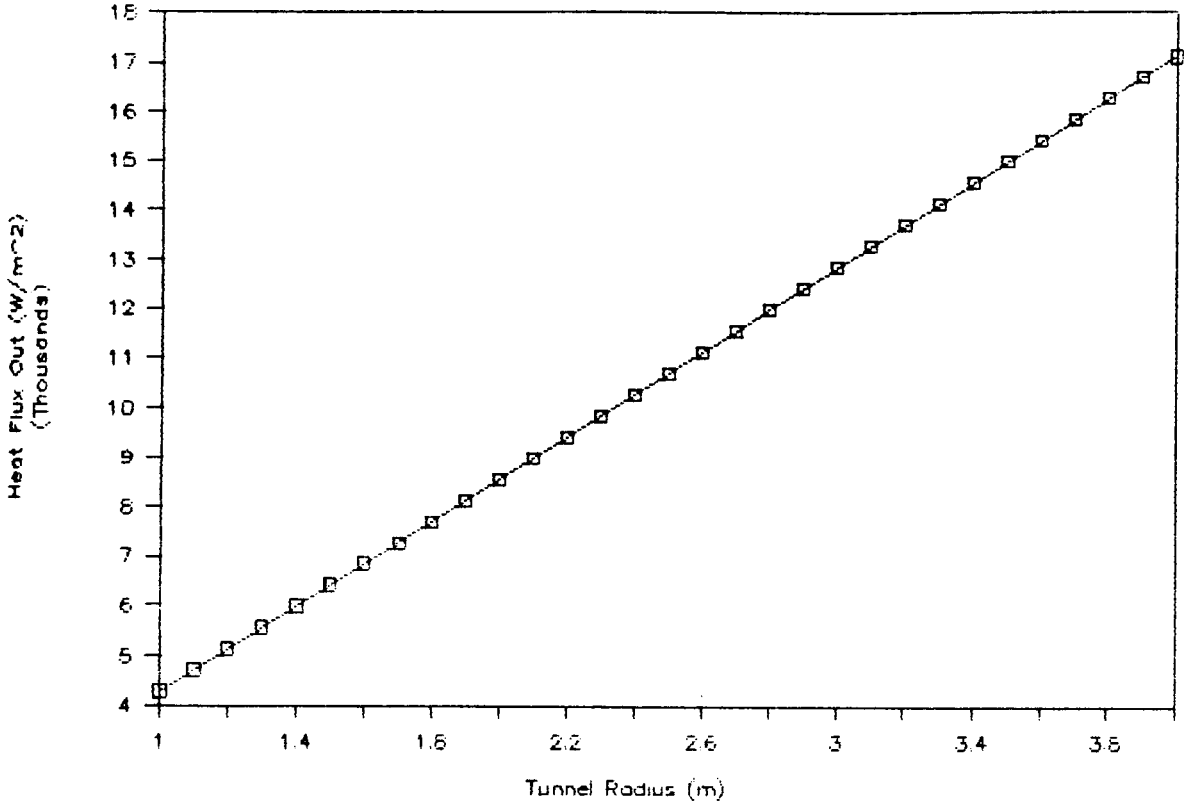

Truck Speed Vs Coolant Tank Length

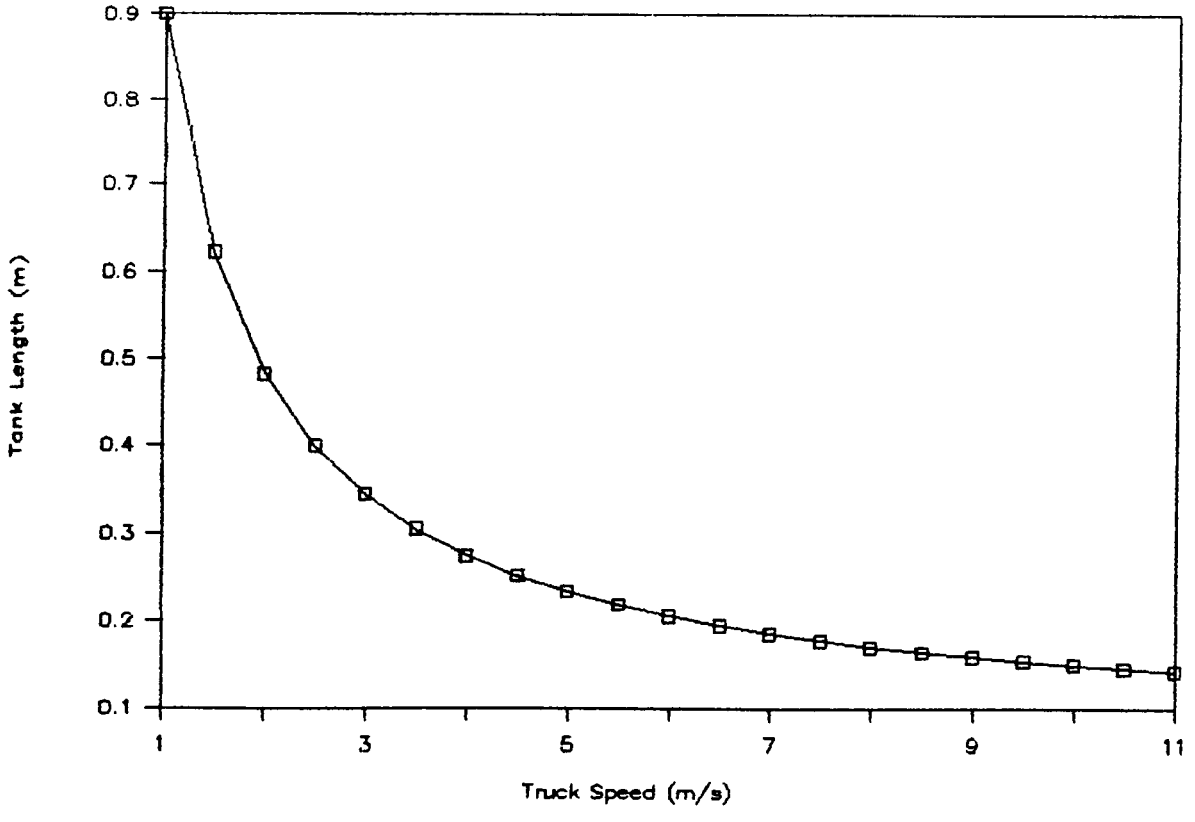

Tunnel Radius Vs Coolant Tank Length

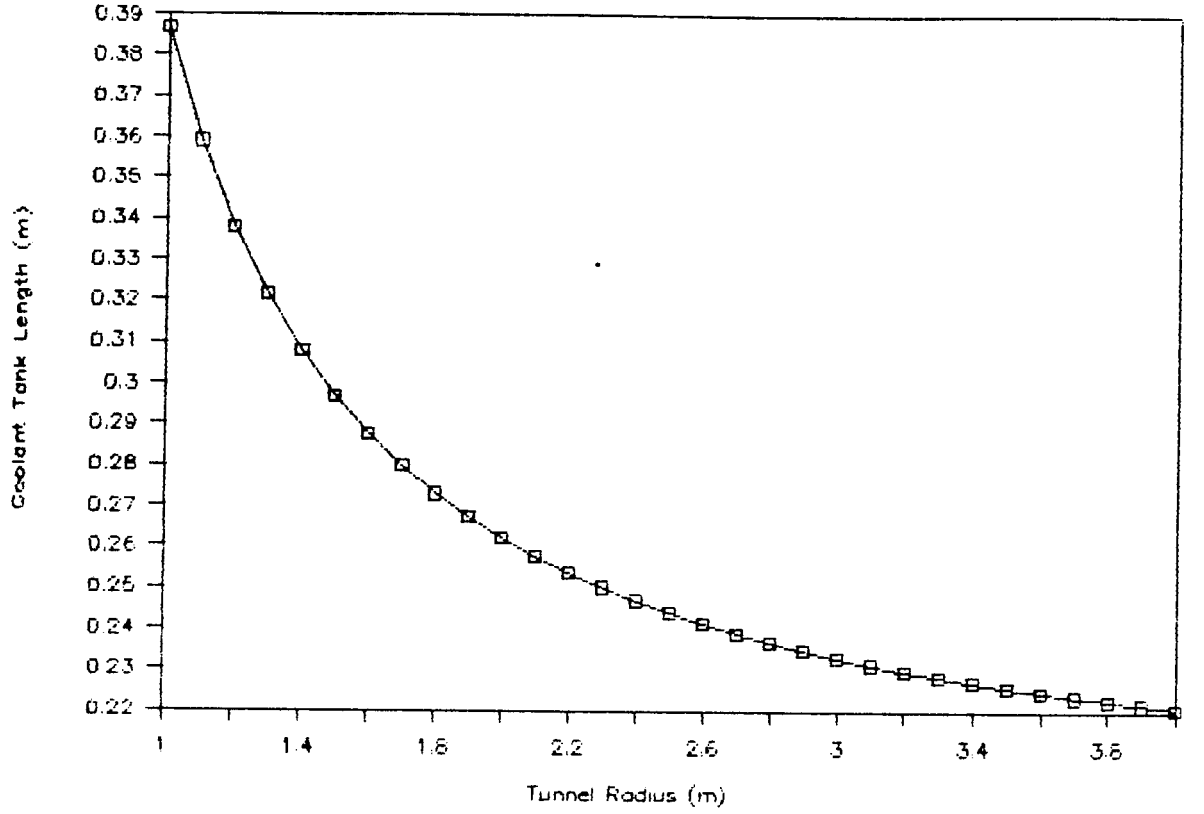

Tunneler Speed Vs Mass Rate of

Wall Coolant

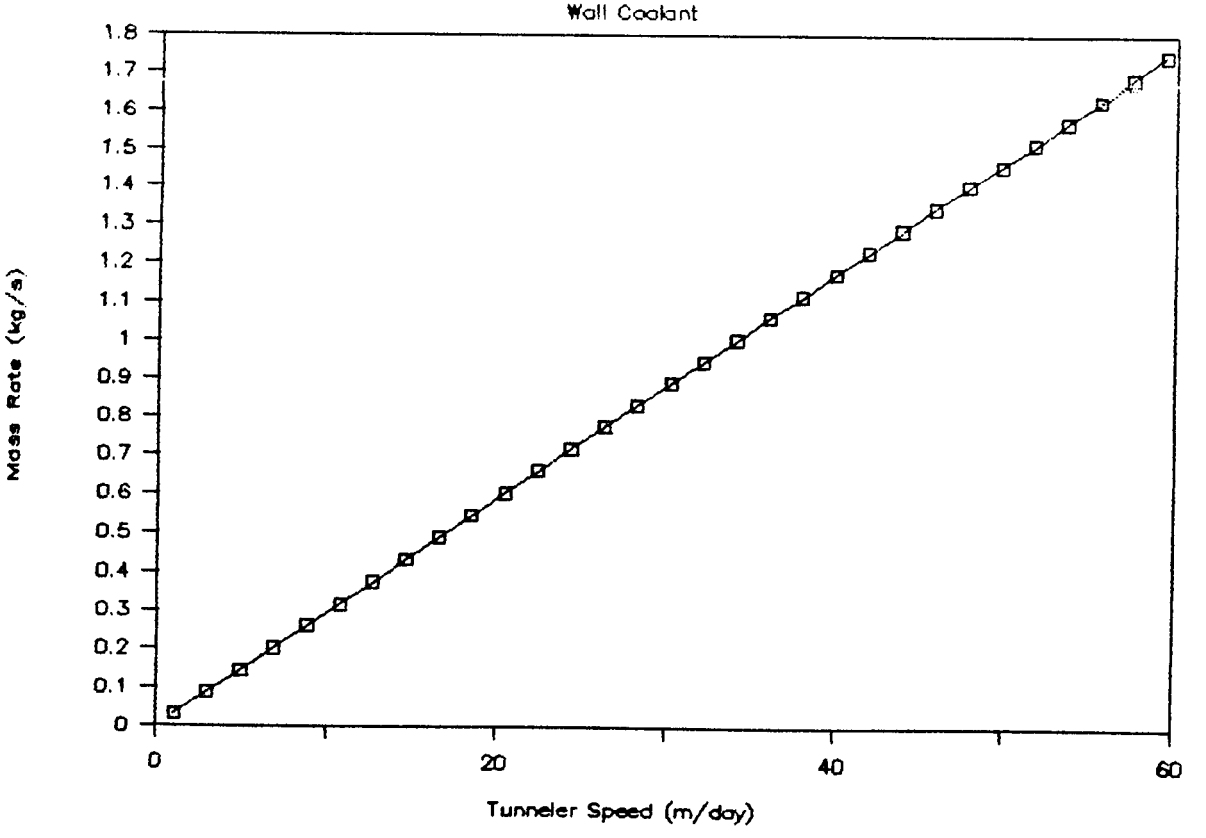

Tunneler Speed Vs Heat Flux In

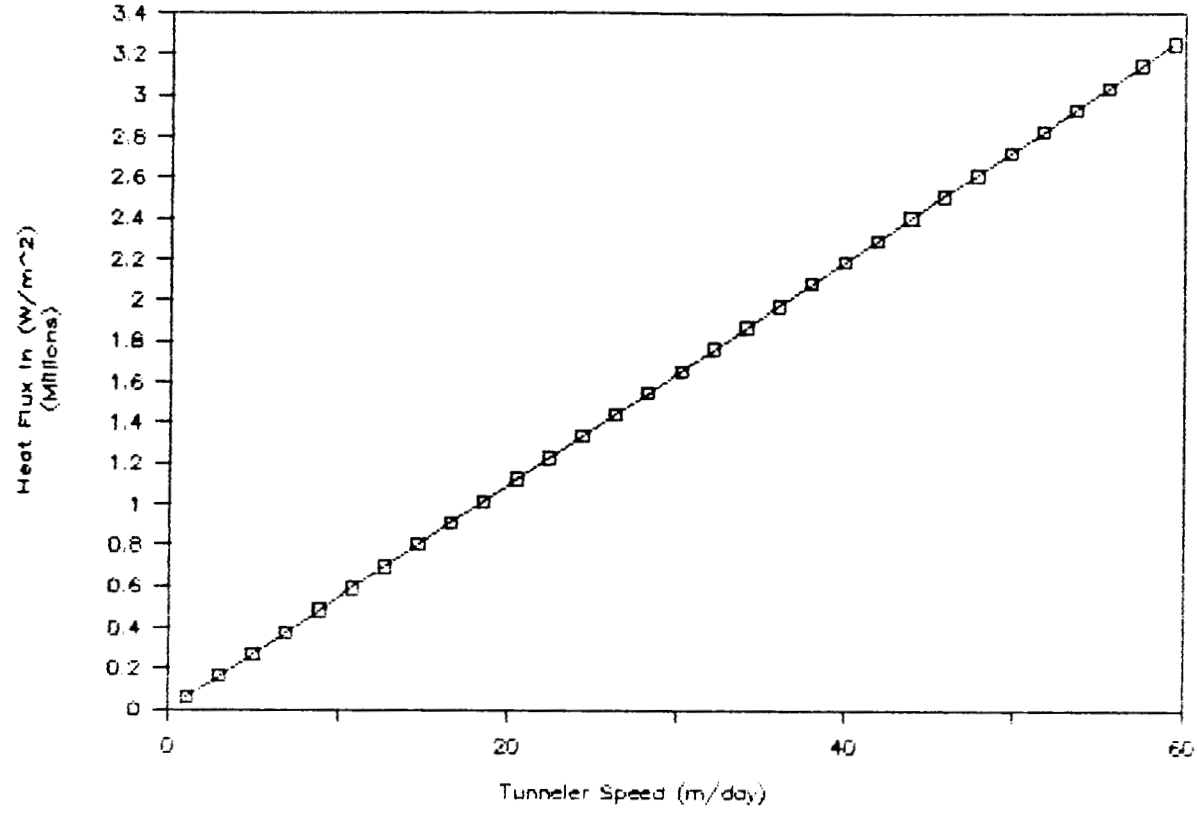

Tunneler Speed Vs Heat Flux Out

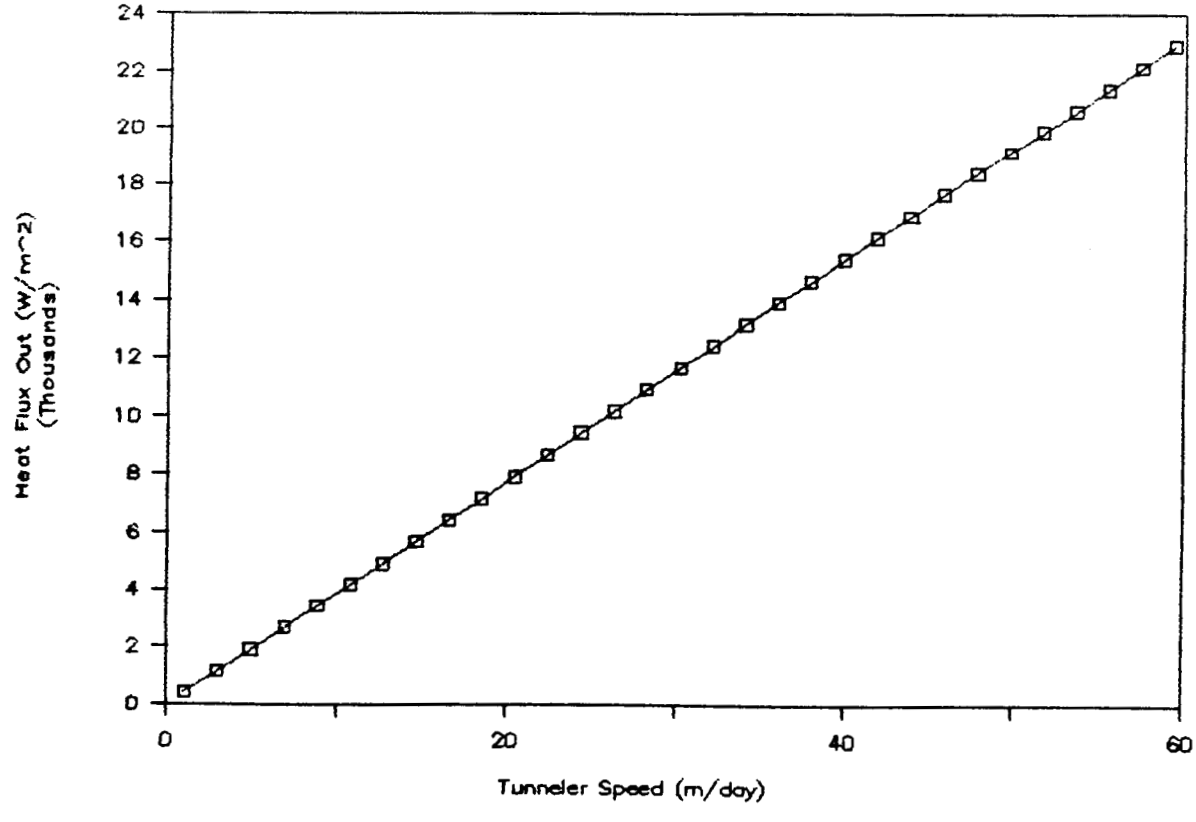

Tunneler Speed Vs Initial Set-Up Time

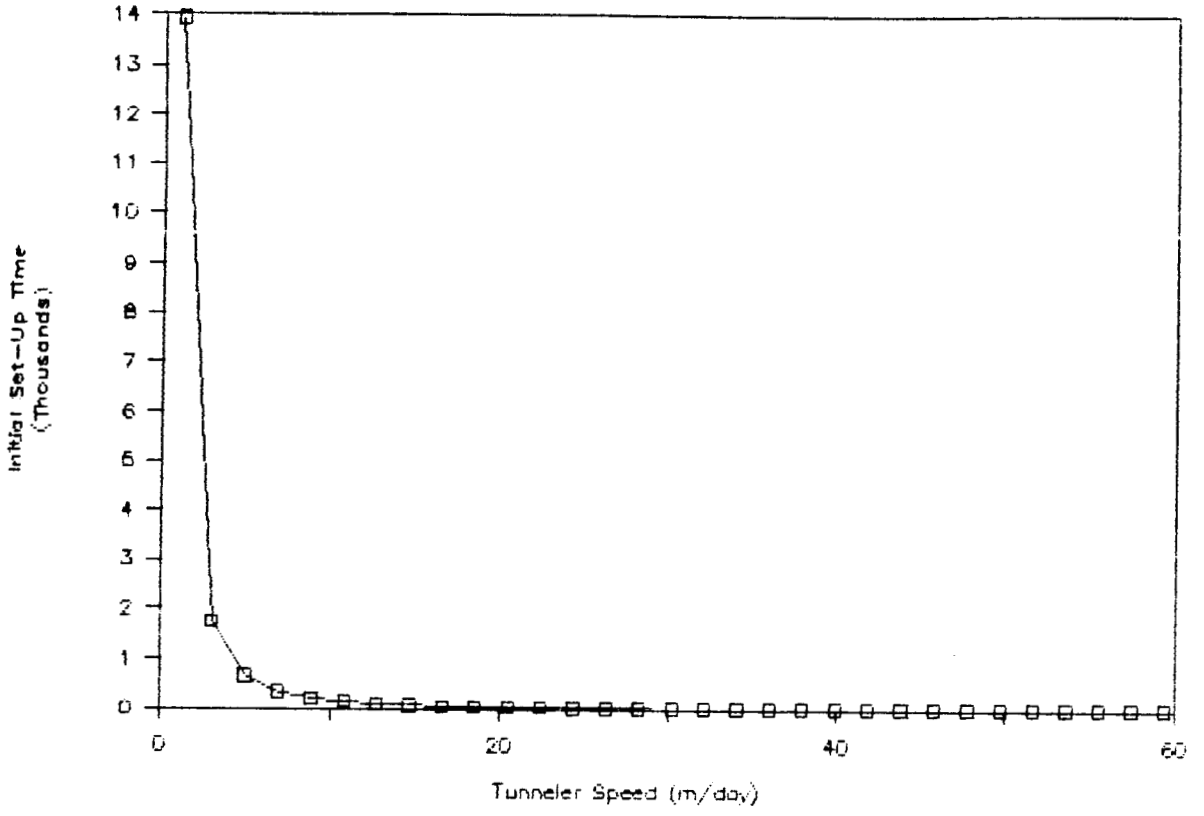

Tunneler Speed Vs Coolant Tank Length

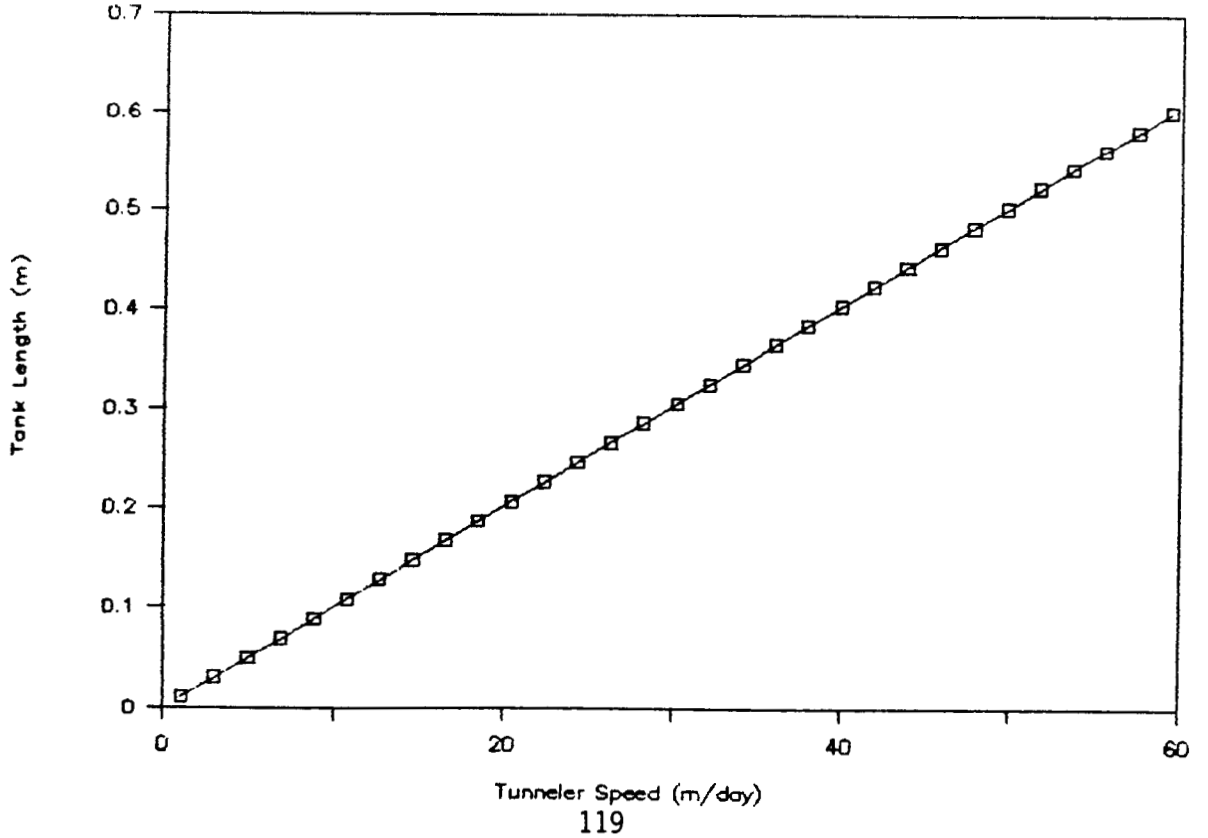

Truck Speed Vs Regolith Tank Length

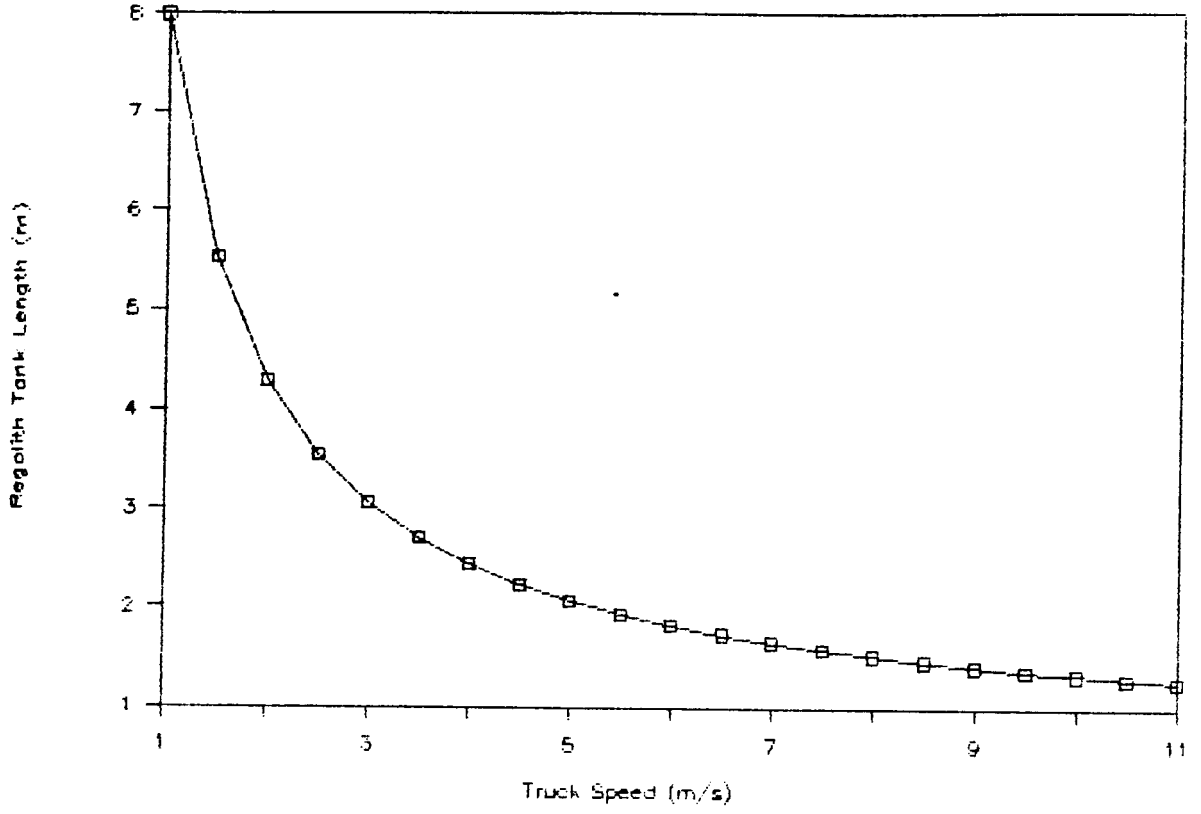

Truck Speed Vs Truck Return Time

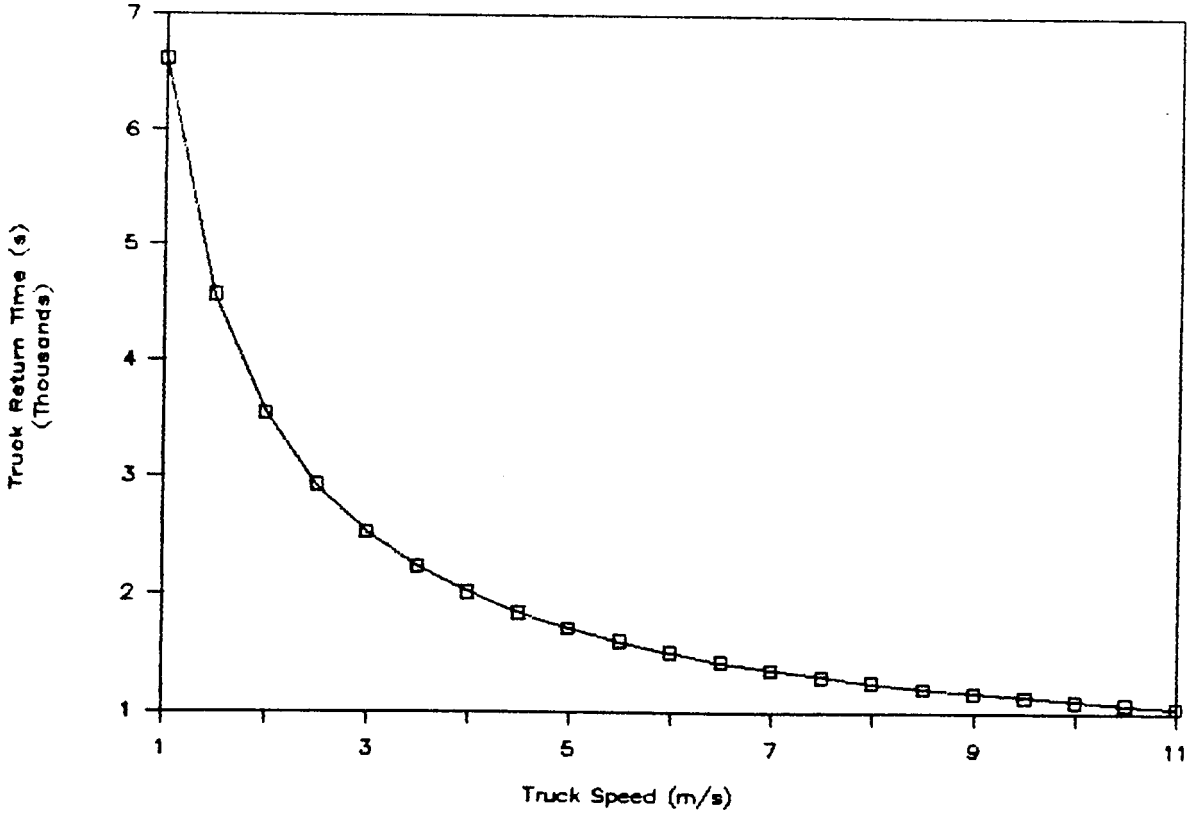

Temperature Gradient

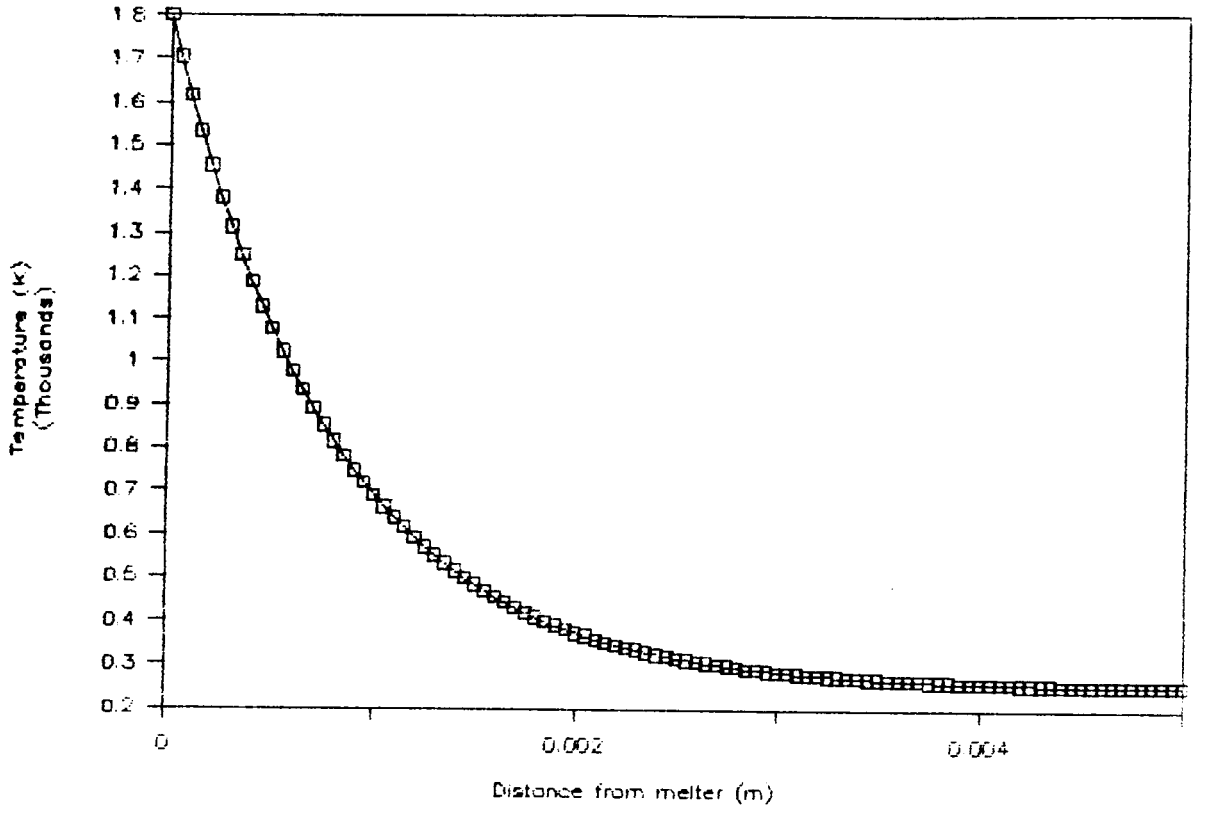

Tunneler Speed Vs Regolith Tank Length

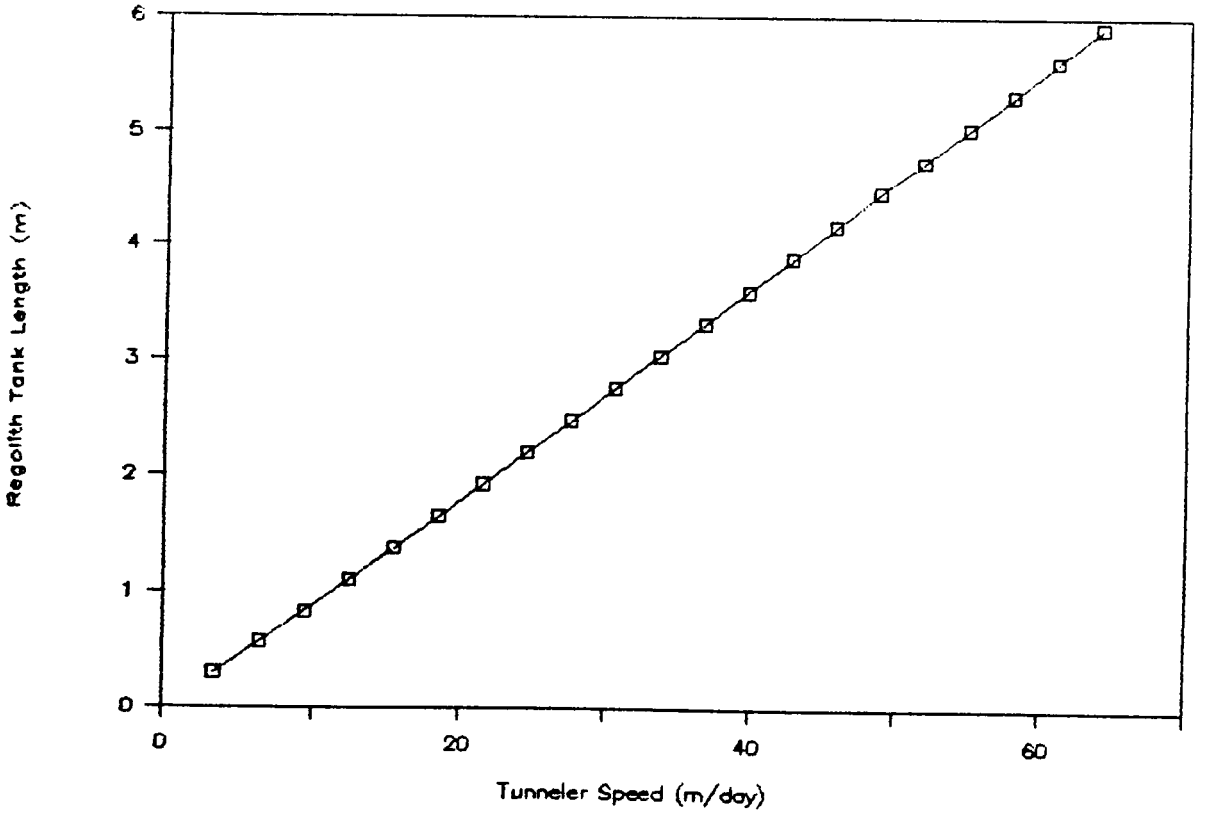

Tunnel Diameter Vs Tank Length of

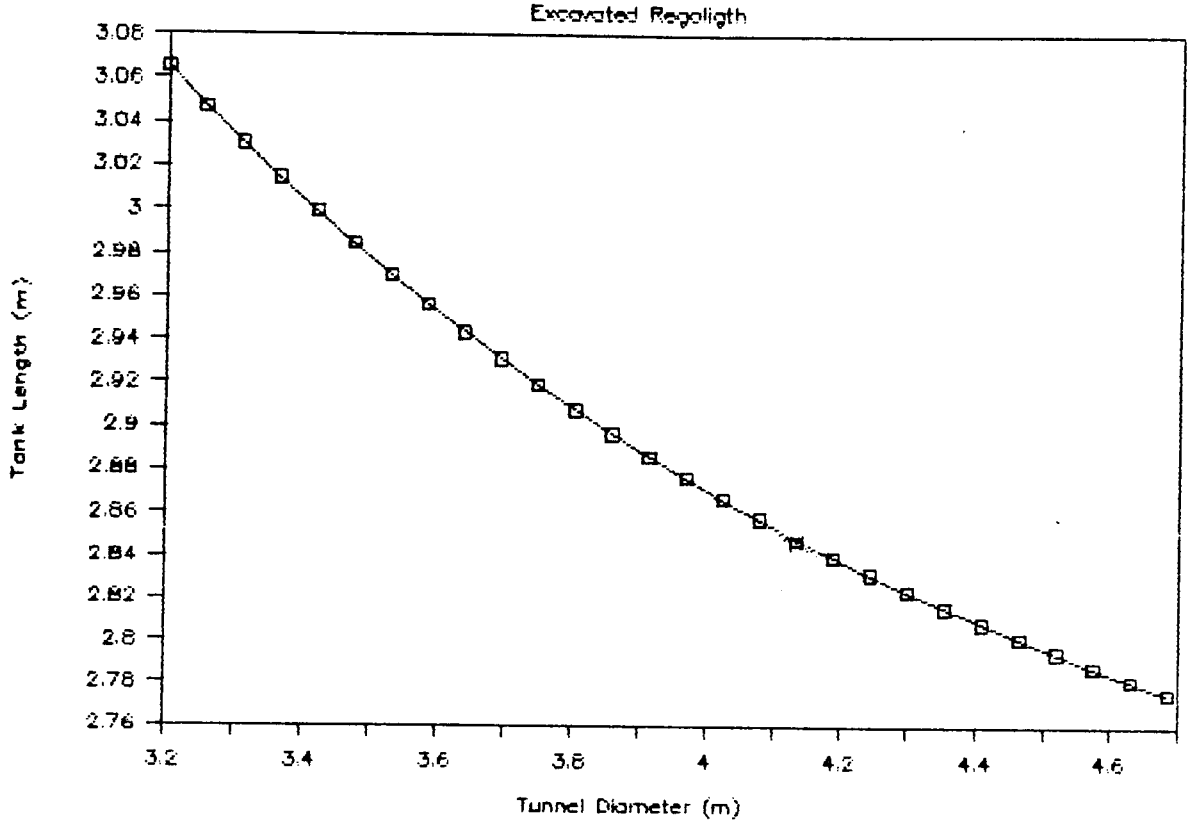

Tunnel Diameter Vs Truck Return Time